CLIMATE CHANGE AND FUTUREPROOFING INFRASTRUCTURE: ETIMESGUT, ANKARA CASE STUDY

A THESIS SUBMITTED TO
THE GRADUATE SCHOOL OF NATURAL AND APPLIED SCIENCES
OF
MIDDLE EAST TECHNICAL UNIVERSITY

BY

SERTAÇ ORUÇ

IN PARTIAL FULFILLMENT OF THE REQUIREMENTS
FOR
THE DEGREE OF DOCTOR OF PHILOSOPHY
IN
DEPARTMENT OF EARTH SYSTEM SCIENCE

JUNE 2018

Approval of the thesis:

CLIMATE CHANGE AND FUTUREPROOFING INFRASTRUCTURE: ETIMESGUT, ANKARA CASE STUDY

Submitted by **SERTAÇ ORUÇ** in partial fulfilment of the requirements for the degree of **Doctor of Philosophy in Earth System Science Department, Middle East Technical University** by,

Prof. Dr. Halil Kalıpçılar _____
Dean, Graduate School of **Natural and Applied Sciences, METU**

Prof. Dr. C. Can Bilgin _____
Head of Department, **Earth System Science, METU**

Prof. Dr. Ayşen Yılmaz _____
Supervisor, **Earth System Science Dept., METU**

Prof. Dr. İsmail Yücel _____
Co-Supervisor, **Civil Engineering Dept., METU**

Examining Committee Members:

Prof. Dr. Elçin Kentel _____
Civil Engineering Dept., METU

Prof. Dr. Ayşen Yılmaz _____
Earth System Science Dept., METU

Prof. Dr. Cemal Saydam _____
Environmental Engineering Dept., Hacettepe University

Assoc. Prof. Dr. Tuğrul Yılmaz _____
Civil Engineering Dept., METU

Assist. Prof. Dr. Melih Çalamak _____
Civil Engineering Dept., TED University

Date: 22.06.2018

I hereby declare that all information in this document has been obtained and presented in accordance with academic rules and ethical conduct. I also declare that, as required by these rules and conduct, I have fully cited and referenced all material and results that are not original to this work.

Name, Last name : Sertaç Oruç

Signature :

ABSTRACT

CLIMATE CHANGE AND FUTUREPROOFING INFRASTRUCTURE: ETIMESGUT, ANKARA CASE STUDY

Oruç, Sertaç
Ph.D., Department of Earth System Science
Supervisor : Prof. Dr. Ayşen Yılmaz
Co-Supervisor : Prof. Dr. İsmail Yücel

June 2018, 115 pages

This study examines the potential impacts of climate change and land use/cover change; investigates how to incorporate these changes into urban stormwater network design. Rainfall analysis with stationary and nonstationary approach for observed and future conditions is performed for the (1950-2015 period) observed data and projections (2015-2098 period) for Ankara province, Turkey. Daily projections are disaggregated to finer scales and used for future period the analysis. Nonstationary Generalized Extreme Value (GEV) models and stationary GEV models for observed and future data is obtained. Also land use/cover change and urbanization in Ankara is investigated in general. Land use/cover situation together with the type and rate of change is examined particularly to obtain a composite runoff coefficient for the pilot study area considering the current and potential development conditions. Stormwater network design is assessed considering the nonstationarities and future conditions for present stormwater network of railway critical infrastructure located in Etimesgut pilot study area. Depending on the models and Representative Concentration Pathways (RCP), there are different results for the future extreme rainfall input; yet all results indicate a decreasing extreme trend. The magnitude of future period extreme rainfall decreases with respect to observations. Return periods of the extreme rainfall increase in the future period therefore, not considering these trends may lead to overdesign of the stormwater network.

Keywords: Climate Change, Stormwater, Nonstationary, Urbanization

ÖZ

İKLİM DEĞİŞİKLİĞİ VE GELECEĞE UYUMLU ALTYAPI: ETİMESGUT, ANKARA ÖRNEĞİ

Oruç, Sertaç
Doktora, Yer Sistem Bilimleri Bölümü
Tez Yöneticisi : Prof. Dr. Ayşen Yılmaz
Ortak Tez Yöneticisi : Prof. Dr. İsmail Yücel

Haziran 2018, 115 sayfa

Bu çalışma, iklim değişikliğinin ve arazi kullanımı/örtüsündeki değişikliğin potansiyel etkilerini incelemekte; bu değişiklikleri kentsel yağmur suyu şebeke tasarımına nasıl dahil edeceğini araştırmaktadır. Gözlem (1950-2015 dönemi) ve projeksiyon (2015-2098 dönemi) yağış verileri için durağan ve durağan olmayan bir yaklaşımla Ankara ili, Türkiye için yağış analizi gerçekleştirilmiştir. Günlük projeksiyonlar daha küçük ölçeklere ayrıştırılarak analizlerde kullanılmıştır. Gözlem ve projeksiyon verileri için Durağan Olmayan Genel Aşırı Değer (GAD) modelleri ve Durağan GAD modelleri elde edilmiştir. Ayrıca Ankara'da arazi kullanımı / örtü değişimi ve kentleşme genel olarak incelenmiştir. Pilot çalışma alanı için mevcut ve potansiyel gelişim koşulları da göz önünde bulundurularak bileşik akış katsayısı elde edilmesi için arazi kullanım / örtü durumu, değişim oranı ve tipi ile birlikte araştırılmıştır. Yağmursuyu şebekesi tasarımı, Etimesgut pilot çalışma alanında bulunan mevcut bir demiryolu kritik altyapısı yağmur suyu şebekesi için durağan olmama durumu ve gelecekteki koşullar dikkate alınarak değerlendirilmiştir. Modellere ve Temsili Konsantrasyon Senaryolarına (TKS) bağlı olarak, gelecekteki aşırı yağış girdisi için farklı sonuçlar tespit edilmiştir ancak tüm sonuçlar aşırı yağışlar için azalan bir eğilimi göstermektedir. Gelecek dönem aşırı yağış büyüklüğü gözlem periyodu büyüklüklerine oranla azalmaktadır. Aşırı yağışların geri dönüş periyotlarının gelecek dönemde artmakta olduğu görülmekte olup söz konusu eğilimler dikkate alınmaksızın yapılacak yağmur suyu şebekesi tasarımı için gereksiz yüklere sebep olabilecektir.

Anahtar Kelimeler: İklim Değişikliği, Yağmur Suyu, Kentleşme, Durağan Olmayan

To My Son and My Wife

Poyraz and Buket

ACKNOWLEDGMENTS

I would like to dedicate my special thanks to my supervisor Prof. Dr. Ayşen Yılmaz and Co-Supervisor Prof. Dr. İsmail Yücel for their patient, valuable contributions, and outstanding guidance during this research and it is my luck to have a chance to work with them. Thanks are also due to all the academic staff of Earth System Science (ESS) department. Special thanks to Aydan Özkil for sharing her work and digitized data. Also thanks to State Meteorological Service, Ministry of Forestry and Water Affairs, General Command of Mapping for the data support. I cordially thank M. Orhan Çevik, Akif Kantar, Nuri Sandıkcıoğlu and Cem Nart for their support.

I cannot find words to express my gratitude to my son Poyraz Oruç for his tolerance and smiling-motivating face and my wife Buket Köksal Oruç for her endless patience, understanding, encouragement and love.

TABLE OF CONTENTS

ABSTRACT v
ÖZ vi
ACKNOWLEDGMENTS viii
TABLE OF CONTENTS ix
LIST OF TABLES xii
LIST OF FIGURES xiv
CHAPTERS
1. INTRODUCTION 1
1.1. CLIMATE CHANGE AND IMPACTS 1
1.1.1. Global and Regional Climate Change: Impacts 1
1.1.2. Climate Change and Alterations in the Precipitation Regime 4
1.1.3. Extreme Precipitations Trends and Intensity–Duration–Frequency (IDF) Curves 5
1.1.4. Climate Change and Future Projections for the Precipitation 6
1.1.5. Climate and Precipitation Regime Changes, Impacts and Future Projections for Turkey and Ankara Province 7
1.2. URBANIZATION AND URBAN STORMWATER NETWORKS 12
1.2.1. Urbanization and Changes in the Land Use/Cover 12
1.2.2. Urban Stormwater Infrastructure System in Changing Conditions - Design for Future 14
1.2.3. General Geographical and Stormwater Network Information for Ankara and Etimesgut Pilot Study Area 16
1.3. RESEARCH QUESTION AND PROBLEM STATEMENT 19
1.4. AIM OF THE STUDY AND OBJECTIVES 19
2. METHODOLOGY 21
2.1. INTRODUCTION 21
2.2. STUDY AREA 22
2.3. DATA COLLECTION AND ANALYSIS - PRECIPITATION 23

2.3.1. Disaggregation 25
2.3.2. Trend Analysis 27
2.3.3. Extreme Value Analysis: Stationary & Nonstationary 28
2.3.4. Goodness of Fit 31
2.4. DATA COLLECTION AND ANALYSIS - LAND USE/COVER CHANGE 32
2.5. DERIVATION OF DESIGN PARAMETERS FOR THE STORMWATER NETWORK OF PILOT STUDY AREA 33
3. CLIMATE CHANGE AND ALTERATIONS IN THE PRECIPITATION REGIME: OBSERVATIONS IN ANKARA PROVINCE 37
3.1. TREND AND CHANGE POINT TESTS 38
3.2. STATIONARY AND NONSTATIONARY ANALYSIS – OBSERVED PRECIPITATION DATA 40
3.2.1. Stationary Analysis – Observed Precipitation Data 40
3.2.2. Non-Stationary Analysis – Observed Precipitation Data 44
4. CLIMATE CHANGE AND ALTERATIONS IN THE PRECIPITATION REGIME: PROJECTIONS FOR ANKARA PROVINCE 51
4.1. TREND TESTS FOR THE PROJECTED DATA 52
4.2. STATIONARY ANALYSIS FOR PROJECTED DATA: RETURN LEVEL ESTIMATES 56
4.3. NON-STATIONARY ANALYSIS FOR PROJECTED DATA AND COMPARISON WITH THE STATIONARY ANALYSIS 60
5. OVERVIEW OF URBANIZATION: ANKARA CASE 71
5.1. LAND USE CHANGE IN ANKARA AND PILOT STUDY AREA 72
6. CLIMATE CHANGE AND ALTERATIONS IN THE PRECIPITATION REGIME: STORMWATER NETWORK ANALYSIS 81
6.1. STORMWATER NETWORK ANALYSIS IN ETIMESGUT PILOT STUDY AREA 82
6.2. STORMWATER NETWORK SYSTEM IN ANKARA PROVINCE: GENERAL ASSESSMENT 94
7. SUMMARY, CONCLUSIONS, AND RECOMMENDATIONS 97
7.1. SUMMARY 97

7.2. CONCLUSIONS 98
7.3. RECOMMENDATIONS 100
REFERENCES 103
CURRICULUM VITAE 115

LIST OF TABLES

TABLES

Table 2.1. Projection Data Stations & Grids (SMS, 2017b) 23
Table 2.2. Description of GEV Distributions (Pinheiro and Grotjahn, 2015). 29
Table 2.3. Non-stationary models with time and covariate (temperature) dependent location and scale parameters 31
Table 3.1. Pettitt Test and Mann-Kendall Results for the Storm Durations 39
Table 3.2. Stationary (St) Return Levels (mm) vs. Return Periods (1950-2015) 40
Table 3.3. Stationary Return Levels (mm) % Change - 1950-2015 vs. 1950-1975 ... 41
Table 3.4. Stationary Return Levels (mm) vs. % Change - 1950-2015 vs. 1976-2015 42
Table 3.5. Stationary Return Levels (mm) % Change - 1976-2015 vs. 1950-1975 ... 42
Table 3.6. Stationary Return Levels (mm) % Change - GEV Stationary Model vs. Turkish State Meteorological Service Return Level Estimates for Ankara 44
Table 3.7. Stationary and Best Fit Nonstationary Model Comparison 44
Table 3.8. Nonstationary Best Fit Return Levels (mm) - Mean Values 45
Table 4.1. Mann-Kendall Results for the Storm Durations of Projected Data Time Series 55
Table 4.2. Ten Minutes Stationary (St) Return Levels (mm) vs. Return Periods Calculated for Projected Data 57
Table 4.3. Fifteen Minutes Stationary (St) Return Levels (mm) vs. Return Periods Calculated for Projected Data 58
Table 4.4. One Hour Stationary (St) Return Levels (mm) vs. Return Periods Calculated for Projected Data 59
Table 4.5. 5 Six Hours Stationary (St) Return Levels (mm) vs. Return Periods Calculated for Projected Data 60
Table 4.6. Diagnostic Values of Stationary and Best Fit Nonstationary Models of Projected Data 61
Table 4.7. Nonstationary Model-Stationary Model Comparison - Mean Value Change for Projected Data 62

Table 4.8. Nonstationary Model-Stationary Model Comparison for Projected Data–Maximum Value Change 64
Table 4.9. Nonstationary Model-Stationary Ensemble Model Comparison for Projected Data - Average and Maximum Values..... 65
Table 5.1. Cover Types and Runoff Coefficient – Pilot Study Area 78
Table 6.1. Percent Fullness of Models without Pipe Revision-Climate Change 83
Table 6.2. Percent Fullness of Models Without Pipe Revision-Climate Change and Land Use Change (C=0,90) 85
Table 6.3. Velocity-Percent Fullness-H Min Results for Models Obtained for Baseline Design System..... 86
Table 6.4. Percent Fullness of Models with Pipe Revision-Climate Change 87
Table 6.5. Percent Fulness of Models with Pipe Revision-Climate Change and Land Use 88
Table 6.6. Pipe Quantities for Models (in meters) Small (200-600 mm) and Large (800-1600 mm) Size-After Revision..... 90
Table 6.7. Pipe Diameter Change for the Models Compared with Baseline Design . 92
Table 6.8. Cost Comparison of Models after Revision (in Euros)..... 93

LIST OF FIGURES

FIGURES

Figure 1.1. Map of the observed surface temperature change from 1901 to 2012. The globally averaged combined land and ocean surface temperature data show a warming of 0.85 [0.65-1.06] °C, over the period of 1880 to 2012 (IPCC, 2013). 2
Figure 1.2. Global mean temperature anomalies, with respect to the 1850–1900 baseline, for the five global datasets (WMO-No. 1212, 2018) 2
Figure 1.3. The GISTEMP monthly temperature anomalies superimposed on a 1980-2015 mean seasonal cycle (retrieved on May 20, 2018, from https://climate.nasa.gov/news/2683/january-2018-was-fifth-warmest-january-on-record/). 3
Figure 1.4. NOAA National Centers for Environmental information, Climate at a Glance: Global Time Series, published April 2018 (retrieved on April 30, 2018, from http://www.ncdc.noaa.gov/cag/). 3
Figure 1.5. Time series of annual a surface air temperature (°C), and b precipitation (mm/day) of CMIP5 model averages over Turkey for the period 2006–2099. The colors indicate different emission scenario simulations (RCP45: blue, and RCP85: red) (Turunçoğlu et. al, 2018) 9
Figure 1.6. Annual count of extreme events in Turkey in the period of 1940-2017 (SMS, 2018). 10
Figure 1.7. Distribution of extreme events and their types in Turkey in 2017 (SMS, 2018)..... 11
Figure 1.8. Changes in the Infiltration due to Urbanization and Changes in the Surface Structure (StormWaterForestry, 2018). 14
Figure 1.9. 3D view of the digital elevation model (DEM) (Yal and Akgün, 2014). 16
Figure 2.1. Railway Maintenance Complex in Etimesgut-Ankara 22
Figure 2.2. Rainfall Data Analyses Framework 25
Figure 2.3. Parameter Derivation for Rational Method 34
Figure 3.1. Storm Durations Used for Stationary Models..... 37

Figure 3.2. Storm Durations Used for Nonstationary Models 38
Figure 3.3. Sub-Hourly Time Series Trend..... 38
Figure 3.4. Hourly Time Series Trend 39
Figure 3.5. Stationary Return Level (mm) Estimates for sub-hourly and hourly storm durations..... 41
Figure 3.6. Average annual maximum rainfall intensities (mm) for sub-hourly and hourly storm durations 43
Figure 3.7. Stationary and Best Fit Nonstationary Model Return Level (mm) Comparison - Return Period vs. Return Level 47
Figure 3.8. Stationary and Best Fit Nonstationary Model IDF Curves..... 48
Figure 4.1. Projected Storm Durations Used for Stationary Models for 2015-2098 period..... 51
Figure 4.2. Projected Storm Durations Used for Nonstationary Models for 2015-2098 period..... 52
Figure 4.3. Projected 10 Minutes Annual Maximum-Time Series in Ankara Province for 2015-2098 period..... 53
Figure 4.4. Projected 15 Minutes Annual Maximum-Time Series in Ankara Province for 2015-2098 period..... 53
Figure 4.5. Projected 1 Hour Annual Maximum-Time Series in Ankara Province for 2015-2098 period 54
Figure 4.6. Projected Six Hours Annual Maximum-Time Series in Ankara Province for 2015-2098 period..... 54
Figure 4.7. Stationary Model Results for Ten Minutes Time Series for Projected Data 57
Figure 4.8. Stationary Model Results for Fifteen Minutes Time Series for Projected Data 58
Figure 4.9. Stationary Model Results for One Hour Time Series for Projected Data 59
Figure 4.10. Stationary Model Results for Six Hours Time Series for Projected Data 60
Figure 4.11. Ten Minutes Ensemble Model Comparison for Projected Data..... 66
Figure 4.12. Fifteen Minutes Ensemble Model Comparison for Projected Data..... 66
Figure 4.13. One Hour Ensemble Model Comparison for Projected Data 66

Figure 4.14. Six Hours Ensemble Model Comparison for Projected Data 66
Figure 4.15. Stationary and Best Fit Nonstationary Model IDF Curves 67
Figure 5.1. Urbanization Effect in a Basin - (surface runoff increases both in volume and in peak discharge value) 71
Figure 5.2. Historical Change of City and Village Population in Ankara - Year vs. Population (in Millions) (*Ankara Development Agency, 2018*) Black: Rural population, Grey: Urban population) 73
Figure 5.3. Areal Ratio with Respect to Late 50s 74
Figure 5.4. Ratio of Green to Urban Area 75
Figure 5.5. Last 60 Years Urban Transformation of Ankara (Black=Urban, Green=Green Areas) 76
Figure 5.6. Urban Transformation of Pilot Study Area- Left 2003 and Right 2018 .. 77
Figure 6.1. Maximum Capacity Experienced during the Projection Period by Each Pipe 84
Figure 6.2. Baseline Design Percent Fullness – C=0.8 and C=0.9 85
Figure 6.3. Small vs. Large Size Pipe Quantities – Baseline and Revised System Pipe Lengths in Meters 91

ABBREVIATIONS

AIC	Akaike Information Criteria
1D	One Dimensional
2D	Two Dimensional
3D	Three Dimensional
A	Area
AIC	Akaike Information Criteria
AM	Annual Maximum
AVG	Average
AWSA	Ankara Water and Sewerage Administration
BAKAY	Greater Ankara Sewerage and Stormwater Project (BAKAY)
BIC	Bayesian Information Criteria
BLRP	Bartlett-Lewis Rectangular Pulse Model
BLRPR	Random Parameter Bartlett-Lewis Rectangular Pulse Model
BM	Block Maxima
C	Runoff Coefficient
CLIMA HYDRO	Climate Change Impacts on Water Resources Project
CNRM-CM5.1	Centre National de Recherches Météorologiques-Model Version 5.1
CMIP	Coupled Model Intercomparison Project
CO2	Carbon dioxide
CORDEX	Coordinated Regional Climate Downscaling Experiment
DEM	Digital Elevation Model
DF	Distribution Function
EVA	Extreme Value Analysis
EVT	Extreme Value Theory
FEH	
GCM	Global Circulation Model
GCoM	General Command of Mapping
GEV	Generalized Extreme Value
GFDL-ESM2M	Geophysical Fluid Dynamics Laboratory Earth System Model
GFDL	GFDL-ESM2M

GHG	Green House Gas
GIS	Geographic Information Systems
GISS	Goddard Institute for Space Studies
GISTEMP	The GISS Surface Temperature Analysis
GL	Generalised Logistic
GPD	Generalized Pareto Distribution
H MINIMUM	Minimum Height in the Pipe
HADGEM2-ES	Hadley Centre Global Environment Model Version 2
HG	HADGEM2-ES
HGK	General Command of Mapping
I	Intensity
IDF	Intensity-Duration-Frequency
IPCC	Intergovernmental Panel on Climate Change
LOTI	Land-ocean temperature index
LU/LC	Land Use Land Cover
MAX	Maximum
MENA	Middle East and North Africa
MIN	Minutes
MK	Mann-Kendal
MLE	Maximum Likelihood Estimate
MPI-ESM-MR	Max Planck Institute – Earth System Model
MPI	MPI-ESM-MR
NASA	National Aeronautics and Space Administration
NLL	Negative Log-Likelihood
NOAA	National Oceanic and Atmospheric Administration
NSTGEV	Nonstationary Generalized Extreme Value
NST	Nonstationary
Ø	Diameter
OBS	Observation
^{o}C	Celsius degree
P	Exceedance Probability
1/P	Return Period

POT	Peak over Threshold
Q	Peak Runoff
q	Runoff
q/Q	Percent Fullness of Pipes
R	The R Project for Statistical Computing
RCM	Regional Climate Model
RCP	Representative Concentration Pathway
RCP 4.5	Representative Concentration Pathway radiative forcing 4.5W/m2
RCP 8.5	Representative Concentration Pathway radiative forcing 8.5W/m2
REGCM4.3	Regional Climate Model
SRES	Special Report on Emissions Scenarios
SREX	Managing the Risks of Extreme Events and Disasters to Advance Climate Change Adaptation
ST	Stationary
SMS	State Meteorological Services
T_c	Time of Concentration
TUİK-TURKSTAT	The Turkish Statistical Institute
V	Velocity
WMO	World Meteorological Organization

CHAPTER 1

INTRODUCTION

1.1. CLIMATE CHANGE AND IMPACTS

1.1.1. Global and Regional Climate Change: Impacts

According to International Government on Climate Change (IPCC) reports (IPCC, 2013; IPCC, 2014b), climate change is observed in all over the world: the atmosphere and oceans are warming, volume of snow and ice covers are diminishing, sea levels are rising and weather patterns are changing. Global warming, which is basically the gradual heating of Earth's surface, oceans and atmosphere, is caused by human activities, primarily through the use of fossil fuels that emit carbon dioxide (CO_2), methane and other greenhouse gases into the atmosphere. If Green House Gasses (GHG's) emissions continue to rise, it is projected that by the end of this century a global average temperature 2.6–4.8 degrees Celsius (°C) higher than the present, and sea levels 0.45–0.82 meters higher than the present will be seen (Chalmers P., 2014; IPCC, 2013). Since 1895, 2016 was the hottest year that is recorded in the world according to NOAA and NASA. Earth's surface temperature was 0.99 °C warmer than the average across the entire 20th century in that year. Also, 2015 was the warmest year globally before 2016. In fact, 16 of the 17 warmest years on record were observed since 2001, according to NASA (See Figures 1.1, 1.2, 1.3, and 1.4).

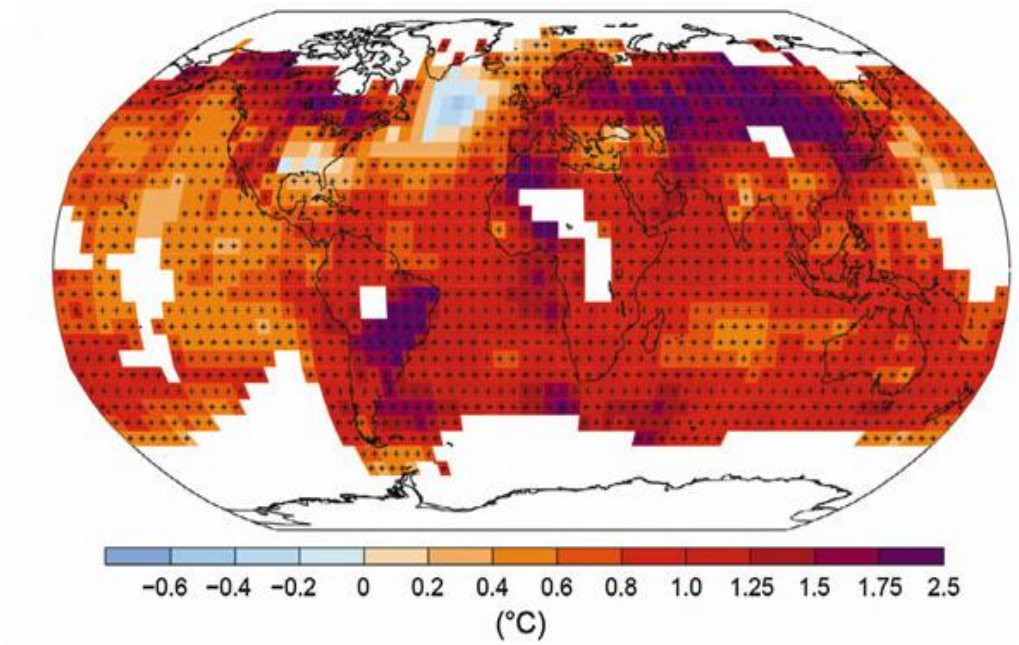

Figure 1.1. Map of the observed surface temperature change from 1901 to 2012. The globally averaged combined land and ocean surface temperature data show a warming of 0.85 [0.65-1.06] °C, over the period of 1880 to 2012 (IPCC, 2013).

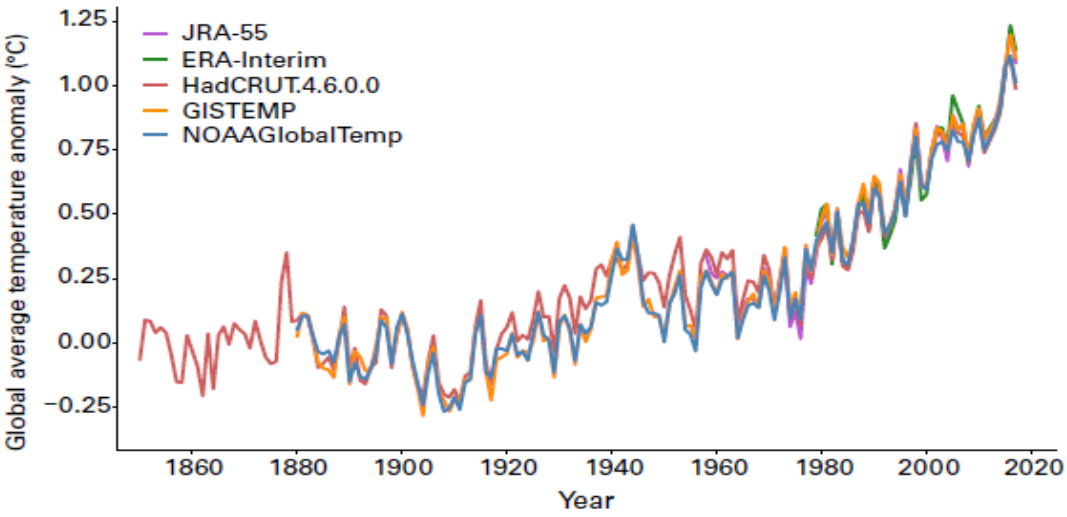

Figure 1.2. Global mean temperature anomalies, with respect to the 1850–1900 baseline, for the five global datasets (WMO-No. 1212, 2018)

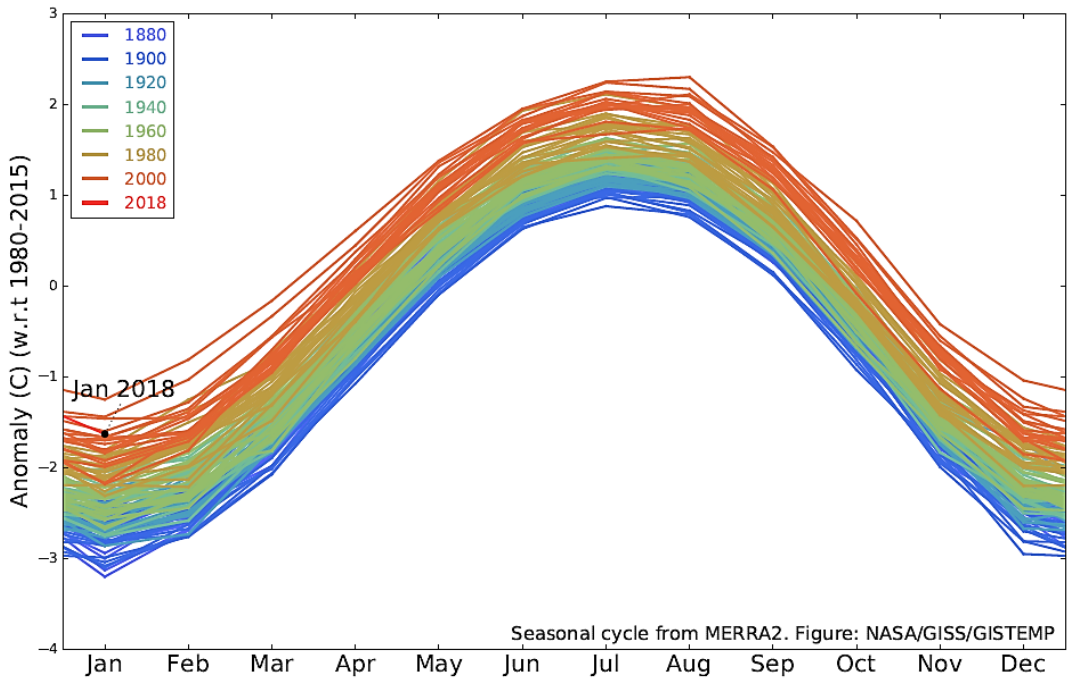

Figure 1.3. The GISTEMP monthly temperature anomalies superimposed on a 1980-2015 mean seasonal cycle (January 2018 was fifth warmest January on record, 2018)

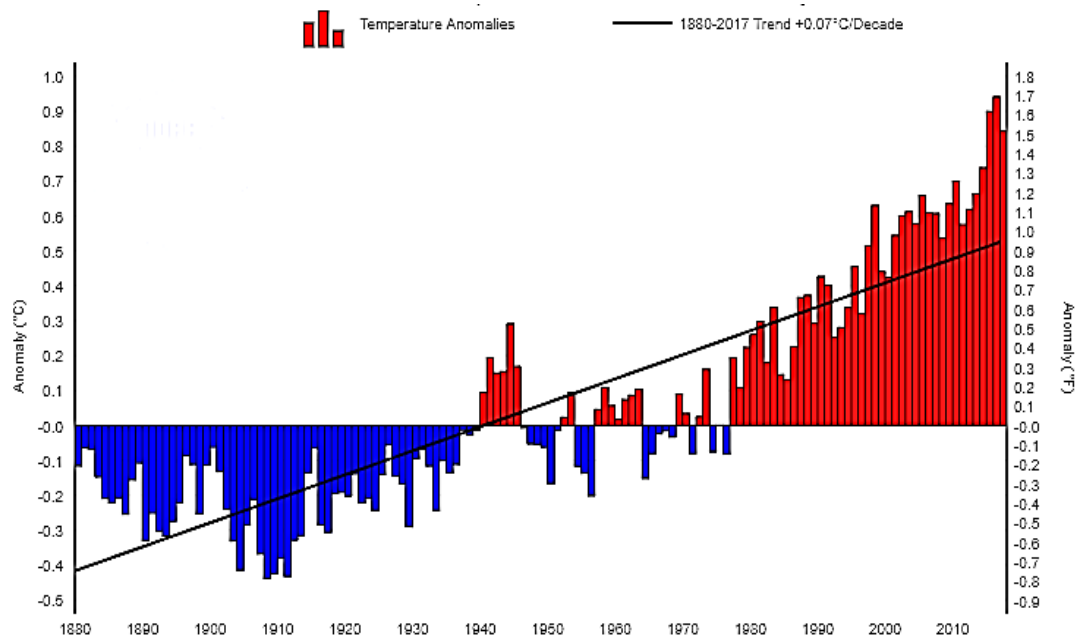

Figure 1.4. Global Land and Ocean Temperature Anomalies, January-December (NOAA, 2018)

Scientists project that due to global warming extreme weather events, such as heat waves, droughts, and rainstorms will continue to occur more frequent and intense. Scientists from the Intergovernmental Panel on Climate Change carrying out global warming research have recently predicted that average global temperatures will probably increase over time (IPCC, 2014a; IPCC, 2014b). Changes resulting from global warming may include rising sea levels due to the melting of the polar ice caps, as well as an increase in occurrence and severity of storms and other severe weather events such as extreme rainfalls (IPCC, 2013).

1.1.2. Climate Change and Alterations in the Precipitation Regime

There are several studies that indicate the effect of climate change on the precipitation regimes and trends. It is a common acceptance that climate change will have significant effects on the water cycle and precipitation patterns (Osborn et al., 2015). In some regions, such changes are expected to change precipitation regimes (e.g. increase in the frequency and intensity of precipitation extremes (Zhou et al., 2012; Papagiannaki et al., 2015). Extreme precipitation events (e.g. fewer rainy days and more extreme rainfalls) are expected by the end of the 21st century under climate change conditions (Willems, 2013; IPCC, 2013; Liew et al., 2014; Pohl et al., 2017). This causes floods with the negative impacts on water infrastructure (e.g. failure of the system, shorten design life of structures), harms on human life, and cause economic losses.

Existing urban infrastructure design criteria and assumptions may underestimate the loads such as peak flow, precipitation height, etc. under changing climate conditions. It has been reported that precipitation pattern that are used as design criteria for urban drainage networks is expected to increase due to climate (van der Linden and Mitchell, 2009; Arnbjerg-Nielsen et al., 2013). This will cause a huge challenge to the current drainage systems which in general designed based on a certain return period (Zhou, 2014). When the consequences of climate change considered, rainfall intensities could be increased, which would lead to an additional impact on stormwater networks, by the shifts in magnitude and frequency of peak flows that the infrastructure, such as stormwater network, faces over the service life. Considering

the potential effects of climate change on extreme rainfall can improve the results of the several methodologies aimed at evaluating potential flood risk and related damages in urban areas or at supporting decision making for flood risk management and urban infrastructure design such as stormwater networks (Notaro et al., 2015).

Local precipitation patterns have been changing due to global warming or atmospheric circulation variations (Zhang et al., 2007) and global exposure to floods would increase depending on the degree of warming, on the other hand flood events will increase in a regional scale instead globally (Hirabayashi et al., 2013). Seneviratne et al. (2012) implies that in south East Asia, north east Europe, tropical Africa, and South America the impact of floods will increase, however these impacts will reverse in central Asia, Eastern Europe, central North America, and Anatolia regions.

Based on the evidence in the SREX (The Special Report on "Managing the Risks of Extreme Events and Disasters to Advance Climate Change Adaptation" of the IPCC report (IPCC, 2012), one can say that there is significant increase in heavy precipitation events at present in more regions than there is significant decreases, but these increase and decrease show various regional and sub-regional trends (Kundzewicz et al., 2014). Similar findings revealed by other studies; extreme weather events stated to occur more frequently and the areas that have not faced extreme events in the past started to encounter these events, moreover both heavy rainfall increase and decrease is observed, but the areas with increasing rainfall getting larger (Li et al., 2017; Hettiarachchi et al., 2018).

1.1.3. Extreme Precipitations Trends and Intensity–Duration–Frequency (IDF) Curves

Climate change may influence extreme climate events, so it is an emerging issue to which the world is paying attention (Crawford and Seidel, 2013). Climate variability and change is important that it has the capacity to make shifts in the extreme event frequencies, intensities and so on. Urban water infrastructure (e.g. sewer and stormwater management systems) and flood control structures (e.g. dams) are

designed based on extreme rainfall properties and these properties are reflected as intensity-duration-frequency (IDF) curves (Peck et al., 2012; Hosseinzadehtalaei et al., 2017). The IDF curves quantify the frequency of occurrence of a storm with a specific intensity at different durations and its application for developing urban design standards (Willems et al., 2012). The IDF curves are, in general, currently based on historical precipitation analysis and statistics. Infrastructure design concepts have considered stationary return levels for a long time, which assume no change to the frequency of extreme event over time however, the frequency of extremes has been changing and this change probably will continue in the future (Cheng and Aghakouchak, 2014). Moreover it is found that neglecting the changing frequency results in IDF curves that can underestimate extreme events (Cheng and Aghakouchak, 2014). Sarhadi et al. (2017) introduced a fully time varying risk framework by Bayesian Markov chain Monte Carlo techniques to incorporate the effect of nonstationarities. The results demonstrate consistent results with those of Cheng and Aghakouchak (2014) and show that stationary approach may underestimate the extreme precipitation events, updated design assumption must be presented in the changing conditions and nonstationary-based IDF curves must replace the stationary-based IDF curves.

1.1.4. Climate Change and Future Projections for the Precipitation

There are studies that analyses future climate projections and their consequences. For instance, Özturk et al. (2018) examine the changes in seasonal precipitation and temperature of CORDEX Middle East and North Africa (MENA) and found out that warmer and drier conditions than present climate conditions are projected to occur more intensely. Furthermore annual average precipitation will increase over the equatorial regions and decrease over the subtropical regions for the annual average precipitation is projected (Kusunoki, 2017). Another study that used multi-model ensemble of regional climate projections to estimate the climate change signal in terms of temperature and precipitation for the city of Aachen, Germany (Buttstadt and Schneider, 2014). The results of the study reveals that rainfall is likely to decrease over the century and the examinations indicates longer and more frequent dry periods in the future. The Norwegian white paper on climate adaptation (Meld.

St. 33, 2013) indicates a rise of 5-30 % in annual mean precipitation by 2100 relative to the period 1961-90 and the number of days with heavy precipitation will rise over this century.

Furthermore in 21st century, a relatively constant runoff volume is expected globally, however, runoff will probably decline substantially in some regions such as Russia, Central Asia, Central Africa, and the Middle East (Miralles-Wilhelm et al., 2017). Future rainfall predictions vary significantly among climate models but a general increase in precipitation are projected for the majority of Canada (Simonovic et al., 2017). Also it is mentioned that the projected increase in annual precipitation is induced primarily by the increases in winter and spring precipitation. Moreover, the projected IDF curves indicate that an overall increase in the intensity of rainfall storms is expected in the majority of cities of Ontario (Wang et al., 2015). Expected changes, however, differ between regions. For instance the most extreme models project changes of mid-twenty-first-century approximately +19 and −25 mm per wet season across the land for Los Angeles Region and ensemble-mean land-average change is −2.5 mm per wet season. (Berg et al., 2015)

1.1.5. Climate and Precipitation Regime Changes, Impacts and Future Projections for Turkey and Ankara Province

Studies support that the global hydrologic cycle will be intensified due to changing climate; wet and dry extremes will be increased which result in floods and droughts (Yoon et al., 2015; Simonovic, 2012; Huntington, 2006). Climate change in Turkey has been evaluated in many different studies with its different aspects. Majority of analysis that are conducted with observed and future data were focused on temperature and precipitation changes which are the most important climate parameters and extreme events.

Sensoy et al. (2013) investigated the extreme climate indices in Turkey for about 109 stations and for the period from 1960 to 2010. The results indicate that annual total precipitation show an increasing in northern parts and a decreasing in Southeastern

Anatolia, Mediterranean and Aegean Regions. Except Aegean and Southeastern Anatolia parts, heavy precipitation days increase in most of the stations. Moreover, in most of the stations maximum 1-day precipitation follow an increasing trend apart from Southeastern Anatolia. Also, there had been many studies investigating rainfall trends in Turkey. Partal and Kahya (2006) applied a trend detection framework and their study identified significant trends in the annual means and in January, February, and September precipitations. The annual mean precipitation showed remarkable decrease mostly in western and southern Turkey. Aşıkoğlu and Çiftlik (2015) studied Aegean Region and they reported that starting in the early 1970s and, in the early 1980s, significant decreases in annual rainfall trends detected and continued afterwards. Except Black Sea Region, there are no significant changes in the amount of the annual precipitation, but number of rainy days has decreased generally in the other regions. Çukur (2011) found out that seasonal amount of precipitation varies with the geographical regions of Turkey. In a recent study for the Rize Province in Turkey, a catchment-scale analysis of extreme rainfall events of the reference (1961–1990) and three future climate periods (2013–2039, 2040–2070, and 2071–2100) is conducted and the results projected a 30% decrease in the median value of extreme rainfall over the study region for the near future (Danandeh Mehr and Kahya, 2016).

Standard duration annual maximum rainfall series with various durations and length of 14 stations up to 2010 in Turkey are used in order to capture the statistical behaviour of series and it is computed that 90% of all studied annual maximum rainfall series are trendless, independent, stationary, homogeneous and it is concluded that IDF curves can be computed in the conventional way for Turkey (Haktanır and Çıtakoğlu, 2014). On the other hand statistically significant increasing trends were found in Antalya Region for at least one extreme rainfall index and frequency analysis conducted by using Generalized Pareto Distribution (GPD) for current and future periods (Yılmaz, 2015). Rainfall intensities for different return periods derived and up to 23% increase was found when compared with the current period (Yılmaz, 2015). Climate change and its urban-induced bias in selected Turkish cities is studied with a quality controlled temperature and precipitation data for the period of 1950–2004 (Tayanç et al., 2009). Larger variability for urban

precipitation is identified which suggests these areas can experience intensified and frequent flood and drought events. The study also identified an increase in the urban precipitation compared to the rural one although not significant however significant warming in southern and southeastern parts of Turkey is detected. Particularly, significant warming is found in almost all of the regions for minimum temperature series and significant decreases of precipitation amounts are identified in the western parts of Turkey (Tayanç et al., 2009). According to Turunçoğlu et al. (2018), for the twenty first century all simulations of CMIP3 and CMIP5 agree on a temperature increase and a precipitation decrease in Turkey.

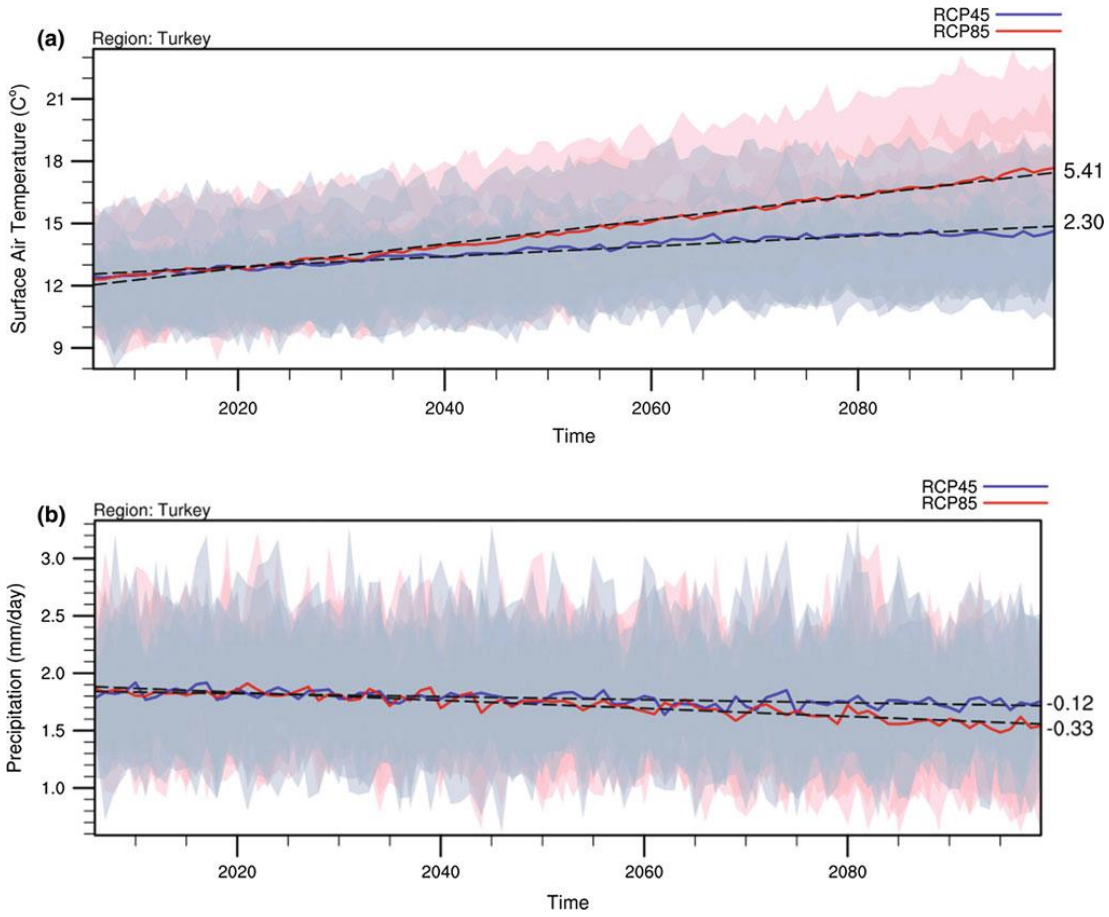

Figure 1.5. Time series of annual a surface air temperature (°C), and b precipitation (mm/day) of CMIP5 model averages over Turkey for the period 2006–2099. The colours indicate different emission scenario simulations (RCP45: blue, and RCP85: red) (Turunçoğlu et al., 2018)

Annual count of extreme events in Turkey shows an increasing trend in 1940-2017 period (See Figure 1.6) according to 2017 Climate Assessment Report (2018) of State Meteorological Service. During 2017 most hazardous extreme events were heavy rain/floods (31%), wind storm (36%), hail (16%), heavy snow (7%), and lightning (4%) (See Fig. 1.7).

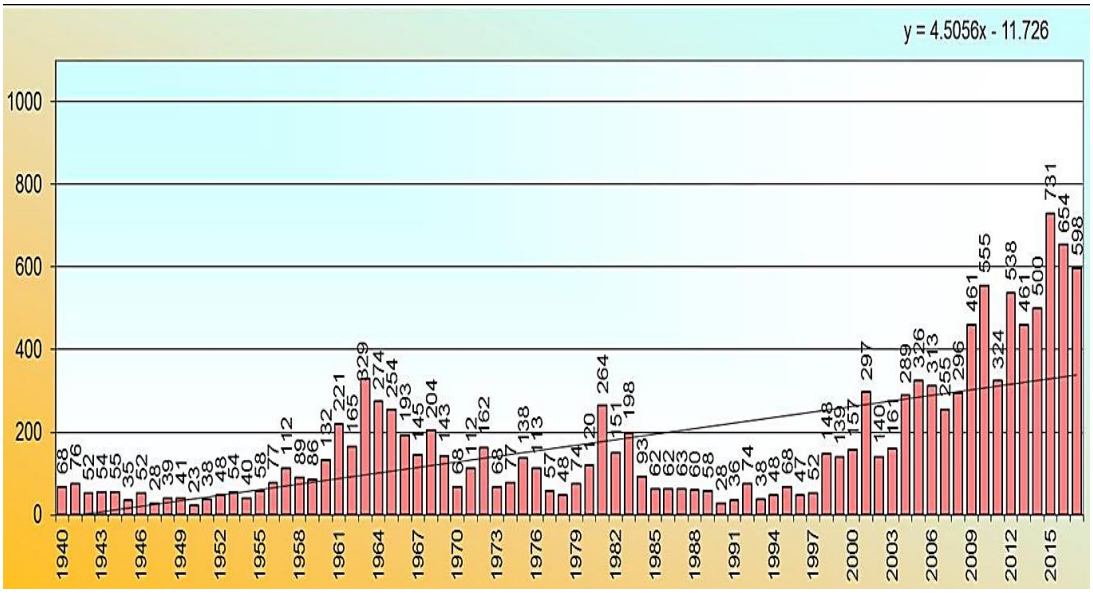

Figure 1.6. Annual count of extreme events in Turkey in the period of 1940-2017 (SMS, 2018).

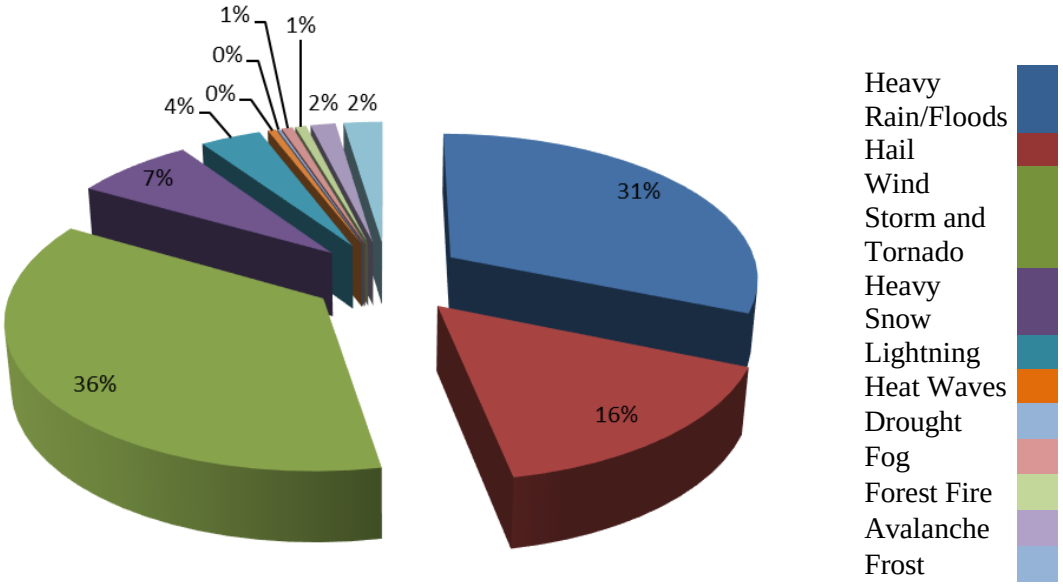

Figure 1.7. Distribution of extreme events and their types in Turkey in 2017 (SMS, 2018).

Climate Change Impacts on Water Resources Project, 2016 (ClimaHydro) by Republic Of Turkey, The Ministry Of Forestry And Water Affairs, General Directorate Of Water Management, has an implementation area of 25 river basins in entire Turkey and the projection period is between 2015 and 2100. The 10-year results of regional, seasonal and yearly changes of precipitation throughout Turkey until 2100 under the RCP 4.5 and the RCP 8.5 scenarios of RegCM4.3 regional climate model solutions based on the HadGEM2-ES, MPI-ESM-MR and CNRM-CM5.1 models have been visualized. For RCP 4.5 and the RCP 8.5 scenarios, precipitations of HadGEM2-ES, MPI-ESM-MR and CNRM-CM5.1 models show that throughout the projection period (2015-2100) regional precipitation increases and decreases will occur based on the ground system models. Generally, during the projection period, it is anticipated that precipitations based on the 10-year averages change between -50 mm and 40 mm for RCP 4.5; -60 mm and 20 mm for RCP 8.5.

Ankara is located within Sakarya and Kızılırmak Basins. According to the results of the projection carried out in ClimaHydro Project for these basins, there is a decrease tendency in the total precipitation compared to the reference period (1971-2000), and

it is predicted that the basins will receive 8% and 6% respectively less rainfall compared to the reference period in 2071-2100 (WRP, 2016). It is expected that rainfall decreases for this period will predominate in the southwestern and north-eastern parts of the Sakarya basin. Also climate projections for Sakarya Basin, which Ankara is located, indicate that number of extreme wet days decrease for future periods, which will have a possible consequence of intensified precipitation (WRP, 2016).

In the last 20 years' flooding observations, heavy rainfall and flash flooding caused various damages. Settlements are damaged due to flooding, agricultural products, environment were damaged due to flooding and agricultural products were damaged due to storm. Moreover road transportation disrupted, people, animals and settlements were damaged also cultivated farmland and vehicles damaged in Ankara, the Capital of Turkey (Supplementary Document of Official Letter of SMS, 2017a).

1.2. URBANIZATION AND URBAN STORMWATER NETWORKS

1.2.1. Urbanization and Changes in the Land Use/Cover

Any surface which water cannot infiltrate is defined as impervious surface. Expansion of impervious surfaces not only increases stormwater runoff volumes but also stream habitat, lake and stream water quality are affected by the rate of increase (Bauer et al., 2007).

The amount of impervious surface in an area is one of the indicators of environmental quality (Arnold and Gibbons, 1996). Impervious surface area increases when rural landscapes changes to urban and suburban areas and effects the amount of runoff, and is also related to urban heat island effects (Bauer et al., 2004). In several regions land surface processes directly affect the extreme temperature and heavy precipitation and these land surface activities projected to expand or intensify in the future (Lawrence et al., 2016).

Urbanization raises the impervious areas, changes land cover types resulting in increase in discharge, volume, and frequency of floods which together with climate change induced intensified rainfalls will have amplified effects on urban stormwater systems (Thakali et al., 2016). Recent data shows the rate of urban sprawl and permanent conversion of agricultural land into urban areas and infrastructure facilities in Europe (EEA, 2017).

The impacts of development on stormwater runoff can lead to increased flooding, degraded water quality, erosion, hydrologic modifications, and destruction of sensitive habitats and landscapes (Figure 1.8.). Urban stormwater runoff results from rain, snow, and other precipitation that lands on roof-tops, roads, sidewalks (pavements), and other surfaces in the urban area. Impervious surfaces shed water, which then becomes runoff that eventually enters the city sewer and stormwater collection system or is discharged directly to adjacent waterbodies. Stormwater runoff flows into separate storm sewers or combined sewer systems. If there is a combined sewer system, stormwater runoff mixes with sanitary flow. If the volume and rate of stormwater and sanitary flow exceeds capacity sewer and stormwater systems (including wastewater treatment plant), street flooding may occur (Guidelines for NYC, 2012).

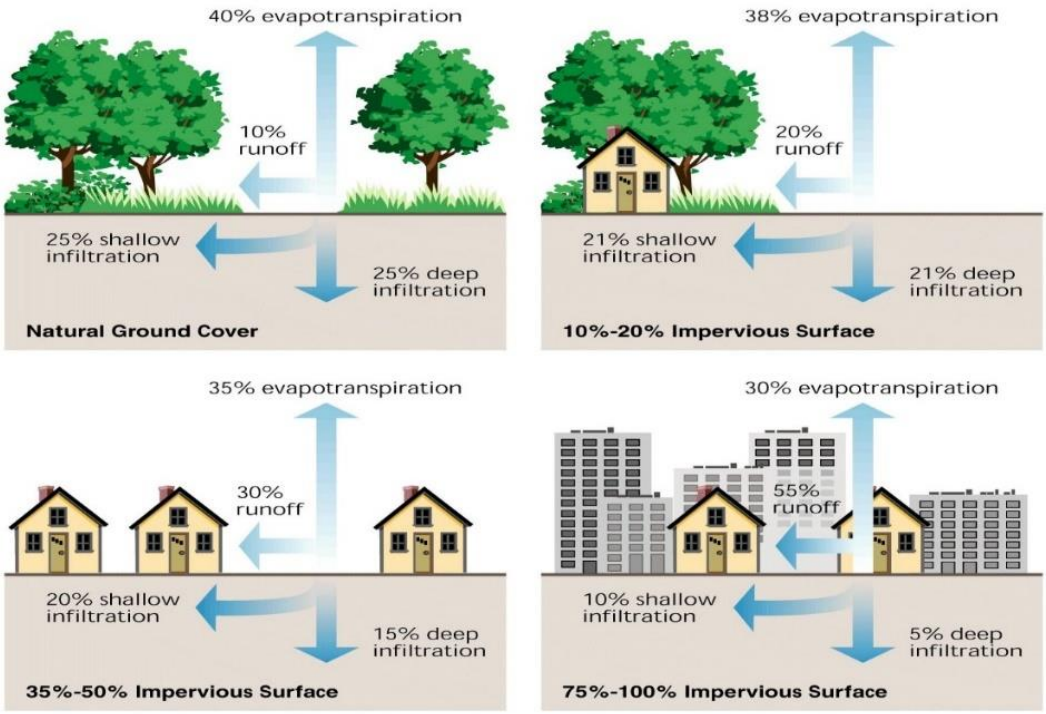

Figure 1.8. Changes in the Infiltration due to Urbanization and Changes in the Surface Structure (StormWaterForestry, 2018).

1.2.2. Urban Stormwater Infrastructure System in Changing Conditions - Design for Future

Climate change and its potential impacts gained importance due to projected changes in temperature and precipitation which can significantly affect the hydrological cycle, land use, extremes and the related infrastructure (Elshorbagy et al., 2018). Stormwater networks can be sensitive to climate change, in particular to extreme rainfall events as they are one of the main variables for design. On the other hand, the design and expected performance of stormwater infrastructure become questionable with the changing climate because the conventional design may not consider the changing climatic conditions (Rosenberg et al., 2010).

For example Osman (2014) analysed future rainfall characteristics and modelled the output to explore the impacts of climate change on the urban drainage system in the Northwest of England during the 21st Century. The results implied that potential

changes in rainfall intensity in the future are expected to alter the performance and serviceability of the system, causing more challenges such as surface flooding and increase in surcharge level in sewers. Bahadur et al. (2016) report that considers urban climate change resilience urges that stormwater management systems will be overwhelmed by the rising intensity of rainfall, and extreme events will damage the infrastructure systems in specific regions of Asia.

There is a need for assessment of uncertainties and hence effects on reliability of design and management of stormwater pipes due to the prevalence of urban floods trigged by modification of land cover and high precipitation intensities respectively due to increasing urbanization and changing climate (Hailegeorgis and Alfredsen, 2017).

Either effected by anthropogenic or natural forcing, climate change will increase the intensity of wet and dry extremes (Simonovic et al., 2016). Moreover, urban runoff and flooding are expected impacts of climate change on urban water systems (Zhou, 2014). The rising trend of rainfall intensities as a result of changing climate or variability is a challenge for infrastructure systems that use particular return levels and periods as design parameters (Zhou, 2014). The adaptation process is not as fast as the changing environmental conditions and increasing exposure to floods therefore result in increased vulnerability (Kundzewicz, 2003; Trenberth, 1998). Older stormwater networks have not been designed to withstand extreme rainfall events, furthermore impervious surfaces increase with urbanization. Additional to extreme rainfall events and urbanization effects, inadequate investment and maintenance of infrastructure further increases exposure to flooding (Simonovic et al., 2016).

Although it is expected that the precipitation intensities tend to change, most of the current infrastructure has been designed with the assumption of a static frequency of extreme climatic events (Cheng & AghaKouchak, 2014). For instance Willems and Lloyd-Huges (2016) found that many of Belgium's sewer systems were designed for storms of a lower intensity than those predicted to occur in the future. Therefore, a

strong need has emerged to study extreme events to reveal potential frequency and intensity alteration under changing climate conditions.

1.2.3. General Geographical and Stormwater Network Information for Ankara and Etimesgut Pilot Study Area

Ankara is located in the northwest of Central Anatolia. The city is like a pot (Figure 1.9) surrounded by four mountains of Anatolia Plateau with an altitude of 850-1000 meters. These mountains are: Karyağdı on the north, İdris on the east, Elmadağ on the south and southeast and Çal on the southwest.

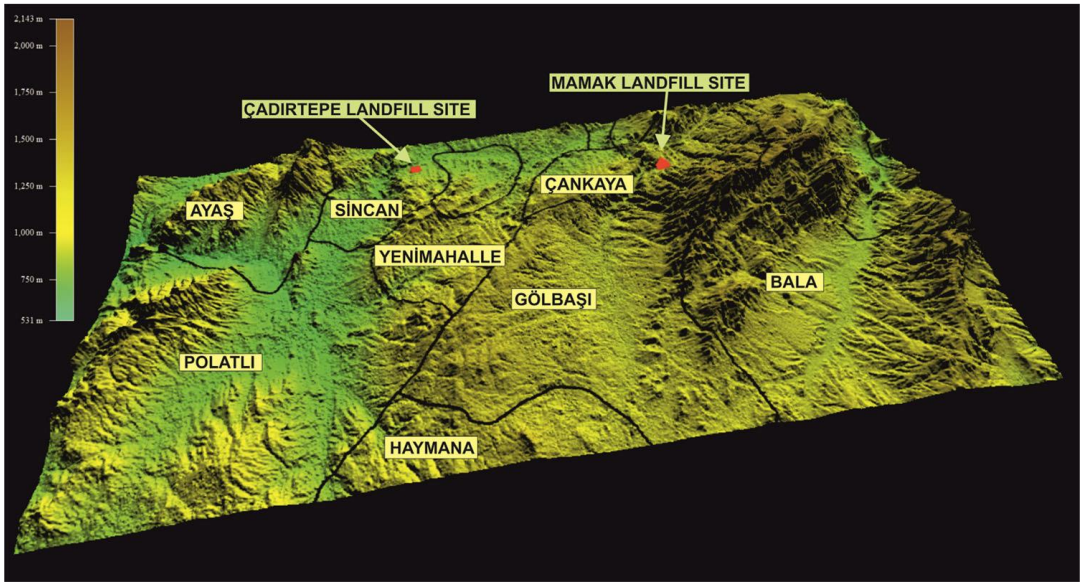

Figure 1.9. 3D view of the digital elevation model (DEM) (Yal and Akgün, 2014).

Between these mountains three rivers run. Çubuk creek between Karyağdı and İdris mountains, Bent Stream between Elmadağ and İdris Mountains and finally İncesu creek between Elmadağ and Çal mountains; these rivers come together between Karyağdı and Çal mountains and flow into Sakarya River as Ankara stream. A population of 5.3 million people (TÜİK, 2016) are living in the capital Ankara and 88% of the population lives in the city center (Governorate of Ankara, 2018).

Ankara is generally known for its twentieth century development as the designed capital of the newly-born Turkish nation-state and the city's growth at the beginning

displayed a typical example of modernization efforts of a nationalist government. The second half of the century compared to the first years, witnessed the uncontrollable expansion and transformation of the city with expanding squatter areas due to heavy migration. Then, the city shaped by urban regeneration projects in the last decades (Batuman, 2013).

Etimesgut District is a district with a total area of 10,153 hectares, located by the Ankara-Sincan highway and by the Ankara Istanbul railway, from 17 km west of the capital Ankara. It is surrounded by Sincan on the west and Yenimalle on the north, south and east. Etimesgut, one of the eight central districts of Ankara Metropolitan, is surrounded by important State Roads. Ankara-İstanbul highway passes through east to the north, Ankara-Eskisehir highway passes through east to the south direction, also the highway (circle freeway) which connects these two roads passes through the west of the city. Also Ankara-Istanbul Railway passes through the centre of district and has 6 subway stations. A military airport (12th Air Base) is located within the boundaries of the district. Etimesgut District is a bowl-shaped valley with a decreasing gradient from east to west. Situated at the base of the valley, the Ankara plain is integrated with the side valleys extending from the top of the hill towards the Ankara Stream and the average elevation is 807 meters (Governorship of Etimesgut, 2018). The pilot study area, which is a heavy maintenance and repair facility for high speed trains, is located in Etimesgut. This area is mostly flat and has an average altitude of 796 meters above Mean Sea Level. The rail service maintenance plant is border with the Ankara River on the northern side, with the existing railway on the southern side line, with the Sugar Factory on the eastern side, and with the E89 road on the western side. The new rail service maintenance plant is located approximately 20 km west of the centre of Ankara.

1990-1998 Period Greater Ankara Sewerage and Stormwater Project (Project BAKAY) and 2006-2007 Period Ankara Central Districts Wastewater and Stormwater Networks Systems Project are the recent and major projects considering the current stormwater network in Ankara. The scope of the BAKAY Project is Detail design for wastewater and stormwater networks, collectors and interceptors to

meet the demand of Ankara where is the capital of Turkey and has 5.500.000 population estimate for the target years of 2025, preparation of the technical specification, pre-qualification and tender documents in accordance with the world bank procedures, evaluation of pre-qualification and bids, contract documents, supervision of construction works and the scope of Ankara Central Districts Wastewater and Stormwater Networks Systems Project is preparation of the detail design for wastewater and stormwater system, river rehabilitation and Wastewater Treatment on the street and avenue in Altındağ, Çankaya, Etimesgut, Gölbaşı, Keçiören, Mamak, Yenimahalle, Sincan districts within the border of Ankara Metropolitan Municipality. Ankara Central Districts Wastewater and Stormwater Networks Systems Project was designed as a separate system (stormwater and wastewater). For the residential centers, only problematic areas are considered for stormwater network and for the rest, free flow is allowed. Considering the stormwater network design in above mention project; Kutter's formula and Rational Method is used for the design of stormwater network system. The time of concentration is chosen 15 minutes and 15 minutes storm duration with 2 years return period rainfall is chosen as the design intensity input. In stormwater channels concrete and reinforced concrete pipes were used. Minimum pipe diameter was chosen 400 mm and percent fullness of pipe (maximum capacity ratio) is chosen 90% in the pipes. Minimum flow velocity employed in the pipes is 0.40 m/s and the maximum is 4.00 m/s. Minimum depth from the ground surface to the top of pipes is 1.40 mt. Due to residential distribution and settlement type in the basins, an average runoff coefficient (C) were calculated for each basin. Topographic information is used at the designation of the basins. Stormwater network is directed to the low elevation areas with collectors and discharged to the creeks/streams (S. Nasuhbeyoğlu, personal communication, March 28, 2018).

Stormwater network of a Railway Maintenance Complex located in Etimesgut Province Ankara as a specific critical infrastructure has been selected as pilot study area. The results of climate change and land use change analysis that are also performed in this study applied to the existing stormwater network of this area. The stormwater network of the pilot study area consists of drainage channels and

drainage manholes. The drainage manholes are connected by circular pipes; the drainage channels and the circular pipes discharge the flow in two main sewer pipes, in an existing sewer, or in the ditches.

1.3. RESEARCH QUESTION AND PROBLEM STATEMENT

Even though floods do not appear with the catastrophic power of other natural hazards, such as earthquakes, their overall impact on society and the economy is very serious (Papagiannaki et al., 2015). In the last 20 years, flooding, heavy rainfall and flash flooding caused various damages. The settlements, agricultural products, environment, people, animals, transportation, cultivated farmland and vehicles are damaged because of flooding, heavy rain fall, flash flooding and storm in Ankara, the Capital of Turkey (Supplementary Document of Official Letter of SMS, 2017a). Climate variability affect the naturel environment from two dimensions: the long term trend of average climate variables may be altered or fluctuations may have a wider ranges which result in changes in the statistical characteristics of climate variables (IPCC, 2013; Yuan et al., 2017).

In this study extreme precipitation and land use properties of Ankara is investigated by using observed (1950-2015) and future (2015-2098) precipitation data together with (1959-2013) land use/cover data of Ankara. Projected precipitation data is disaggregated to finer scales and Generalized Extreme Value (GEV) is used to analyse observed and future data considering the stationary and nonstationary models. The effect of changing climatic and land use/cover conditions are studied and the results are applied for a newly built stormwater network of a pilot study area in Etimesgut, Ankara. Performance of the system investigated under current and changing conditions and different approaches such as stationary and nonstationary assumption.

1.4. AIM OF THE STUDY AND OBJECTIVES

Climatic and land use/cover conditions are investigated for Ankara in general and stormwater network of railway critical infrastructure located in Etimesgut is selected

as the pilot study area to apply the results. The main goal of this study is to incorporate climate change into urban stormwater network design by using stationary and non-stationary GEV models for extreme rainfall analysis together with land use/cover change and urbanization data. The research objectives in reaching this main goal are presented as follows:

- Disaggregate daily future projections to finer scales.

- Investigate superiority of nonstationary GEV models to stationary GEV models for observed and future precipitation data.

- Calculate return level values; the value expected to be exceeded on average once every interval of time; for observed and future period rainfall with stationary and nonstationary GEV models.

- Analyse of land use/cover change between 1950-2013 period in order to show the long term chances in the permeability at the surface due to urbanisation for Ankara in general.

- Calculate a composite runoff coefficient for the pilot study area.

- How these changing climatic and land use/cover conditions will impact a current stormwater network in the pilot study area?

CHAPTER 2

METHODOLOGY

2.1. INTRODUCTION

Observed (1950-2015) annual maximum precipitation data (height in mm) were acquired from State Meteorological Service for sub-hourly and hourly storm durations. These observed time-series data sets were used directly in the analysis. Additionally, daily projected (2015-2099) precipitation and temperature data sets acquired from SMS (Supplementary Document of Official Letter of SMS, 2017b). Since daily time scale is relatively a large scale and low resolution for design practices; rainfall disaggregation, which is obtaining small scale-high resolution (eg. hourly, sub-hourly) rainfall using their low resolution (eg. daily, monthly) rainfall values is used. Daily projections of rainfall were disaggregated into finest scale (5 minutes) and then aggregated to next analysis time scales (10, 15 minutes and 1, 6 hours) and these values used in the analysis as well. Moreover land use/cover analysis conducted by using the digitized data of maps that were obtained from General Command of Mapping for Ankara and Maps acquired from State Railways for the pilot study area.

The precipitation and land use/cover analysis results were then applied to the pilot study area stormwater network. GEV stationary and nonstationary models were constructed and return level vs. return period results were obtained for the observed and future data. The return level value is defined as a value that is expected to be equalled or exceeded on average once every interval of time (t) (with a probability of 1/t) so t is the return period (Gavidel and Rickli, 2015). Urban transformation of Ankara in general is investigated by using maps of late 1950s, early 1980s, mid

1990s and 2013. Composite runoff coefficient is calculated for Pilot Study area by using the weighted average of land use/cover types.

2.2. STUDY AREA

Precipitation analysis is conducted for the capital city of Ankara, which is a highly urbanized city. A population of 5.3 million people (TURKSTAT, 2016) are living in the capital Ankara, 88% of the population lives in the city centre. The information obtained from the analyses is transformed and applied to test the runoff and hydraulic performance of an actual stormwater network of a Railway Maintenance Complex (Figure 2.1) located in Etimesgut Ankara Province as a specific critical infrastructure (Turkish State Railways, 2018).

Figure 2.1. Railway Maintenance Complex in Etimesgut-Ankara

The study area is mostly flat and has an average altitude of 796 meters above Mean Sea Level. The rail service maintenance plant has border on the northern side with the Ankara River, on the southern side with the existing railway line, on the eastern side with the Sugar Factory, and on the western side with the E89 road. The new rail service maintenance plant is located approximately 20 km west of the centre of Ankara, the capital of Turkey. The stormwater network of this area consists of drainage channels and drainage manholes. The drainage manholes are connected by circular pipes; the drainage channels and the circular pipes discharge the flow in two main sewer pipes, in an existing sewer, or in the ditches. In addition to these

solutions, some ditches have been included in the project to protect the rail service maintenance plant and the road. In these ditches is also conveyed part of the rain water of the rail service plant. The stormwater network cover a 342,000 m2 basin which is divided into 38 sub basins for the calculations. Single runoff coefficient is applied to the basin which is equal to 0.80. Kutter formula is used to calculate the velocity of the discharge. The stormwater network used for the calculations consist of 218 separate pipes in various length and size. For the calculations rainfall height is converted to l/sec/ha and used to calculate the peak runoff.

2.3. DATA COLLECTION AND ANALYSIS - PRECIPITATION

The annual maximum precipitation data of 5, 10, 15, 30 minutes and 1, 2, 3, 6 hour for 1950-2015 period for Ankara province is obtained to conduct data analysis for the observation period. This data is officially acquired from State Meteorological Service (SMS).

Daily precipitation projection data from SMS is reanalysed for future extreme value analysis. Table 2.1 shows the location of meteorological stations and nearest projection grids to these stations as well as their altitudes. The data consists of daily projections covering 2015-2099 period however because of missing data for 2099, 2015-2098 period is used for the analyses. Also, 1971-2000 is chosen as model validation period. Three global climate models (GCM) are used; namely HadGEM2-ES, MPI-ESM-MR and GFDL-ESM2M. These models are operated with the RCP 4.5 and RCP 8.5 emission scenarios. A fine scaled regional climate model (RCM) coupled to these GCMs and provide the outputs.

Table 2.1. Projection Data Stations & Grids (SMS, 2017b)

No	Station	Grid	Station			Grid		
			Latitude	Longitude	Altitude mt	Latitude	Longitude	Altitude mt
17129	**ETİMESGUT HAVALİMANI**	**2733**	39,9558	32,6854	806	39,9661	32,6608	1028
17131	**ANKARA GÜVERCİNLİK HAVALİMANI**	**2733**	39,9343	32,7387	820	39,9661	32,6608	1028

Rainfall/frequency analysis is conducted for daily projections of three model and two scenarios of grid no 2733 for the projection (2015-2098) period. However, daily temporal resolution from projection data is not well suited for the extreme value analysis. Urban flash flooding is caused by heavy rainfalls over short durations such as in a few minutes to hours therefore it is essential to analyse extreme rainfalls for shorter durations such as sub-daily or sub-hourly. For this reason daily RCM output data is disaggregated to finer time scales such as hourly and sub-hourly to use future projections for extreme value analysis (Kossieris et al., 2016a). For the disaggregation process; temporal stochastic simulation of rainfall process at high resolution (fine time scales), based on the Bartlett-Lewis rectangular pulse model (Kaczmarska et al., 2015; Ritschel et al., 2017) is used.

Stationary and nonstationary rainfall return levels (in mm) for return periods 2, 5, 10, 20, 25, 50, 100, 200 years are derived for observed (1950-2015) and projected data (2015-2098) for extreme rainfall time series of the sub-hourly and hourly annual maximum data.

The methodology of precipitation analysis in this study consists of;

(1) Projected data is disaggregated into finest scale (5 minutes) and then it is aggregated to next analysis time scales (10, 15, and 30 minutes) because each run generates rainfall depths that are independent from the other runs and subsequently the data at higher time scales may be inconsistent.

(2) Trend analysis is carried out for observed and projected data.

(3) Stationary GEV (St) models are developed; return levels are derived for desired return periods considering single and multi-time periods for observed and projected data.

(4) Non-stationary GEV (NSt) models are developed; return levels are derived for desired return periods for observed and projected data.

A general framework for rainfall analyses used in this study can be seen in Figure 2.2.

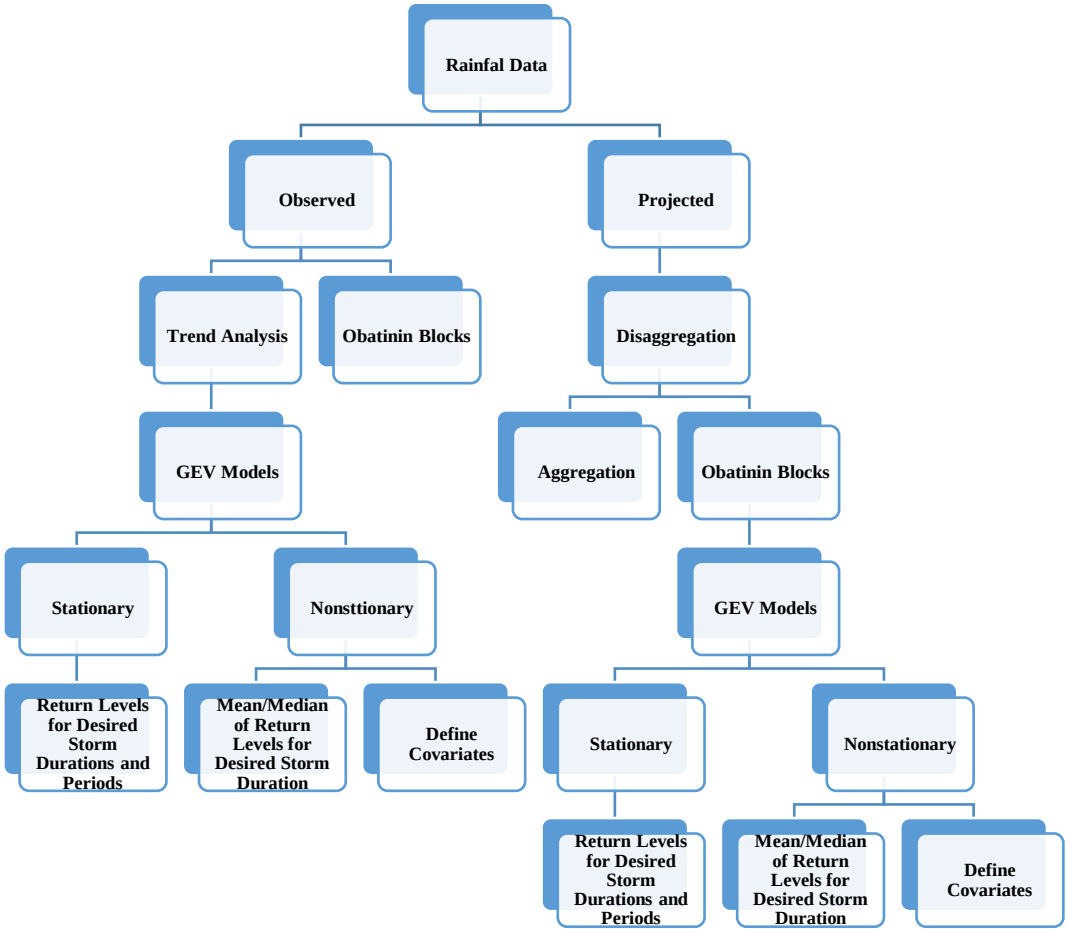

Figure 2.2. Rainfall Data Analyses Framework

2.3.1. Disaggregation

Assessment of climate change impact on hydrological systems requires finer temporal resolution at hourly or less particularly for extreme events occurring in a small-scale area however climate change projection results from GCM/RCM couplings cannot be directly used for the impact studies (Yucel et al., 2016, Abdellatif et al., 2013). Rainfall intensity is one of the main input variables in many hydrological analyses and modelling. Unfortunately, reliable records are available at coarse intervals such as yearly, monthly or daily and rainfall data is generally low

quality. Short interval rainfall records are limited due to the high cost and insufficiency of reliable measurement and the monitoring systems (Harisaweni and Fadhilah, 2016). In this context, disaggregation can be employed to take the advantage of using long term data which exist in low resolution or larger time scales such as daily or above (Kossieris et al., 2016b).

Daily projected precipitation data first disaggregated to 5 minutes duration and then for the use of GEV analyses aggregated to 10, 15 minutes and 1, 6 hours storm duration. A complete software package for the temporal stochastic simulation of rainfall process at fine time scales which is developed in the R programming environment, HyetosMinute, is used to prepare daily data for extreme value analysis and used for the disaggregation process in this study. Disaggregation is based on the Bartlett-Lewis rectangular pulse model (Kossieris et al., 2016a; Kossieris et al., 2016b; Kossieris et al., 2012) which provides temporal stochastic simulation of rainfall process at fine time scales.

The Bartlett–Lewis Rectangular Pulses (BLRP) model is used in many studies to disaggregate daily observed rainfall to finer scales and belongs to the general category of Poisson-cluster models that simulate rainfall events via clusters of rectangular pulses that occur in continuous time (Rodriguez-Iturbe et al., 1987a , 1987b; Abdellatif et al., 2013; Ritschel et al., 2017; Villani et al., 2016).

The initially proposed model has 5 parameters denoted with λ, β, γ, η, and μX (Lu and Qin, 2012; Villani et al., 2016). To enhance the model's flexibility in generating a greater diversity of rainfalls, parameter η is randomly varied from storm to storm according to the gamma distribution with a shape parameter α and a rate parameter v so the Random Parameter Bartlett-Lewis Rectangular Pulse Model (BLRPR) can have 6 parameters: $\{\lambda, \alpha, \nu, \kappa, \varphi, \mu X\}$, which is the preferred model in this study. (Rodriguez-Iturbe et al., 1987a; Kaczmarska et al., 2015; Kossieris et al., 2016a). In order to calculate model parameters for this study, an enhanced version of the evolutionary annealing-simplex optimization method is used (Kossieris et al., 2016b; Rozos et al., 2004; Efstratiadis and Koutsoyiannis, 2002). Mean, variance,

covariance and probability of dry days are used as historical statistics for the objective function of the desired time scale (in this case five minutes). It is stated that the distribution of the maximum rainfall depths/heights can be better derived if the inter-annual variability of monthly statistics is incorporated in the parameter estimation process of the model. Therefore in this study only the historical daily parameters are used for the optimization process and to make an adequate estimation every month is calculated separately and then combined by year. In the end, a set of parameters are obtained for implementation in disaggregation.

2.3.2. Trend Analysis

The statistical tools that provide trend tests to detect time series' trends are commonly divided into two: Parametric and non-parametric methods and non-parametric tests are said to be more appropriate for hydro-meteorological time series data, which are generally non-normally distributed and censored (Yilmaz and Perera, 2014).

Mann-Kendall (MK) trend test is one of the non-parametric tests for trend detection and is used to detect the trends of precipitation time series in this study. MK test is a rank based tests which have been commonly applied to hydrometeorological time series data to detect trends (Yilmaz and Perera, 2014; Cheng and AghaKouchak, 2014; Onyutha et al., 2015). The purpose of the Mann-Kendall (MK) test (Mann, 1945, Kendall, 1975, Gilbert, 1987) is to statistically detect if there is a monotonic upward or downward trend over time for the corresponding variable.

Although normally distributed data assumption is not applicable for MK test, data independency remains as an assumption and the presence of serial dependence increases the probability of rejecting the null hypothesis (no trend) (Yilmaz and Perera, 2014; Helsel and Hirsch, 2002). So, autocorrelation of data is checked before using them in MK test for detection of trends.

Time series behaviour is not only detected for entire period but also multi period analysis is carried out. Therefore any significant change points for the time series are

investigated. Climate change, anthropogenic activities, and observational errors in monitoring, change in recording methodology or use of different equipment can be the reason of occurrence the change point. It is possible to detect change point in a time series visually from time series graphs; however it is useful to employ a statistical approach for this purpose (Yilmaz and Perera, 2014). In this study Petitt's change point test is also applied to time series (Kundzewicz and Robson, 2004).

2.3.3. Extreme Value Analysis: Stationary & Nonstationary

Recently, climatic extremes have widely been subject of many studies at various spatial and temporal scales (Wehner et al. 2018; Busuioc et al. 2015; Zscheischler et al., 2018; Ekström et al., 2018; Gilleland et al., 2016). There are several approaches to simulate the frequency of extreme events, these being (1) parametric, (2) non-parametric, (3) stochastic methods and (4) Extreme Value (Goldstein et al., 2003).

Extreme Value Analysis (EVA) is a tool used commonly for investigating meteorological extremes (e.g. Scotto et al., 2011; Vahedifard et al., 2017; Cheng et al., 2015; Fix et al., 2018). Extreme value theory (EVT) is concerned with the statistical properties of the tails of distributions and by providing the necessary methods to estimate the distribution of the extremes of a time series (Umbricht et al., 2013). By this way quantification of the return values and return periods of extreme events become possible.

Extreme Value Theory (EVT) uses probabilistic distribution functions such as Generalised Extreme Value (GEV) or Generalised Logistic (GL) function to annual maximum (AM) series or Generalised Pareto Distribution (GPD) function which is fitted on peak-over-threshold (POT) series (Collet et al., 2017). GEV distribution function is used in the present study to fit the observed and future precipitation data. The methodology is widely used in engineering applications that need an assessment of extreme environmental conditions (Coles and Sparks, 2006).

The generalized extreme value (GEV) distribution function has theoretical justification for fitting to block maxima (maxima of long blocks of data, e.g., annual maximum values of daily precipitation height) of data. The GEV df is given by (2.1);

$$G(z) = \exp[-\{1 + \xi\left(\frac{z-\mu}{\sigma}\right)\}_{+}^{-\frac{1}{\xi}}] \quad (2.1)$$

where y+ = max{y, 0}, $\sigma > 0$ and $-\infty < \mu, \xi < \infty$ (Coles 2001).

Equation 2.1 covers three types of df's depending on the sign of the shape parameter, ξ. The heavy-tailed Fréchet df results from $\xi > 0$, and the upper bounded Weibull df when $\xi < 0$. The Gumbel type is obtained by taking the limit as $\xi \rightarrow 0$ (Gilleland and Katz, 2016). Brief description of GEV distributions can be seen in Table 2.2.

Table 2.2. Description of GEV Distributions (Pinheiro and Grotjahn, 2015).

	GEV
Description	Distribution function of standardized maxima (or minima)-block maxima/minima
Parameters	Location μ: position of the GEV mean
	Scale σ: multiplier that scales function
	Shape ξ: Parameter that describes the relative distribution of the probabilities.
General function	for extreme value z, $G(z) = \exp[-\{1 + \xi\left(\frac{z-\mu}{\sigma}\right)\}_{+}^{-\frac{1}{\xi}}]$
Limit as; ξ→0 ξ>0 ξ<0	 Gumbel Fréchet Weibull
Interpretation of results	Return level: value z_p that is expected to be exceeded on average once every 1/p periods,

The block maxima (BM) approach aims to describe the probability distribution of the maxima of a block. In the block maxima approach, equal length of blocks are selected and maximum values from each block are determined and subsequently the GEV distribution is fitted to the obtained maxima series to estimate the exceedance

probability (p), calculate return period (1/p) and its return level z_p. The size of the block is important because the distribution of the maximum series of the parent distribution may not converge to the GEV distribution as expected for the block maxima approach because of small number of blocks and block size caused biases and errors (Wang et al., 2016; Cai and Hames, 2010; Umbricht et al., 2013). Yearly maximum time series generated from 1950-2015 and 2015-2098 periods provide time series that are relatively long enough in this study.

The GEV distribution has three parameters including location (μ), scale (σ) and shape (ξ) parameters. Yilmaz and Perera (2014) indicate that Maximum Likelihood Estimation (MLE) method is a preferred method for parameter estimation of nonstationary models due to its suitability for incorporating nonstationarity into the distribution parameters as covariates, is also the preferred parameter estimation method in this study. R package extRemes is used for the analysis. It is a suite of functions for carrying out analyses on the extreme values of a process of interest (Gilleland and Katz, 2016, Gilleland, 2016).

First for the stationary case and the non-stationary case, extreme value analysis is applied. Estimated distribution parameters, standard error estimates, estimated parameter covariance matrix and model performance criteria results are computed.

Non-stationarity can occur either as a gradual trend or a sudden shift (Bayazit, 2015). Time (and other covariates) variant/dependent parameters are used to capture the non-stationarity of the time series (Pohlert, 2016; Gül et al., 2014). It is a common practice to incorporate time dependency into the location parameter of the GEV distribution to investigate how extremes are changing in time (Yilmaz and Perera, 2014; Cheng and AghaKouchak, 2014). Nonstationarity can also be expressed incorporating time dependency by scale parameter. On the other hand it is not a realistic attempt to estimate the shape parameter as a function of time because it is difficult to estimate the shape parameter precisely when it is time dependent (Coles, 2001).

For non-stationary case, the location parameter and/or scale parameter are set to be a function of time or other variants such as annual precipitation or temperature. Different combinations for nonstationary cases are tested and compared to find out the best fitted model among stationary and nonstationary models. In the present study, all model parameters set constant for the stationary case, and location and/or scale parameters assumed to be a function of time and/or temperature for the nonstationary case. The non-stationary models that describe each of these cases with their developed parameters are explained in Table 2.3.

Table 2.3. Non-stationary models with time and covariate (temperature) dependent location and scale parameters

Model	Location	Scale	Shape
NStGEV1	$\mu t = \beta 0 + \beta 1 t$	σ (constant)	ξ (constant)
NStGEV2	$\mu t = \beta 0 + \beta 1 t$	$\sigma t = \beta 0 + \beta 1 t$	ξ (constant)
NStGEV3	μ (constant)	$\sigma t = \beta 0 + \beta 1 t$	ξ (constant)
NStGEV4	$\mu t = \beta 0 + \beta 1$temperature	σ (constant)	ξ (constant)
NStGEV5	$\mu t = \beta 0 + \beta 1 t$	$\sigma t = \beta 0 + \beta 1$exp(temperature)	ξ (constant)
NStGEV6	$\mu t = \beta 0 + \beta 1$exp(temperature)	$\sigma t = \beta 0 + \beta 1$exp(temperature)	ξ (constant)
NStGEV7	$\mu t = \beta 0 + \beta 1$exp(temperature)	σt = (constant)	ξ (constant)
NStGEV8	μ (constant)	$\sigma t = \beta 0 + \beta 1$temperature	ξ (constant)

2.3.4. Goodness of Fit

Performance of fitted models is inspected by goodness-of-fit indicators such as, Akaike Information Criterion (AIC), Bayesian Information Criterion (BIC), the likelihood-ratio test, and Negative Log-Likelihood (NLL) (Šraj et al., 2016; Cheng, 2014; Wang and Lui, 2006; Sienz et al., 2010; Umbricht et al., 2013). Goodness of fit of the GEV models is determined based on these statistical tests.

Both AIC and BIC are capable of model selection and were designed to be used with maximum likelihood estimates which is the parameter estimation method in this study; AIC is good at finding appropriate predictive models, BIC was developed primarily for model averaging and is good for small sets of well-justified models (Wang, and Liu, 2006; Hooten and Hobbs, 2015).

Similar to ordinary least squares, the negative of the log-likelihood is used to determine the most likely value of the parameter and it is the one that makes the negative log-likelihood as small as possible; thus, the maximum likelihood estimate is equal to the minimum negative log-likelihood estimate (McGarigal, 2017).

Additionally, the likelihood-ratio test was performed to test whether the inclusion of the covariates into the stationary model provide significant improvement among nested models (stationary and its corresponding nonstationary model) (Coles, 2001; Gilleland and Katz, 2011; Šraj et al., 2016).

2.4. DATA COLLECTION AND ANALYSIS - LAND USE/COVER CHANGE

Impervious surfaces are generally human-made (such as buildings, roads) and pervious surfaces include vegetation, water bodies, and bare soil. During the data acquisition processes, these areas had been transferred to the digital medium as it is in the original. (Özkil, 2015).

Maps produced by the General Command of Mapping (GCoM) were analysed as the most suitable data set by Özkil (2015). Since it is examined as a subject of national security, maps had been acquired from the Military by special consent for scientific research (Regarding this, none of the maps that have been presented in this study can be used or reproduced without permission of concerning bodies). It has been identified that there are 4 different versions of maps covering the area of interest, available in the GCoM archives. They represent late 50s, early 80s, mid 90s and lately the year of 2013.

Initially, the classification of land is done by extracting the image bands with the pixels grouping to each image segment. Classification (e.g. urban area, green area, soil, road etc.) is performed based on the land use conditions. Polygons are created in advance during the digitizing process and then appropriate projection system is defined for that polygons to calculate the geometry. Finally, urban and green areas (impervious and pervious surfaces) are calculated as the surface area per parcel.

The methodology of land use/cover analysis in this study consists of;

(1) Data digitalized and classified as urban and green area and also transportation networks such as, road, rail, etc. for Ankara

(2) Area of urban and green and length of road network computed in ArcGIS for Ankara

(3) Change and trend of urban and green area together with road network is investigated for Ankara; a potential development rate and developable part of the pilot study area assessed

(4) Land use/cover types of pilot study area is calculated for Pilot Study area

(5) Composite runoff coefficient is calculated for Pilot Study area

2.5. DERIVATION OF DESIGN PARAMETERS FOR THE STORMWATER NETWORK OF PILOT STUDY AREA

Rational formula is used to for the recalculation the peak runoff of pilot study area stormwater network. The rational method makes the basic assumption that the peak rate of surface outflow from a given watershed is proportional to the watershed area and average rainfall intensity over a period of time just sufficient for all parts of the watershed to contribute to the outflow (Burke, T. and Burke, B., 2015). The rational formula is written as: Q=CIA, where Q is the peak runoff, C (runoff coefficient), is the ratio of peak runoff rate to average rainfall rate over the watershed during the time of concentration, I is the rainfall intensity and A is the contributing area of watershed under consideration (TDT, 2016; Burke, T. and Burke, B., 2015).

Use of the rational method includes some assumptions and limitations that makes it relatively easy to apply but also limits its application area. The limitations and assumptions are as follow for the rational method:

to apply the method, time of concentration for the drainage area must be less than the duration of peak rainfall intensity, runoff is directly proportional to the rainfall intensity and rainfall intensity is uniform throughout the storm duration. The frequency of occurrence for the peak discharge is the same as the frequency of the rainfall producing that event, rainfall is distributed uniformly over the drainage area. The minimum duration to compute the rainfall intensity is 10 minutes and if the

calculated T_c is less than 10 minutes, then 10 minutes should be adopted for rainfall intensity computations. The rational method does not consider any storage in the area. Because of the assumptions and limitations, the rational method is applied to watersheds 200 acres (80 hectares) or smaller (TDT, 2016).

The following procedure is used to apply the Rational Method (TDT, 2016; Burke, T. and Burke, B., 2015). Step 1: Define contributing area A (acres or hectares). Step 2: Estimate the runoff coefficient due to land use/cover. If the land use is mixed, calculate a composite runoff coefficient Step 3: Determine the time of concentration. Step 4: Determine the intensity and return period. An intensity-duration-frequency curve can be used to identify intensity for the storm duration equal to the time of concentration and selected return period. This is then multiplied by the area and runoff coefficient to determine the peak discharge rate. Parameter derivation for rational method is conducted as presented in Figure 2.3.

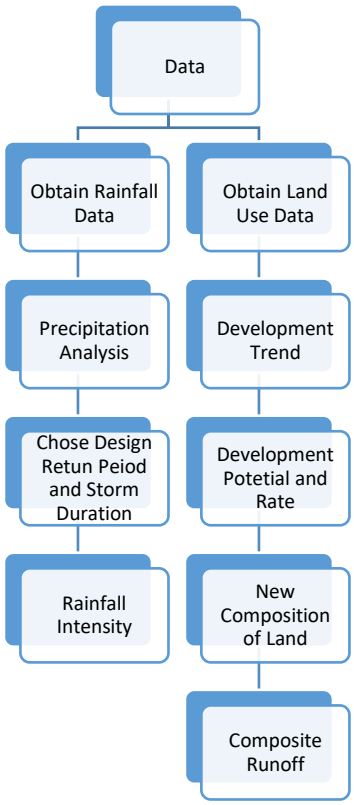

Figure 2.3. Parameter Derivation for Rational Method

Data from observation and projection period precipitation analyses results are used to calculate the rainfall intensities to calculate the peak discharge. Rainfall intensity at a duration equal to the time of concentration (T_c) is used to calculate the peak flow in the Rational Method. Time of concentration and return period is chosen 15 minutes and 2 years respectively according to design standards of General Directorate of Ankara Water and Sewage Administration (AWSA) and the design values used for the baseline (current) stormwater network. For the calculations, rainfall heights or intensity are converted to l/sec/ha and used to calculate the peak runoff. Return level values (in mm) are first converted to mm/minutes and then to l/sec/ha in this study. This is then multiplied by the area and runoff coefficient to determine the peak discharge rate. Moreover the 15 minutes - 5 years storm depths were also used for the performance analysis of baseline storm sewer design. Kutter formula is used to calculate the velocity of the discharge.

In the pilot study area, there are several type of cover such as building (roof), parking lot, asphalt, slab on grade (concrete), bituminous sub-ballast, etc. These cover types have different range of runoff coefficients (TDT, 2016; Burke, T. and Burke, B., 2015) not only related with the material but also related with the slope of the cover. Where a drainage area is composed of subareas with different runoff coefficients, then the summation of the products of corresponding runoff coefficients and subareas divided by the total area and a composite coefficient for the total drainage area is computed. In order to find a better runoff coefficient both current land use type and the potential development of the undeveloped area are considered that is applicable to entire area and a composite runoff coefficient is calculated by using weighted average of the current and future land cover types.

CHAPTER 3

CLIMATE CHANGE AND ALTERATIONS IN THE PRECIPITATION REGIME: OBSERVATIONS IN ANKARA PROVINCE

This chapter presents the development of stationary and nonstationary models, based on block maxima of sub-hourly and hourly storm durations, to investigate the return level and return period of extreme rainfall events. Stationary and nonstationary models are applied to a 5-10-15-30 minutes and 1-2-3-6 hours observed (1950-2015) annual maximum storm durations for Ankara province. Several variables such as temperature, time are tried to be incorporated into non-stationary models as covariates to capture the changes in extreme precipitation characteristics. If a statistically significant trend in time series is detected then it is accepted that the assumption of stationarity is violated in this study. However, time series that did not present significant trend also revealed superior results in terms of nonstationary models.

Storm durations that used for stationary and nonstationary models can be seen in Figure 3.1 and Figure 3.2. The model names that are derived from stationary and nonstationary models with various storm durations are abbreviated for convenience and to avoid confusion. For instance Nonstationary model results for 30 minutes storm duration is abbreviated as NstThirtyMin or stationary models 3 hours storm duration can be found as StThreeHour in the text.

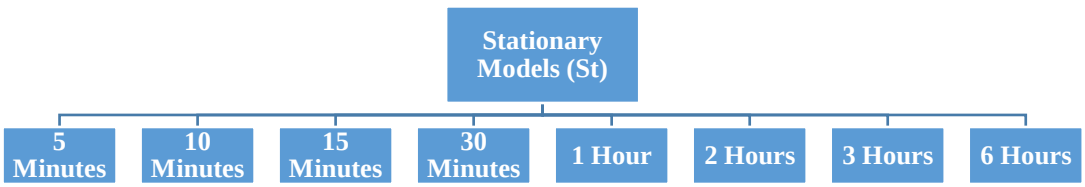

Figure 3.1. Storm Durations Used for Stationary Models

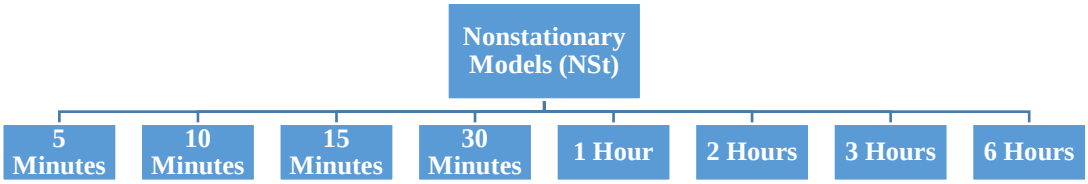

Figure 3.2. Storm Durations Used for Nonstationary Models

3.1. TREND AND CHANGE POINT TESTS

Trend tests are used to figure out if a time series has an increasing or decreasing trend. Visual inspection is an alternative to make rough inferences but for reliable determination, especially with complex variations and long term series, statistical tests are needed. Figure 3.3 and Figure 3.4 demonstrate the trend for observed sub-hourly (5-10-15-30 minutes) and hourly (1-2-3-6 hours) time series annual maximum rainfall intensities with a linear trend line between 1950-2015 period. It can be inferred that simple linear trend line visually indicate the downward (decreasing) trend.

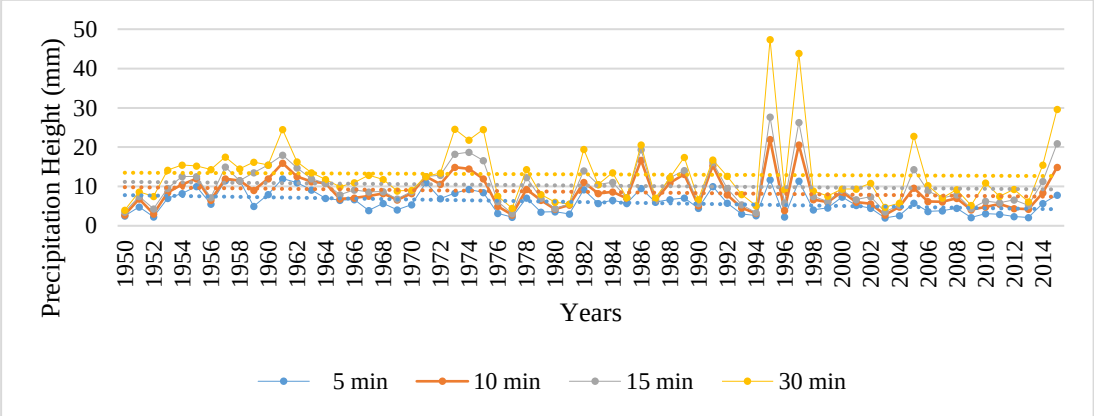

Figure 3.3. Sub-Hourly Time Series Trend

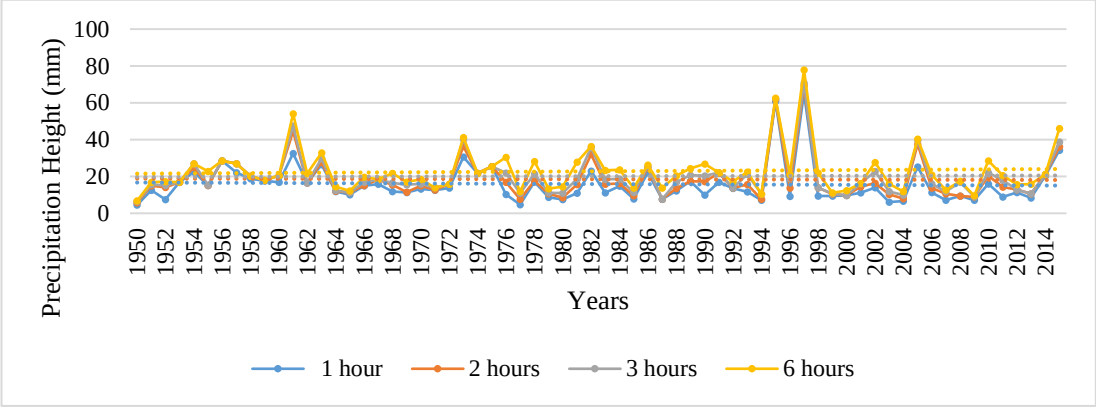

Figure 3.4. Hourly Time Series Trend

Time series for all storm durations, Mann Kendall Trend test is applied and results are shown in Table 3.1. Subsequently, together with trend test, change point detection is conducted by Pettitt test and stationary models were derived for two time periods that are decided based on the change point test results. Trend test and change point results, according to Mann-Kendall and Pettitt Test for all durations are shown in Table 3.1. Bold ones indicate significant change point and/or trend for 0.05 and 0.10 significant level. Trends in short (in particular sub-hourly) and long storm durations are largely different in terms of statistical significance but not in direction. According to MK statistics; the null hypothesis that there is no trend is rejected for the 5-10-15-30 minutes and 1-2 hours time series and the results suggest that there is significantly a downward monotonic trend between 1950-2015 periods.

Table 3.1. Pettitt Test and Mann-Kendall Results for the Storm Durations

Storm Duration	**Probable Change Point**	**Change Point Statistic**	**p-Value**	**MK Statistic**	**p-Value**
5 Minutes	**43**	**K = 391**	**0.01754**	**tau = -0.260**	**0.0021616**
10 Minutes	**26**	**K = 368**	**0.05604**	**tau = -0.187**	**0.027951**
15 Minutes	**26**	**K = 340**	**0.09958**	**tau = -0.143**	**0.091372**
30 Minutes	**26**	**K = 363**	**0.0877**	**tau = -0.148**	**0.080262**
1 Hour	**26**	**K = 402**	**0.04548**	**tau = -0.189**	**0.025699**
2 Hour	**27**	**K = 299**	**0.2373**	**tau = -0.136**	**0.10726**
3 Hour	48	K = 210	0.6805	tau = -0.0565	0.50656
6 Hour	49	K = 189	0.8359	tau = -0.0266	0.75662

As seen in the Table 3.1, there is an important difference between short and long storm duration time series data for the change point results. On the other hand for the majority of the storm durations change point is constructed around mid-1970s so it is decided to derive models for 1950-1975 and 1976-2015 periods.

3.2. STATIONARY AND NONSTATIONARY ANALYSIS – OBSERVED PRECIPITATION DATA

3.2.1. Stationary Analysis – Observed Precipitation Data

In Table 3.2 and Figure 3.5, return level estimates for 2-5-10-20-25-50-100 and 200 year return periods between 1950-2015 years are represented for all annual maximum time series with stationary approach. Stationary return levels (mm) vs. return periods considering 1950-1975 and 1976-2015 periods for 2-5-10-20-25-50-100 and 200 year return periods are compared (% change) with 1950-2015 whole period respectively for all annual maximum time series with stationary approach and represented in Table 3.3 and Table 3.4.

Table 3.2. Stationary (St) Return Levels (mm) vs. Return Periods (1950-2015)

Model	2-year	5-year	10-year	20-year	25-year	50-year	100-year	200-year
StFiveMin	5.54	8.14	9.82	11.39	11.88	13.38	14.84	16.26
StTenMin	7.72	11.48	14.13	16.83	17.71	20.53	23.47	26.56
StFifteenMin	8.95	13.60	17.12	20.86	22.13	26.32	30.90	35.95
StThirtyMin	10.90	17.09	22.31	28.36	30.53	38.08	47.06	57.77
StOneHour	12.91	20.49	27.10	34.97	37.84	48.00	60.39	75.57
StTwoHours	15.36	23.51	30.52	38.76	41.74	52.20	64.83	80.10
StThreeHours	17.18	25.62	32.57	40.48	43.28	52.91	64.17	77.38
StSixHours	19.97	29.04	36.13	43.87	46.54	55.47	65.50	76.79

Stationary (St) models are derived for sub-hourly (5-10-15-30 minutes) and hourly (1-2-3-6 hours) time series annual maximum rainfall heights (mm) entitled as abbreviation such as StTenMin which is the model for storm duration of Ten minutes constructed with stationary approach.

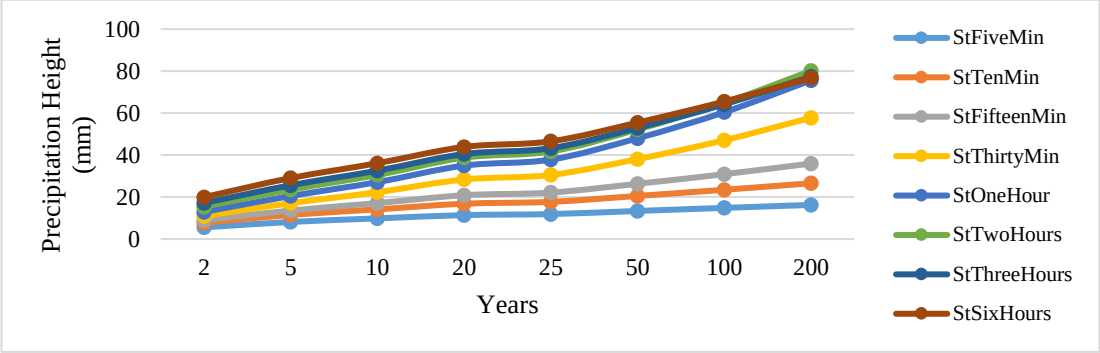

Figure 3.5. Stationary Return Level (mm) Estimates for sub-hourly and hourly storm durations

For the 1950-2015 whole period, all storm durations' return levels decrease for shorter return periods such is 2 years and 5 years, in comparison with the 1950-1975 period return levels; ranging from 36% to 2% while for 10 years and above return periods, return level of whole time series exhibit greater values except five minutes data. Whole period return level values increase in accordance with the return period. It can be generalized that 1950-1975 period has higher return levels for shorter return periods but for the medium and long duration return periods whole period (1950-2015) return levels get higher values with an increasing trend (Table 3.3).

Table 3.3. Stationary Return Levels (mm) % Change - 1950-2015 vs. 1950-1975

Storm Duration	2-year	5-year	10-year	20-year	25-year	50-year	100-year	200-year
FiveMin	-36%	-20%	-10%	-1%	2%	9%	16%	21%
TenMin	-29%	-11%	1%	12%	15%	24%	31%	38%
FifteenMin	-28%	-10%	3%	15%	18%	28%	36%	44%
ThirtyMin	-26%	-7%	6%	18%	22%	32%	41%	50%
OneHour	-29%	-11%	2%	15%	19%	30%	40%	49%
TwoHours	-17%	-7%	2%	11%	13%	21%	29%	37%
ThreeHours	-9%	-1%	4%	11%	13%	19%	24%	30%
SixHours	-2%	3%	8%	12%	14%	18%	22%	27%

For the 1950-2015 whole period, all storm durations' return levels increase for shorter return periods such as 2 or 5 years but this increase exhibit a decreasing trend with increasing storm duration when compared with the 1976-2015 period (Table 3.4).

Table 3.4. Stationary Return Levels (mm) vs. % Change - 1950-2015 vs. 1976-2015

Storm Duration	2-year	5-year	10-year	20-year	25-year	50-year	100-year	200-year
FiveMin	21%	17%	11%	3%	1%	-9%	-20%	-33%
TenMin	16%	12%	6%	-2%	-5%	-16%	-28%	-42%
FifteenMin	15%	10%	4%	-3%	-6%	-15%	-26%	-38%
ThirtyMin	16%	10%	1%	-11%	-16%	-33%	-55%	-81%
OneHour	14%	12%	8%	3%	1%	-7%	-15%	-25%
TwoHours	12%	7%	-1%	-12%	-17%	-33%	-53%	-77%
ThreeHours	7%	3%	-4%	-12%	-15%	-26%	-39%	-54%
SixHours	3%	-1%	-7%	-14%	-16%	-25%	-35%	-47%

In comparison with the 1976-2015 period return levels; there is up to 21% increase for 1950-2015 entire period considering the 2 years and 5 years return periods. On the other hand this increase returns to decrease after 10 years return period for hourly storm durations except one hour time series and after 20 years return period for sub-hourly storm durations except five minutes. Entire period return level values decreases in accordance with the return periods compared with 1976-2015 period. It can be generalized that 1976-2015 period has higher return levels for mid and longer return periods while for shorter return periods, 1950-2015 whole period return levels get higher values. Besides comparing with the whole period, 1950-1975 and 1976-2015 periods are compared with each other in Table 3.5.

Table 3.5. Stationary Return Levels (mm) % Change - 1976-2015 vs. 1950-1975

Storm Duration	2-year	5-year	10-year	20-year	25-year	50-year	100-year	200-year
FiveMin	-73%	-45%	-23%	-4%	1%	17%	30%	41%
TenMin	-54%	-26%	-4%	14%	19%	34%	46%	57%
FifteenMin	-50%	-22%	-1%	17%	22%	37%	49%	59%
ThirtyMin	-51%	-20%	5%	26%	32%	49%	62%	72%
OneHour	-50%	-27%	-7%	13%	18%	35%	48%	59%
TwoHours	-34%	-15%	3%	20%	26%	41%	54%	64%
ThreeHours	-17%	-4%	8%	20%	24%	35%	46%	55%
SixHours	-5%	5%	14%	23%	26%	34%	43%	50%

The return level estimates for 1950-1975 and 1976-2015 periods, models show different behaviour; shorter return periods exhibit greater return values for 1950-

1975 period especially for short storm durations while with the increasing return period; 1976-2015 period return level values gets higher.

Also average and maximum annual rainfall intensities for two periods compared and shown in Figure 3.6 for sub-hourly and hourly time series. When compared with the return level estimates for two and single period, average annual maximum rainfall intensities during change phases show more coherent and substantial distinction. First period average return level values are greater than the second period and whole period values, and whole period return level values are greater than second period values. Maximum rainfall intensities observed in the whole period are mostly coming from the second period except five minutes maximum value. Moreover the direction of maximum and average return level values are not same for when compared whole period to first period; first period return level estimates are greater than the whole period ones on the other hand whole period maximum values are greater than the first period values.

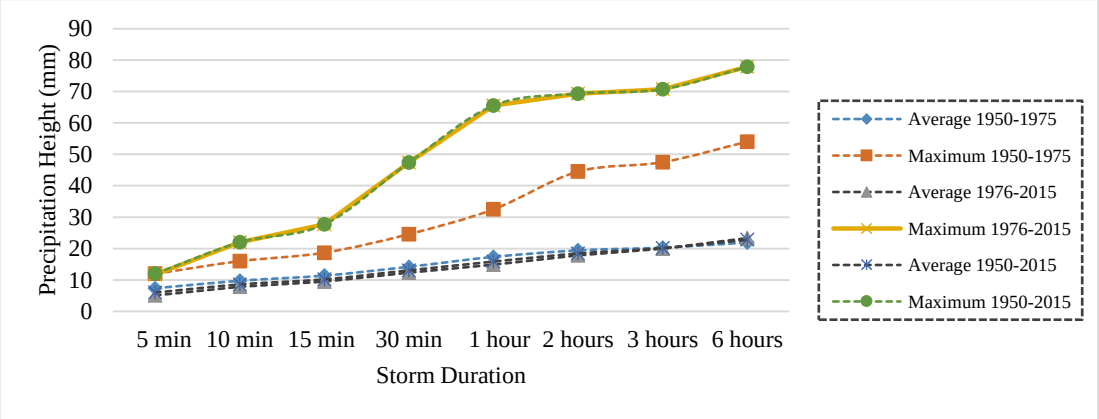

Figure 3.6. Average annual maximum rainfall intensities (mm) for sub-hourly and hourly storm durations

In Table 3.6, comparison of stationary GEV model return levels (mm) with Turkish State Meteorological Service return levels can be seen. Five minutes storm duration return levels decreases for all return periods for the GEV stationary model data. However, ten, fifteen, thirty minutes and one, two and three hours storm durations show an increasing trend with regard to return levels. Six hours storm duration data

decreases with increasing return period for GEV stationary model data. The comparison indicate various return level changes considering stationary return levels (mm) GEV stationary model and Turkish State Meteorological Service return level estimates ranging from -4% to 12% according to storm duration and return period.

Table 3.6. Stationary Return Levels (mm) % Change - GEV Stationary Model vs. Turkish State Meteorological Service Return Level Estimates for Ankara

Storm Duration	2-year	5-year	10-year	25-year	50-year	100-year	200-year
FiveMin	-1%	-1%	-2%	-2%	-2%	-2%	-3%
TenMin	-2%	-1%	0%	1%	3%	4%	5%
FifteenMin	-2%	0%	1%	3%	6%	8%	10%
ThirtyMin	-4%	-2%	0%	3%	6%	9%	12%
OneHour	-3%	-2%	-1%	1%	3%	6%	8%
TwoHours	-1%	-1%	0%	1%	2%	3%	5%
ThreeHours	0%	0%	0%	0%	0%	0%	0%
SixHours	2%	2%	1%	-1%	-3%	-5%	-6%

3.2.2. Non-Stationary Analysis – Observed Precipitation Data

Stationary and nonstationary models are constructed for observed precipitation data and compared for time series between years 1950-2015. Stationary and nonstationary models' negative log-likelihood (NLL), AIC and BIC values are used to capture the best fit nonstationary model among the others. Table 3.7 presents the diagnostic values of stationary and best fit nonstationary models.

Table 3.7. Stationary and Best Fit Nonstationary Model Comparison

Model	N L L	AIC	BIC		Model	N L L	AIC	BIC
StFiveMin	160	327	333		**StTenMin**	182	369	376
NStFiveMin	139	288	298		**NStTenMin**	166	342	353
StFifteenMin	194	394	401		**StThirtyMin**	210	426	432
NStFifteenMin	173	356	367		**NStThirtyMin**	190	390	401
StOneHour	222	451	457		**StTwoHours**	228	461	468
NStOneHour	201	412	423		**NStTwoHours**	205	420	431
StThreeHours	231	468	474		**StSixHours**	237	480	487
NStThreeHours	209	428	439		**NStSixHours**	216	442	452

Small negative log-likelihood and AIC/BIC values infer the superiority of the model to the other ones. First nonstationary models compared among themselves then nonstationary model with the best fit diagnostic values compared with stationary model (Table 3.7). In addition to diagnostic value check likelihood ratio test is also conducted between stationary and best fit nonstationary models to explore the superiority of models. Stationary model has standard three parameters of GEV distribution however nonstationary models' parameters depends on the number of covariates. Likelihood-ratio test can be used to find out whether or not inclusion of the covariate/covariates is statistically significant. The values in Table 3.7 tell that nonstationary models exhibit superiority in terms of negative log-likelihood and AIC/BIC (smaller values) when compared with their corresponding stationary models.

Return levels of best fit nonstationary models results are shown in Table 3.8. Generally mean or median values are computed to simplify the results of nonstationary models because nonstationary return level values gets different values for every single year.

Table 3.8. Nonstationary Best Fit Return Levels (mm) - Mean Values

	2-year	**5-year**	**10-year**	**20-year**	**25-year**	**50-year**	**100-year**	**200-year**
NStFiveMin	5.31	7.86	9.32	10.57	10.94	12.00	12.95	13.80
NStTenMin	6.77	10.14	12.66	15.33	16.23	19.18	22.38	25.89
NStFifteenMin	8.83	13.08	16.13	19.24	20.27	23.56	27.03	30.70
NStThirtyMin	10.95	16.53	21.03	26.06	27.82	33.82	40.72	48.69
NStOneHour	12.06	19.42	26.24	34.76	37.95	49.63	64.55	83.66
NStTwoHours	15.36	22.89	29.34	36.90	39.63	49.20	60.72	74.61
NStThreeHours	17.22	24.93	31.02	37.72	40.04	47.84	56.66	66.68
NStSixHours	20.13	28.70	35.34	42.55	45.02	53.28	62.50	72.83

In this study, mean values of nonstationary model results are used. Nonstationary model results are compared with respect to stationary model results of each storm duration and in Figure 3.7, stationary and nonstationary mean return level estimates for every storm duration are given respectively. In figure 3.8 IDF curves of observed stationary and nonstationary results can be seen. By examining storm durations, it is found that the shorter the duration the larger the differences between the non-

stationary and stationary extremes. As an example, for the 100-year return period, the differences between stationary and nonstationary return level of 5 minutes and 30 minutes events 15% and 16%, while for a 6 hours storm, the difference is 5%. Also among the storm durations, only one hour time series exhibit larger values for its nonstationary model return level values, however this is not valid for shorter return periods such as 5 years or 20 years.

Sub-hourly nonstationary return level values show an increasing difference between stationary model return level values with the rising return period, except ten minutes data nonstationary model results. While the difference is 4% for five and fifteen minutes 5 years return period return level values; this difference gets 11% and 12% for 50 years return period and 15% and 14% for 100 years return period. On the other hand ten minutes data follows the opposite direction for the alteration of nonstationary and stationary return level results with respect to time, such as 14% and 12% difference for 2 and 10 years return period and 5% for 100 years return period. The hourly time series demonstrate similar behaviour to sub-hourly time series. While two, three and six hours time series' difference enlarge with increasing return period, one hour time series show that after 25 years return period, nonstationary return level values gets larger than the stationary one hour model return level results. The difference between the stationary and nonstationary return levels is not following a linear trend but to make a general inference sub-hourly storm durations indicate larger difference than hourly storm durations and non-stationary estimates are smaller than their corresponding stationary values. In this circumstances for a worst case scenario it is better to use stationary return level estimates when observed data is considered.

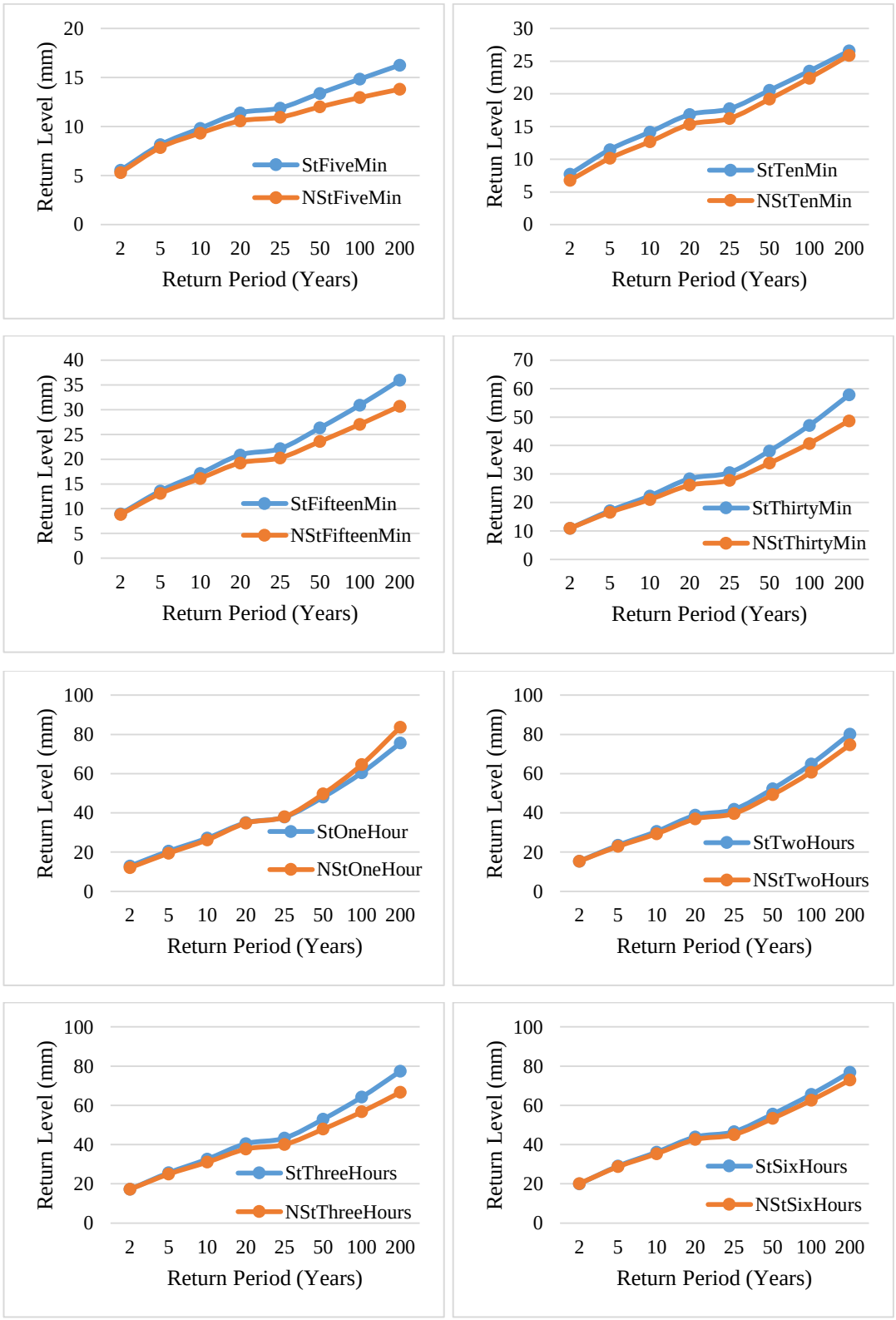

Figure 3.7. Stationary and Best Fit Nonstationary Model Return Level (mm) Comparison - Return Period vs. Return Level

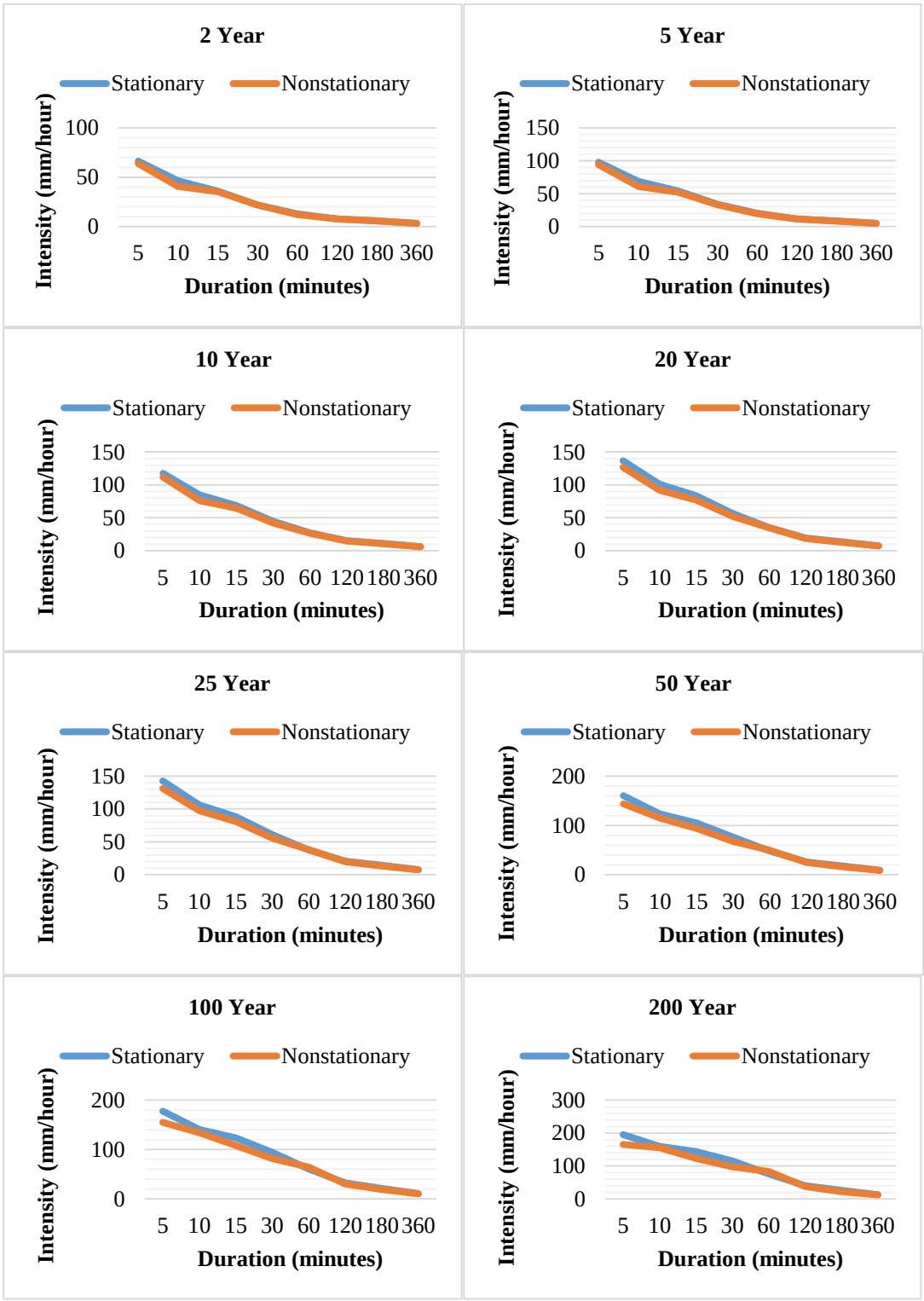

Figure 3.8. Stationary and Best Fit Nonstationary Model IDF Curves

In the analyses statistically significant extreme rainfall trends were detected for storm durations considering the data from 1950 to 2015. Also evidence of non-stationarity exits according to partial period GEV analysis (1950-1975, 1976-2015) results. Statistical tests indicate that there is a significant downward monotonic trend between 1950-2015 periods for 5-10-15-30 minutes and 1-2 hours time series. Besides, with regard to single change point analyses, majority of change points are constructed around 1975-1976. So the stationary analyses is conducted for 1950-2015, 1950-1975, and 1976-2015 periods. 1950-1975 period has higher return levels for shorter return periods but for the medium and long duration return periods whole period (1950-2015) return levels get higher values with an increasing trend. On the other hand, 1976-2015 period has higher return levels for mid and longer return periods while for shorter return periods, 1950-2015 whole period return levels get higher values.

The return level estimates for 1950-1975 and 1976-2015 periods, models show different behaviour among themselves; shorter return periods exhibit greater return values for 1950-1975 period especially for short storm durations while with the increasing return period; 1976-2015 period return level values gets higher. Moreover, stationary GEV model return levels (mm) compared with Turkish State Meteorological Service return level observations (Supplementary Document of Official Letter of SMS, 2017a). The comparison indicates various return level changes considering stationary return level (mm) GEV stationary model and Turkish State Meteorological Service return level observations which ranges from -4% to 12% according to storm duration and return period.

Nonstationary models are constructed and compared with stationary model results. Negative log-likelihood (NLL), AIC and BIC values are computed and the best fit nonstationary models are determined. Nonstationary model results which in general exhibit smaller return level values are compared with respect to stationary model results of each storm duration; by examining storm durations, it is found that mainly the shorter the duration the larger the differences between the non-stationary and stationary extremes.

With the rising return period generally the difference between stationary and nonstationary model return level values increased but this is not valid for ten minutes data nonstationary model results. The hourly time series demonstrate similar behaviour to sub-hourly time series. While two, three and six hour time series' difference between stationary and nonstationary return level values increase in accordance with the return period, one hour time series show different results after 25 years return period. To make a general inference for the difference between the stationary and nonstationary return levels; sub-hourly storm durations indicate larger difference than hourly storm durations with regard to their corresponding stationary results and non-stationary estimates are smaller than their corresponding stationary values so it is better to use stationary return level values for a worst case scenario when the observation period data is considered.

Non-stationary GEV models perform better than the stationary models according to diagnostic tests and values. The results of nonstationary analyses exhibit similar results in terms of model fit with other studies in this research area. As an example Šraj et al. (2016) found that all non-stationary models that are used in their analyses show a better fit to the maximum annual flood data than the stationary model. Cheng (2014) shows that nonstationary return level estimates are more accurate than stationary assumption and ignoring the stationary assumption may cause to underestimation of extremes. Eckersten (2016) used a Bayesian approach similar with the methodology Cheng (2014) has developed with non-stationary assumption to calculate return levels using the General Extreme Value distribution with time-dependent parameters. The differences in design rainfall estimates between two observation periods (1950-1975 and 1976-2015), entire period and nonstationary assumption models support the need to update the current information, with the most recent data and approaches. The variations among the time periods also reveal the need to conduct analysis using future climate data as stated in the literature (e.g. Yilmaz and Perera 2014, Kirshen et.al. 2014, Cheng and AghaKouchak 2014). On the other hand unlike the results of other studies, nonstationary model results exhibit smaller return level values than stationary models results for the observed data.

CHAPTER 4

CLIMATE CHANGE AND ALTERATIONS IN THE PRECIPITATION REGIME: PROJECTIONS FOR ANKARA PROVINCE

This chapter presents the development of stationary and nonstationary models, based on block maxima of future sub-hourly and hourly storm durations. Data is derived from daily projections of precipitation, to investigate the return levels and return periods of extreme rainfall events. At first daily precipitation values of projection period is disaggregated to 5 minutes storm durations, then five minutes time series aggregated to the storm durations that are subject of interest. Stationary and nonstationary models are applied to a 10-15 minute and 1-6 hour projected (2015-2098) annual maximum storm durations for Ankara province. Three models and two RCP scenario matrix for storm durations of stationary and nonstationary models are given in Figure 4.1 and Figure 4.2.

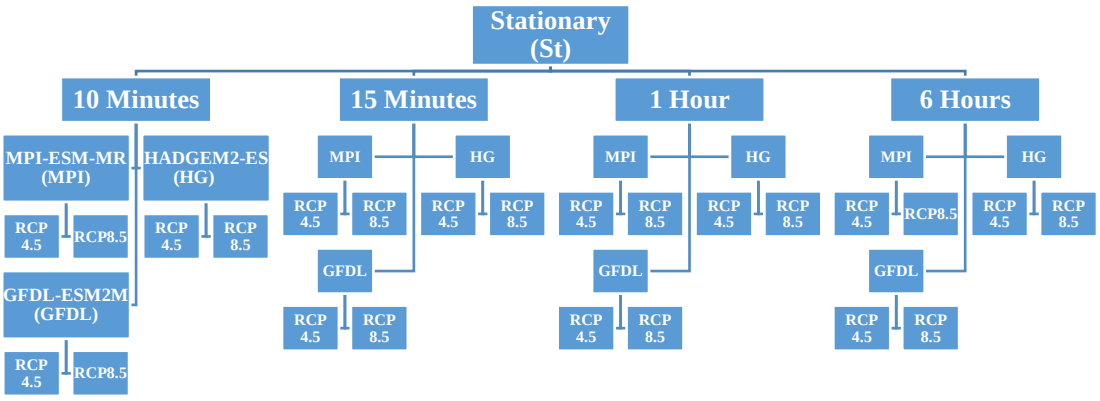

Figure 4.1. Projected Storm Durations Used for Stationary Models for 2015-2098 period

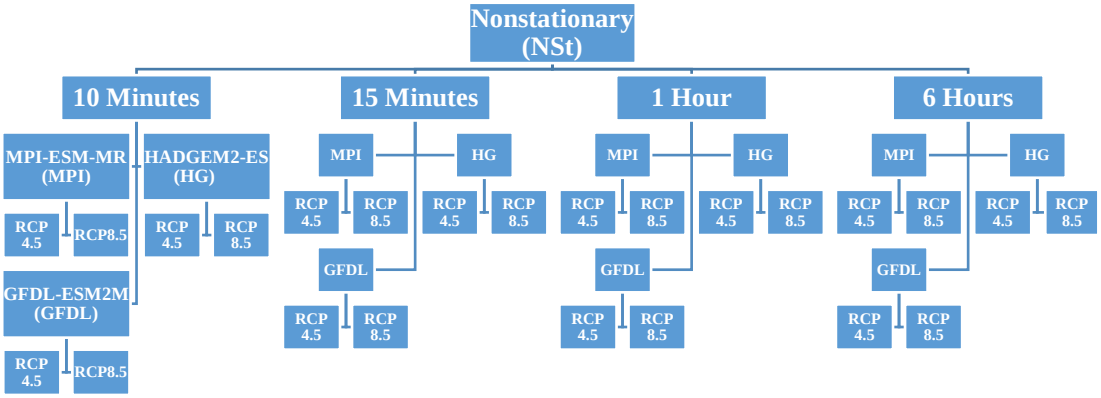

Figure 4.2. Projected Storm Durations Used for Nonstationary Models for 2015-2098 period

The model explanations that are derived from stationary and nonstationary models for storm durations and model vs. RCP combinations are abbreviated for convenience and to avoid confusion as it is done in Chapter 3. This time GCM name and RCP scenario information is also added. For instance Nonstationary model results for 15 minutes storm duration data, which is derived from MPI-ESM-MR model with RCP 8.5 scenario, is abbreviated as NstFifteenMinMPI85 or stationary models that uses 6 hours storm duration that is obtained from HADGEM2-ES model with RCP 4.5, can be found as StSixHourHG45 in the text.

4.1. TREND TESTS FOR THE PROJECTED DATA

Trend tests are used to figure out if a time series has an increasing or decreasing trends. Visual inspection is an alternative to make rough inferences but for reliable determination, especially with complex variations and for long term series, statistical tests are needed. Figure 4.3 shows the sub-hourly time series of interest, annual maximum rainfall intensities for storm duration of 10 minutes for three models and two RCP scenarios, between 2015-2098 periods.

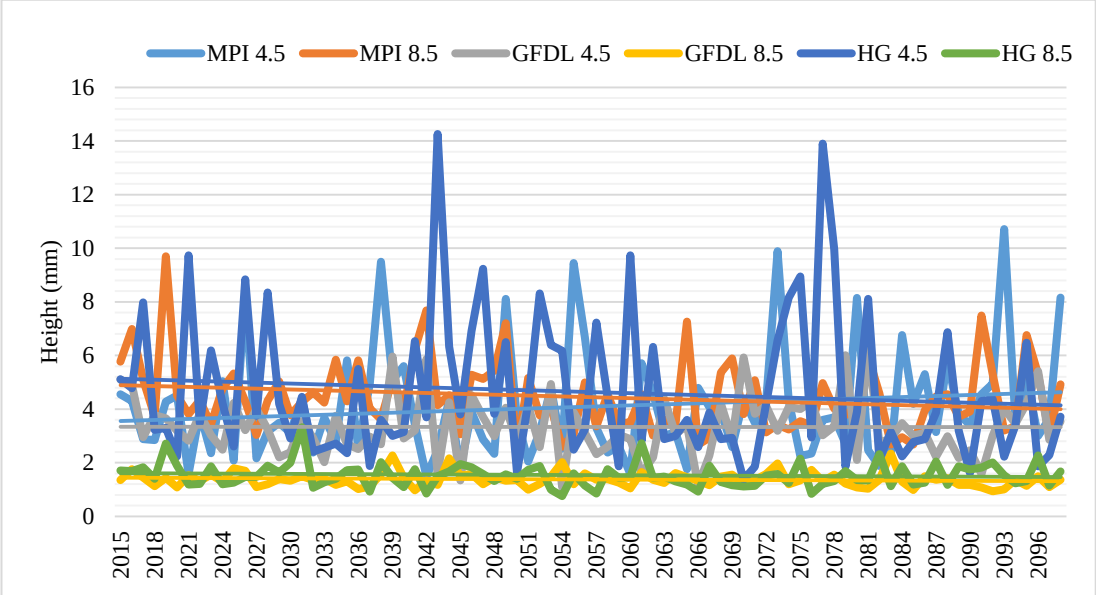

Figure 4.3. Projected 10 Minutes Annual Maximum-Time Series in Ankara Province for 2015-2098 period

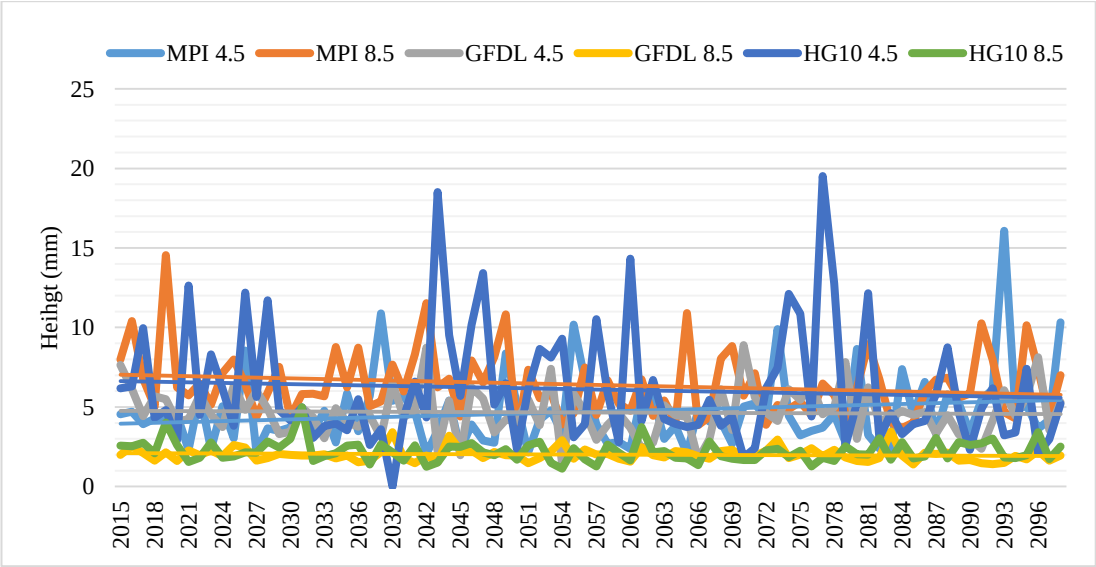

Figure 4.4. Projected 15 Minutes Annual Maximum-Time Series in Ankara Province for 2015-2098 period

Figure 4.4, Figure 4.5 and Figure 4.6 also demonstrate the trend for (15 minutes, 1-6 hours) time series with a linear trend line. It can be inferred that simple linear trend line visually indicate the downward (decreasing) and upward (increasing) trends.

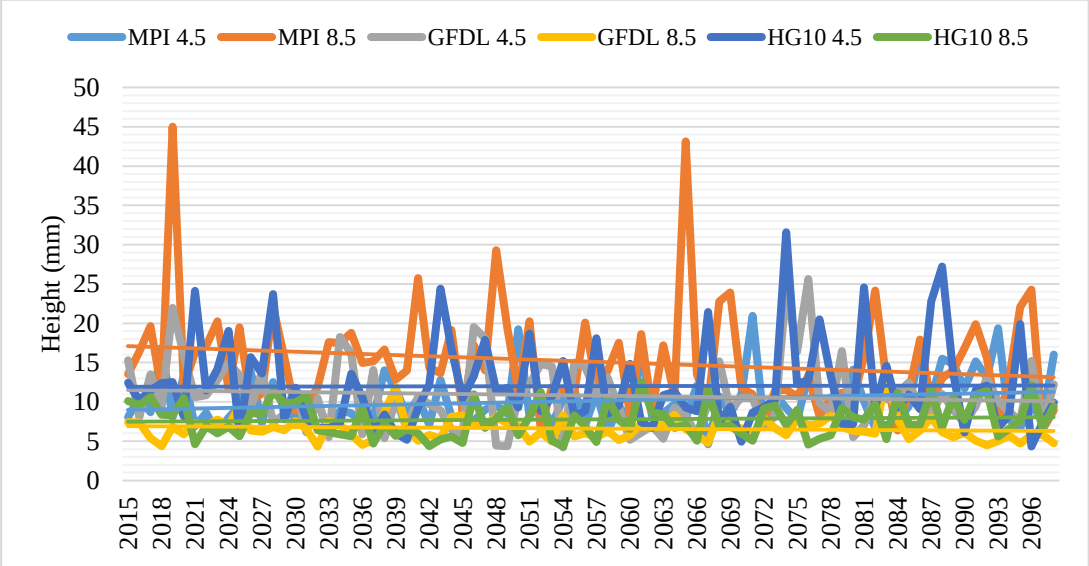

Figure 4.5. Projected 1 Hour Annual Maximum-Time Series in Ankara Province for 2015-2098 period

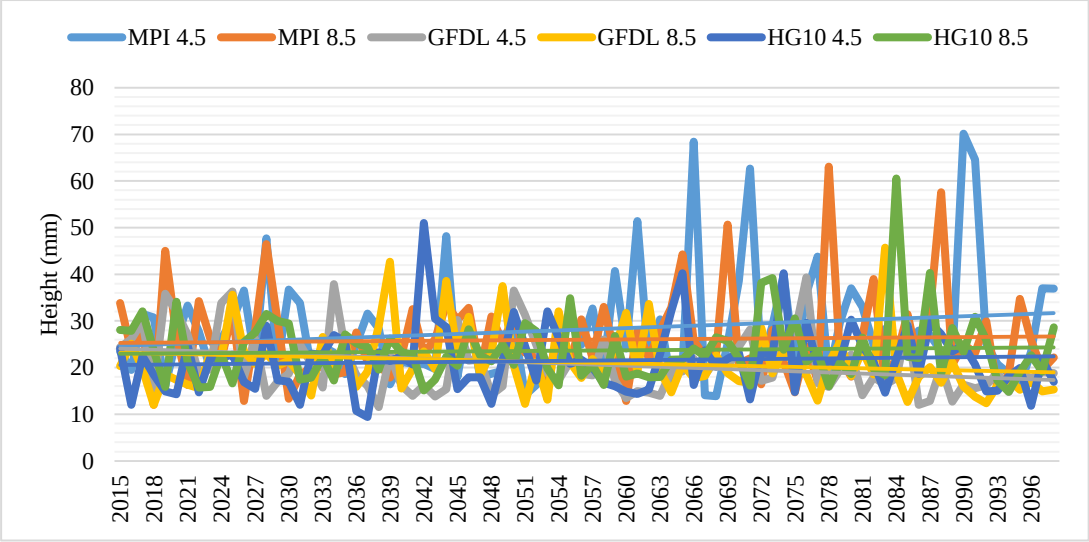

Figure 4.6. Projected Six Hours Annual Maximum-Time Series in Ankara Province for 2015-2098 period

According to MK statistics; the null hypothesis that there is no trend is rejected for the 10 minutes data but only for the MPI model RCP 8.5 time series indicated a significant trend. Fifteen minutes time series exhibited downward trend except MPI 45 but only MPI 85 and GFDL 85 results are significant. For One hour time series, MPI model RCP 8.5 and GFDL model RCP 8.5 time series have significant

downward trends. Six hours time series' GFDL model results suggest that there is significantly a downward monotonic trend for both 4.5 and 8.5 RCP scenarios.

Trend test results, according to Mann-Kendall Test for all durations are shown in Table 4.1. The sign of the MK statistic tau determine the direction of trend, if it is (-) it can be inferred that there is a monotonic downward trend and if it is (+) there is an upward trend exists. Significance of the trend is decided due to the p-Value of the test results. A 2-sided p-value smaller than 0.10 supports the significance of the trend. Trends in short (in particular sub-hourly) and long storm durations are largely different in terms of statistical significance and directions for model and scenario combinations. On the other hand all significant trends and most of the trends are downwards.

Table 4.1. Mann-Kendall Results for the Storm Durations of Projected Data Time Series

Storm Duration	MK Statistic	p-Value
TenMinutesMPI45	0.0947	0.20374
TenMinutesMPI85	-0.14	0.05940
TenMinutesGFDL45	-0.0175	0.8167
TenMinutesGFDL85	-0.105	0.15966
TenMinutesHG45	-0.0967	0.19428
TenMinutesHG85	-0.0531	0.47717
FifteenMinutesMPI45	0.0895	0.22959
FifteenMinutesMPI85	-0.118	0.11235
FifteenMinutesGFDL45	-0.0459	0.53906
FifteenMinutesGFDL85	-0.122	0.10142
FifteenMinutesHG45	-0.0938	0.20789
FifteenMinutesHG85	-0.0422	0.57273
OneHourMPI45	0.112	0.1339
OneHourMPI85	-0.143	0.05535
OneHourGFDL45	-0.0694	0.35185
OneHourGFDL85	-0.141	0.05888
OneHourHG45	-0.0402	0.59128
OneHourHG85	0.0499	0.50392
SixHoursMPI45	0.0602	0.41944
SixHoursMPI85	-0.0115	0.88024
SixHoursGFDL45	-0.173	0.01983
SixHoursGFDL85	-0.199	0.00759
SixHoursHG45	0.0422	0.57274
SixHoursHG85	-0.0143	0.84986

4.2. STATIONARY ANALYSIS FOR PROJECTED DATA: RETURN LEVEL ESTIMATES

In Table 4.2, 4.3, 4.4, and 4.5, return level estimates for 2-5-10-20-25-50-100 and 200 year return periods for 2015-2098 period are represented for all annual maximum time series with stationary approach. Ten and fifteen minutes, one hour and six hours storm durations' return level estimates for all model and RCP scenarios are represented respectively. Also average and maximum of four storm durations are given. For instance, when the MPI model RCP scenario 8.5 projection results used in the stationary GEV model; 3.58 mm return level (height) for 2 years return period is computed; average value for this (ten minutes) storm duration is the mean value of all three models vs. two RCP results such as the 10 years return period average value is 4.93 mm. For the maximum value, the largest value for the corresponding return period is chosen. For example 100 year return periods maximum return level is 19,07 mm which is the largest among the 100 years return period values of six different return level results.

Models and scenario caused differences can be seen from the Tables 4.2, 4.3, 4.4, 4.5 and Figures 4.7, 4.8, 4.9, and 4.10 for all the storm durations. The return level estimates for ten minutes stationary models show different behaviour, MPI model shows a slight difference within scenarios MPI 4.5 and MPI 8.5, this difference increases with the increasing return periods. GFDL and HG models have greater difference than MPI model within RCP scenarios. Among the model results, HG model RCP 4.5 represent the highest return level values especially for 50 and longer return periods, GFDL and HG models RCP 8.5 scenarios represent the lowest return level values. For instance, highest 100 year return level is 19.07 mm and the lowest return level estimate is 2.43 mm. This difference is valid for both short and long return periods of ten minutes stationary models results. Maximum values for the ensemble return levels are mostly coming from the HG model RCP 4.5 results.

Table 4.2. Ten Minutes Stationary (St) Return Levels (mm) vs. Return Periods Calculated for Projected Data

	2-year	5-year	10-year	20-year	25-year	50-year	100-year	200-year
StTenMinMPI45	3.58	5.27	6.61	8.07	8.58	10.29	12.22	14.42
StTenMinMPI85	4.18	5.35	6.16	6.99	7.25	8.11	8.99	9.92
StTenMinGFDL45	3.24	4.23	4.81	5.30	5.45	5.88	6.27	6.62
StTenMinGFDL85	1.33	1.57	1.74	1.90	1.95	2.11	2.27	2.43
StTenMinHG45	3.79	6.09	8.15	10.66	11.59	14.92	19.07	24.24
StTenMinHG85	1.47	1.86	2.12	2.35	2.43	2.65	2.87	3.09
Average	2.93	4.06	4.93	5.88	6.21	7.33	8.62	10.12
Max	4.18	6.09	8.15	10.66	11.59	14.92	19.07	24.24

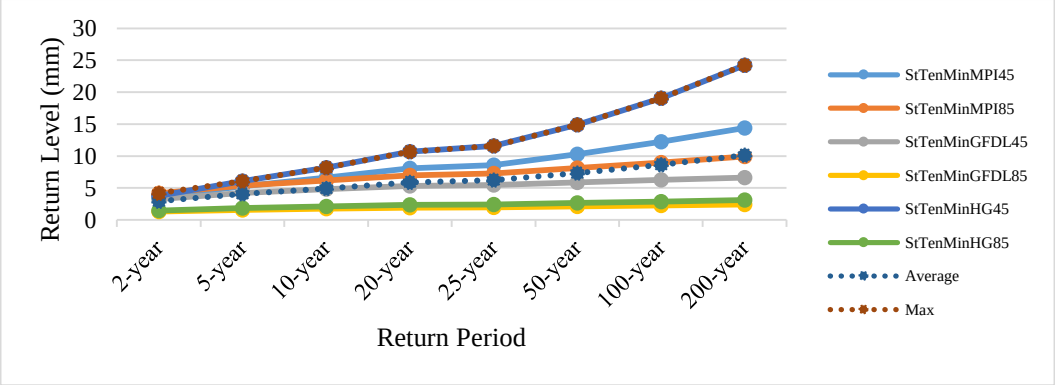

Figure 4.7. Stationary Model Results for Ten Minutes Time Series for Projected Data

Fifteen minutes stationary model results also represent variations; MPI model has greater values for RCP 8.5 for short and mid-term return periods but GFDL and HG models' RCP 4.5 scenario return level values are higher than RCP 8.5 values. Return level of 50 years return period is 11.55 mm for MPI 45 and 12,12 mm for MPI 85 on the other hand for 100 years MPI 45 return level is 13.77 mm and MPI 85 return level is 13.53 mm, since this difference increases with the increasing return period. Maximum return level values, except 2 years return period, are based on HG model

RCP 45 time series results, average return levels estimates are coherent with GFDL and MPI 45 results for short return periods.

Table 4.3. Fifteen Minutes Stationary (St) Return Levels (mm) vs. Return Periods Calculated for Projected Data

	2-year	5-year	10-year	20-year	25-year	50-year	100-year	200-year
StFifteenMinMPI45	4.12	5.94	7.40	9.04	9.61	11.55	13.77	16.33
StFifteenMinMPI85	5.97	7.77	9.05	10.34	10.76	12.12	13.53	15.02
StFifteenMinGFDL45	4.55	5.90	6.67	7.33	7.53	8.09	8.58	9.03
StFifteenMinGFDL85	1.94	2.29	2.54	2.78	2.86	3.11	3.36	3.62
StFifteenMinHG45	5.01	7.98	10.65	13.89	15.09	19.39	24.74	31.42
StFifteenMinHG85	2.12	2.69	3.07	3.43	3.54	3.89	4.23	4.58
Average	3.95	5.43	6.56	7.80	8.23	9.69	11.37	13.33
Max	5.97	7.98	10.65	13.89	15.09	19.39	24.74	31.42

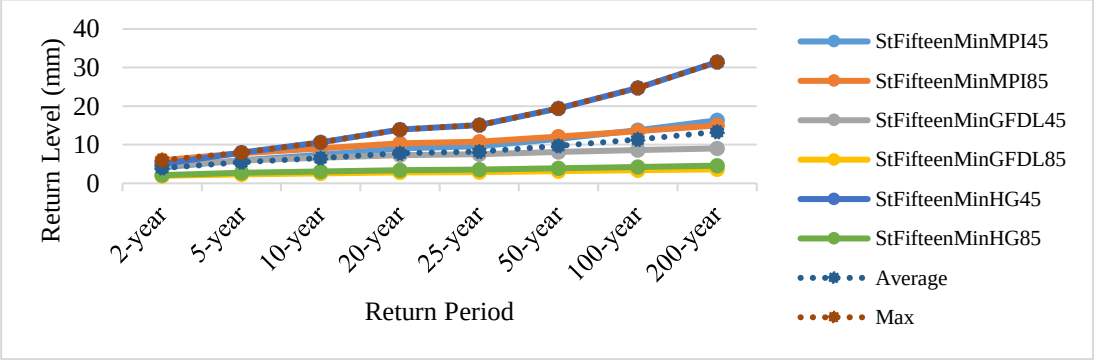

Figure 4.8. Stationary Model Results for Fifteen Minutes Time Series for Projected Data

One hour stationary model results also represent variations; MPI model has greater values for RCP 8.5 but GFDL and HG models' RCP 4.5 scenario return level values are higher than RCP 8.5 values. Maximum return level values are based on MPI model RCP 8.5 time series results, average return levels estimates are coherent with

GFDL and MPI 45 results. GFDL and MPI 45 (average), GFDL and HG 85 (lower), MPI 85 and HG 45 (higher) results have similar outcomes.

Table 4.4. One Hour Stationary (St) Return Levels (mm) vs. Return Periods Calculated for Projected Data

	2-year	5-year	10-year	20-year	25-year	50-year	100-year	200-year
StOneHourMPI45	9.40	12.20	14.26	16.41	17.13	19.46	21.97	24.67
StOneHourMPI85	13.67	19.02	23.03	27.25	28.67	33.32	38.38	43.89
StOneHourGFDL45	9.99	13.89	16.55	19.16	20.01	22.64	25.32	28.05
StOneHourGFDL85	6.36	7.65	8.53	9.37	9.64	10.49	11.33	12.19
StOneHourHG45	10.59	15.28	18.98	23.04	24.44	29.15	34.48	40.52
StOneHourHG85	7.52	9.45	10.58	11.58	11.87	12.74	13.53	14.25
Average	9.59	12.92	15.32	17.80	18.63	21.30	24.17	27.26
Max	13.67	19.02	23.03	27.25	28.67	33.32	38.38	43.89

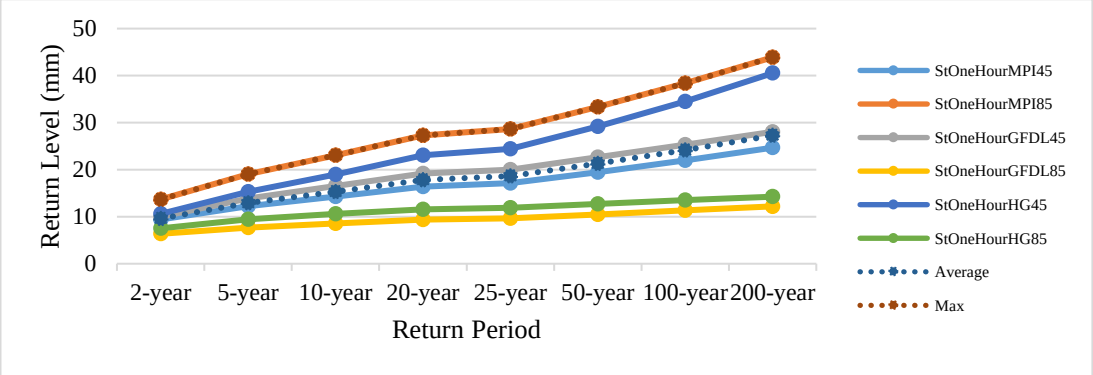

Figure 4.9. Stationary Model Results for One Hour Time Series for Projected Data

Six hours stationary MPI model results has greater values for RCP 4.5 but HG models' RCP 8.5 return level values are higher than RCP 4.5 values. GFDL model RCP 8.5 return level values are greater for short return periods on the other hand RCP 4.5 values get larger than RCP 8.5 values with the increasing return periods. For instance 5 years return period return level for GFDL 45 is 24.69 mm and GFDL 85 is 25.17 mm but 50 years return period values are 41.17 mm and 39.43 mm

respectively. Maximum return level values are based on MPI model RCP 4.5 time series results, average return levels estimates are coherent with HG 85 for short return periods and MPI 85 results for longer return periods. MPI 45 has the highest return level values, GFDL 45, 85 and HG 45 have smallest values. Also MPI model results are greater than HG and GFDL model return level results for all durations.

Table 4.5. 5 Six Hours Stationary (St) Return Levels (mm) vs. Return Periods Calculated for Projected Data

	2-year	5-year	10-year	20-year	25-year	50-year	100-year	200-year
StSixHoursMPI45	25.00	34.49	42.32	51.24	54.40	65.26	77.97	92.88
StSixHoursMPI85	24.16	31.96	37.48	43.06	44.89	50.71	56.78	63.14
StSixHoursGFDL45	19.02	24.69	29.12	33.94	35.61	41.17	47.41	54.44
StSixHoursGFDL85	19.66	25.17	29.22	33.44	34.85	39.43	44.35	49.65
StSixHoursHG45	20.41	26.50	30.51	34.32	35.53	39.24	42.90	46.52
StSixHoursHG85	22.08	27.81	32.15	36.80	38.37	43.57	49.28	55.58
Average	21.72	28.44	33.47	38.80	40.61	46.56	53.12	60.37
Max	25.00	34.49	42.32	51.24	54.40	65.26	77.97	92.88

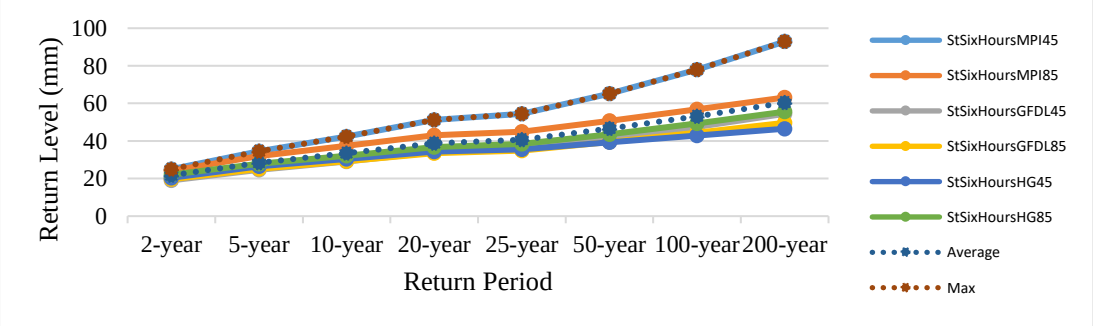

Figure 4.10. Stationary Model Results for Six Hours Time Series for Projected Data

4.3. NON-STATIONARY ANALYSIS FOR PROJECTED DATA AND COMPARISON WITH THE STATIONARY ANALYSIS

Additionally, nonstationary models are constructed for the future (projected) precipitation data and compared with stationary models. First nonstationary models

compared among themselves then nonstationary model with the best fit diagnostic values compared with stationary models. AIC, BIC and NLL values of stationary models and their corresponding best fit nonstationary ones are presented in Table 4.6. Moreover as the scale parameter of GEV distribution must be >0, for all nonstationary best fit models and every single point (in this case year) of these models' scale parameters are computed and checked whether or not it is appropriate.

Table 4.6. Diagnostic Values of Stationary and Best Fit Nonstationary Models of Projected Data

Model	Stationary			Best Fit Nonstationary		
	N L L	**AIC**	**BIC**	**N L L**	**AIC**	**BIC**
TenMinMPI45	160.49	329.98	334.27	159.58	327.15	336.88
TenMinMPI85	132.92	271.84	279.13	128.45	264.91	274.63
TenMinGFDL45	124.99	255.97	263.26	123.57	255.15	267.87
TenMinGFDL85	2.65	11.31	18.60	-1.81	6.38	18.53
TenMinHG45	181.79	369.57	376.86	180.24	368.47	378.20
TenMinHG85	43.77	93.53	100.83	43.21	94.42	104.15
FifteenMinMPI45	165.88	337.76	345.05	164.76	337.52	347.24
FifteenMinMPI85	169.16	344.31	351.61	166.22	340.43	350.16
FifteenMinGFDL45	151.40	308.81	316.10	149.05	306.10	315.83
FifteenMinGFDL85	33.81	73.61	80.91	31.63	71.25	80.98
FifteenMinHG45	203.40	412.81	420.10	201.64	411.29	421.013
FifteenMinHG85	74.74	155.48	162.78	74.03	156.06	165.78
Model	**Stationary**			**Best Fit Nonstationary**		
	N L L	**AIC**	**BIC**	**N L L**	**AIC**	**BIC**
OneHourMPI45	205.35	416.71	424.00	203.77	415.55	425.27
OneHourMPI85	258.91	523.82	531.11	252.66	513.33	523.05
OneHourGFDL45	235.48	476.96	484.25	234.06	476.13	485.85
OneHourGFDL85	142.67	291.34	298.63	138.44	286.87	299.03
OneHourHG45	246.33	498.66	505.95	244.51	497.02	506.74
OneHourHG85	181.81	369.61	376.91	179.66	367.33	377.05
SixHoursMPI45	303.82	613.65	620.94	302.85	613.71	623.43
SixHoursMPI85	292.30	590.61	597.90	281.20	572.41	584.56
SixHoursGFDL45	262.57	531.13	538.43	258.63	527.27	539.42
SixHoursGFDL85	261.93	529.86	537.15	252.61	515.21	527.37
SixHoursHG45	273.65	553.29	560.59	252.01	514.01	526.17
SixHoursHG85	264.12	534.24	541.53	264.08	536.17	545.89

For every model and its corresponding RCP scenarios, mean and maximum nonstationary return level estimate results compared with stationary model results (e.g. best fit nonstationary model for MPI RCP 4.5 time series' return level estimates are compared with stationary MPI RCP 4.5 time series'). Also for all storm durations (e.g. 10-15 minutes and 1-6 hours) stationary and nonstationary average and

maximum return level estimates (average and maximum of all model and RCP combination stationary results and average and maximum of all model and RCP combination nonstationary best fit results) are computed.

Best fit nonstationary return level results are compared with stationary model return level values of every model and RCP scenarios in Table 4.7 (mean values) and in Table 4.8 (maximum values). There are various increases and decreases which can be seen among the time series' results. Ten minutes stationary and best fit nonstationary results for time series of all models and RCP scenarios are evaluated. Return periods over 100 years for HG 45 time series show increase for nonstationary return levels with increasing trends. GFDL and MPI85 45 time series results show that nonstationary model results are decreasing with increasing return periods.

Table 4.7. Nonstationary Model-Stationary Model Comparison - Mean Value Change for Projected Data

		2-year	5-year	10-year	20-year	25-year	50-year	100-year	200-year
Ten Minutes	**MPI45**	0%	0%	0%	0%	0%	0%	0%	0%
	MPI85	0%	-1%	-1%	-2%	-2%	-2%	-2%	-2%
	GFDL4	-1%	-1%	0%	0%	0%	1%	1%	1%
	GFDL4	-1%	-1%	0%	0%	0%	1%	1%	2%
	GFDL8	1%	0%	0%	-1%	-1%	-1%	-2%	-2%
	HG45	0%	-1%	0%	0%	1%	2%	2%	4%
	HG85	0%	0%	0%	0%	0%	0%	0%	1%
Fifteen Minutes	**MPI45**	0%	0%	0%	0%	0%	1%	2%	3%
	MPI85	0%	-1%	-1%	-1%	-2%	-2%	-2%	-3%
	GFDL4	-1%	-1%	-1%	0%	0%	0%	0%	1%
	GFDL4	-1%	-1%	-1%	0%	0%	0%	1%	1%
	GFDL8	0%	0%	-1%	-1%	-1%	-1%	-1%	-1%
	GFDL8	0%	0%	0%	-1%	-1%	-1%	-1%	-2%
	HG45	-1%	-1%	0%	1%	2%	3%	5%	6%
	HG85	0%	0%	0%	0%	0%	0%	0%	1%
One Hour	**MPI45**	-1%	-1%	-1%	-1%	-1%	-2%	-2%	-2%
	MPI85	0%	-2%	-2%	-2%	-1%	-1%	0%	1%
	GFDL4	-1%	0%	0%	1%	1%	2%	3%	4%
	GFDL8	0%	0%	-1%	-2%	-2%	-3%	-3%	-4%
	HG45	0%	-1%	-1%	0%	0%	0%	0%	1%
	HG85	0%	-1%	-1%	-1%	-1%	-1%	-1%	-1%
Six Hours	**MPI45**	0%	-1%	-1%	-1%	-2%	-2%	-3%	-4%
	MPI85	-25%	-30%	-31%	-32%	-32%	-32%	-32%	-31%
	GFDL4	3%	0%	-3%	-6%	-8%	-12%	-17%	-23%
	GFDL8	4%	4%	1%	-2%	-3%	-8%	-13%	-19%
	HG45	7%	5%	5%	7%	8%	10%	13%	17%
	HG85	10%	14%	15%	15%	15%	14%	12%	11%

Fifteen minutes stationary and best fit nonstationary results for time series of all models and RCP scenarios; HG 45 time series show increase for nonstationary return levels with an increasing trend. Other model and RCP combinations do not change significantly for fifteen minutes time series projections.

Considering one hour stationary and best fit nonstationary results for time series of all models and RCP scenarios; GFDL 45 time series show increase for nonstationary return levels with increasing trends and GFDL 85 time series results show that nonstationary model results are decreasing with increasing return periods, but these nonstationarity effect is significant only for longer return periods.

Six Hours stationary and best fit nonstationary results for time series of all models and RCP scenarios are evaluated, percent changes over 3% and below -3% are accepted significant. HG 45 and 85 time series show increase for nonstationary return levels for all return periods. HG 45 has an increasing trend with increasing return period, besides HG 85 return level increases for short return periods, reaches its highest value for mid-level return periods and then decreases with the increasing return periods. GFDL 45 and 85 results show that nonstationary return levels decrease with increasing return period.

Additionally, maximum values of all best fit nonstationary models and stationary models are compared in Table 4.8 and it can be generalized that most of the nonstationary model maximum results are significantly higher than stationary model maximum return level results for all storm durations and return periods. As three models and two RCP scenarios are used, there are 6 different return level estimates for each storm duration. Each storm duration-model-RCP combination is compared among itself. Stationary and best fit nonstationary model of each combination are compared.

Table 4.8. Nonstationary Model-Stationary Model Comparison for Projected Data–Maximum Value Change

		2-year	5-year	10-year	20-year	25-year	50-year	100-year	200-year
Ten Minutes	**MPI45**	8%	5%	4%	4%	3%	3%	3%	3%
	MPI85	15%	11%	9%	8%	8%	6%	6%	5%
	GFDL45	14%	11%	10%	9%	9%	9%	9%	9%
	GFDL45	6%	4%	4%	4%	4%	4%	4%	5%
	GFDL85	3%	4%	4%	4%	4%	4%	4%	4%
	HG45	9%	6%	5%	4%	4%	4%	4%	5%
	HG85	13%	11%	10%	9%	9%	8%	8%	7%
Fifteen Minutes	**MPI45**	9%	6%	5%	5%	5%	5%	5%	5%
	MPI85	13%	10%	8%	7%	6%	5%	4%	3%
	GFDL45	17%	13%	12%	11%	11%	11%	11%	10%
	GFDL45	7%	5%	5%	4%	4%	5%	5%	5%
	GFDL85	5%	4%	4%	3%	3%	3%	2%	2%
	GFDL85	3%	3%	4%	4%	4%	4%	4%	4%
	HG45	9%	6%	5%	5%	5%	6%	7%	8%
	HG85	15%	12%	11%	10%	10%	9%	8%	8%
One Hour	**MPI45**	1%	6%	8%	10%	10%	11%	12%	12%
	MPI85	18%	12%	10%	8%	8%	8%	7%	8%
	GFDL45	3%	10%	13%	16%	16%	18%	20%	21%
	GFDL85	3%	3%	3%	2%	2%	2%	1%	1%
	HG45	13%	9%	7%	6%	6%	5%	5%	5%
	HG85	24%	20%	18%	17%	16%	15%	15%	14%
Six Hours	**MPI45**	2%	7%	9%	10%	10%	11%	11%	11%
	MPI85	-11%	-8%	-7%	-5%	-5%	-3%	-2%	0%
	GFDL45	17%	15%	13%	10%	9%	6%	2%	-2%
	GFDL85	8%	12%	11%	9%	8%	5%	1%	-3%
	HG45	8%	6%	6%	8%	9%	12%	15%	19%
	HG85	11%	16%	18%	18%	18%	17%	16%	14%

Also the average and maximum of stationary and nonstationary model-RCP combinations of each storm duration are computed. Stationary return level averages and maximum of MPI, GFDL, HG models RCP 4.5 and 8.5 results and nonstationary return level means and maximum of MPI, GFDL, HG models RCP 4.5 and 8.5 in order to make the comparison easier, more general in order to give a different perspective. These results (in mm) are given in Table 4.9 and in the following tables to figure out the superiority effect of nonstationarity.

Table 4.9. Nonstationary Model-Stationary Ensemble Model Comparison for Projected Data - Average and Maximum Values

	2-year	**5-year**	**10-year**	**20-year**	**25-year**	**50-year**	**100-year**	**200-year**
NStTenMinAvg	2.97	4.06	4.89	5.78	6.09	7.14	8.34	9.75
NStTenMinMax	4.91	6.45	8.54	11.11	12.07	15.56	19.96	25.53
StTenMinAvg	2.93	4.06	4.93	5.88	6.21	7.33	8.62	10.12
StTenMinMax	4.18	6.09	8.15	10.66	11.59	14.92	19.07	24.24
Nst/St Avg	**1%**	**0%**	**-1%**	**-2%**	**-2%**	**-3%**	**-3%**	**-4%**
Nst/St Max	**15%**	**6%**	**5%**	**4%**	**4%**	**4%**	**4%**	**5%**
	2-year	**5-year**	**10-year**	**20-year**	**25-year**	**50-year**	**100-year**	**200-year**
NStFifteenMinAvg	3.76	5.06	6.04	7.11	7.48	8.73	10.17	11.87
NStFifteenMinMax	6.87	8.61	11.20	14.61	15.89	20.55	26.50	34.10
StFifteenMinAvg	3.95	5.43	6.56	7.80	8.23	9.69	11.37	13.33
StFifteenMinMax	5.97	7.98	10.65	13.89	15.09	19.39	24.74	31.42
Nst/St Avg	**-5%**	**-7%**	**-9%**	**-10%**	**-10%**	**-11%**	**-12%**	**-12%**
Nst/St Max	**13%**	**7%**	**5%**	**5%**	**5%**	**6%**	**7%**	**8%**
	2-year	**5-year**	**10-year**	**20-year**	**25-year**	**50-year**	**100-year**	**200-year**
NStOneHourAvg	9.56	12.80	15.19	17.68	18.51	21.24	24.21	27.45
NStOneHourMax	16.59	21.62	25.53	29.76	31.21	36.05	41.45	47.50
StOneHourAvg	9.59	12.92	15.32	17.80	18.63	21.30	24.17	27.26
StOneHourMax	13.67	19.02	23.03	27.25	28.67	33.32	38.38	43.89
Nst/St Avg	**0%**	**-1%**	**-1%**	**-1%**	**-1%**	**0%**	**0%**	**1%**
Nst/St Max	**18%**	**12%**	**10%**	**8%**	**8%**	**8%**	**7%**	**8%**
	2-year	**5-year**	**10-year**	**20-year**	**25-year**	**50-year**	**100-year**	**200-year**
NStSixHoursAvg	21.84	28.36	33.10	38.00	39.64	44.98	50.73	56.98
NStSixHoursMax	25.51	36.99	46.33	56.84	60.54	73.16	87.76	104.71
StSixHoursAvg	21.72	28.44	33.47	38.80	40.61	46.56	53.12	60.37
StSixHoursMax	25.00	34.49	42.32	51.24	54.40	65.26	77.97	92.88
Nst/St Avg	**1%**	**0%**	**-1%**	**-2%**	**-2%**	**-4%**	**-5%**	**-6%**
Nst/St Max	**2%**	**7%**	**9%**	**10%**	**10%**	**11%**	**11%**	**11%**

It can be concluded that on average nonstationary models produce mostly lower return levels for mid and longer return periods for all durations and similar results for short (2 and 5 years) return periods except one hour storm duration. To illustrate stationary and nonstationary return level plots for different return periods and storm durations (10 minutes, 15 minutes, 1 hour, 6 hours) are presented in the Figures 4.11, 4.12, 4.13, 4.14 and IDF curves for various return periods are given in Figure 4.15.

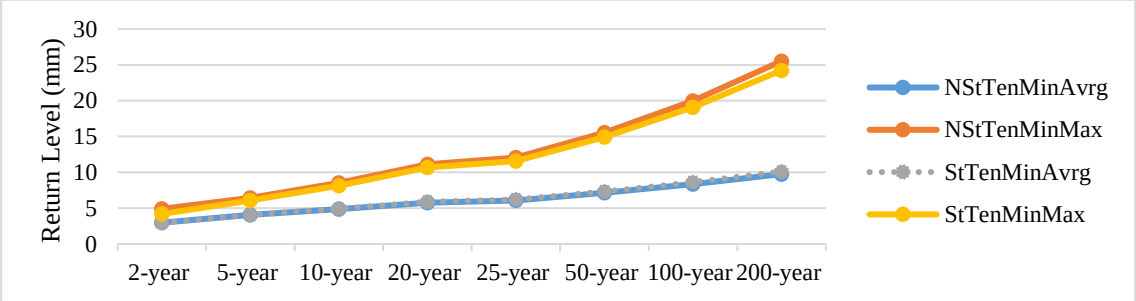

Figure 4.11. Ten Minutes Ensemble Model Comparison for Projected Data

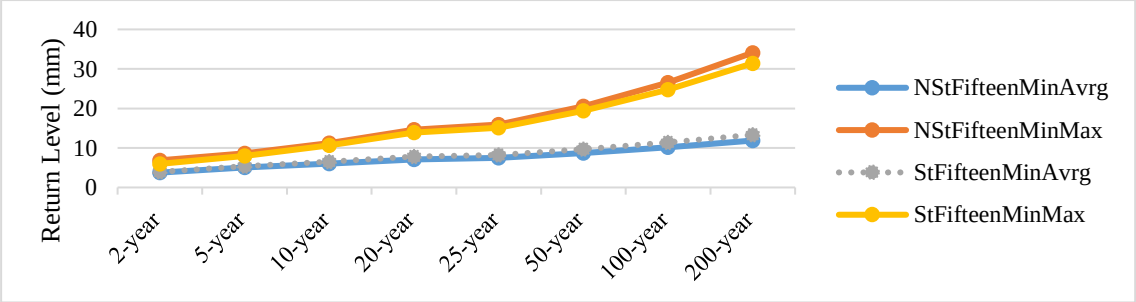

Figure 4.12. Fifteen Minutes Ensemble Model Comparison for Projected Data

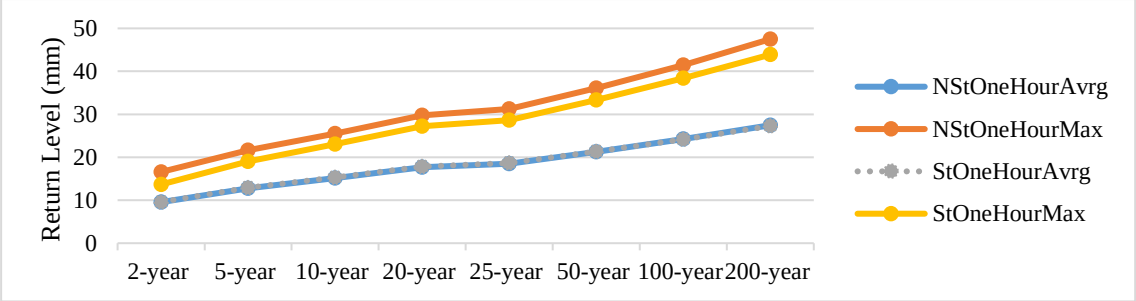

Figure 4.13. One Hour Ensemble Model Comparison for Projected Data

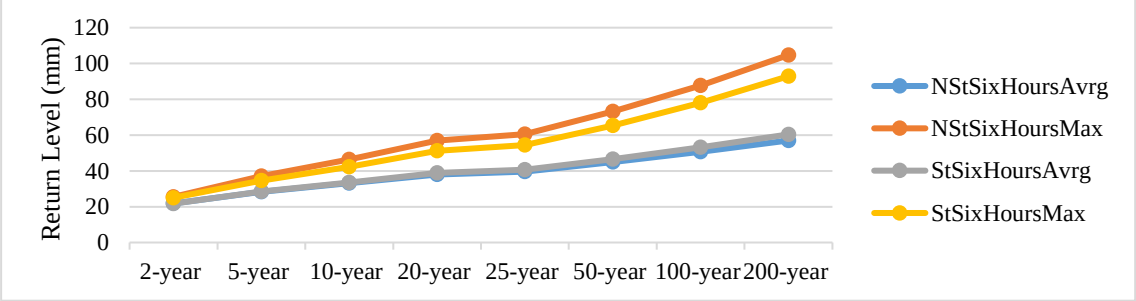

Figure 4.14. Six Hours Ensemble Model Comparison for Projected Data

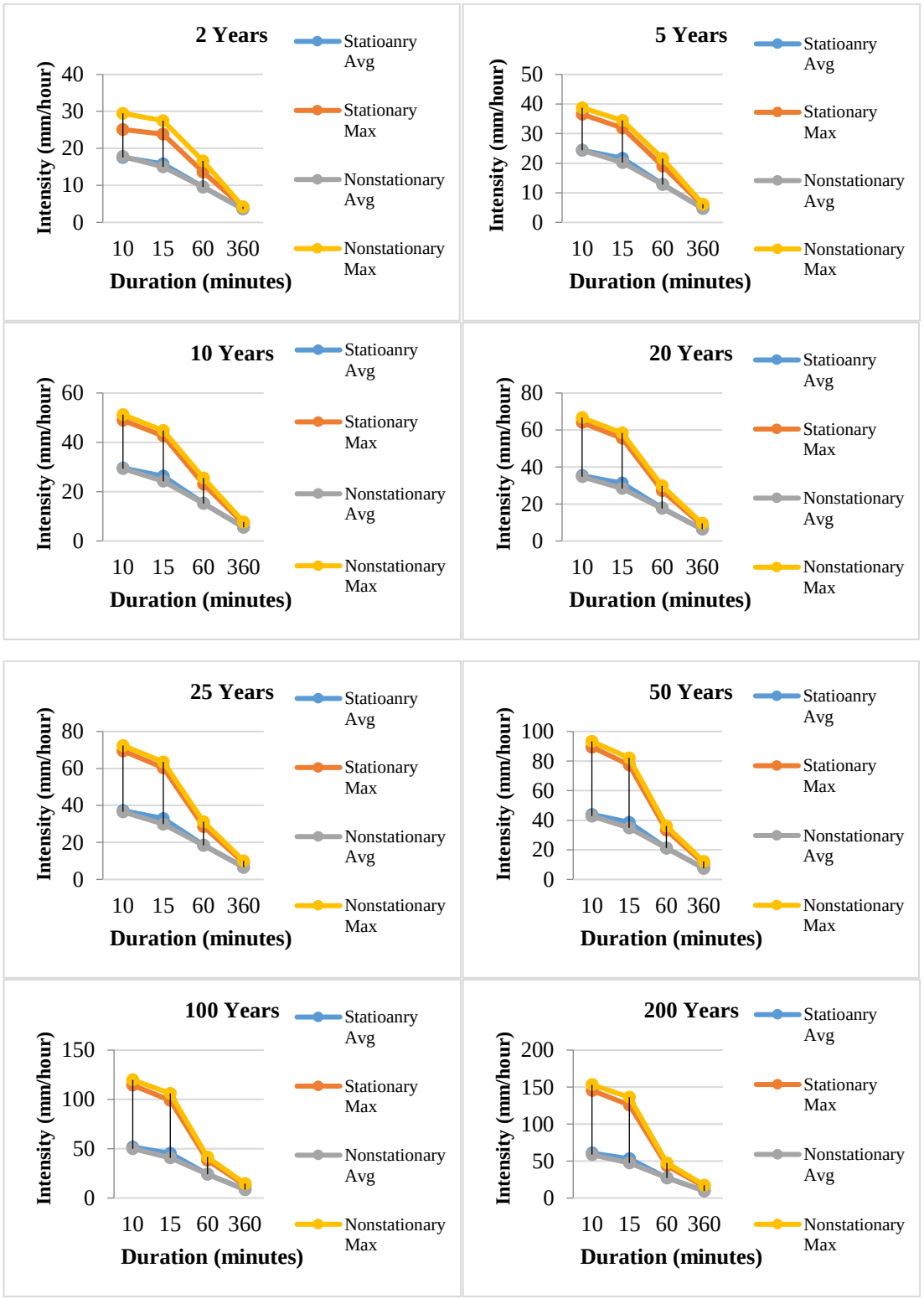

Figure 4.15. Stationary and Best Fit Nonstationary Model IDF Curves

Daily projection results are disaggregated to finer scales in order to derive annual maximum of subhourly and hourly data sets, to apply the methodology and make sensible comparison with the observation period data. The models are applied to a 10-15 minute and 1-6 hour projected (2015-2098) annual maximum storm durations and results of these models are compared with their corresponding observation period results. It is observed that trends in short (in particular sub-hourly) and long storm durations are largely different in terms of statistical significance and directions for model and scenario combinations. On the other most of the trends that are observed are downwards for the projected annul maximum time series. According to projected data driven stationary model results, RCP 8.5 scenarios reveal smaller return level values for GFDL and HG models, except six hours storm duration while stationary MPI model results are greater for RCP 8.5 for storm durations fifteen minutes and one hour and smaller for storm durations ten minutes and six hours. The variations among models and RCP scenarios also identified by other studies. Alam (2014) focus on to derive future IDF curves for Saskatoon, Canada, with possible climate change scenarios and find out that the sign and the magnitude of future variations in extreme precipitation quantiles are dependent to the selection of GCMs and/or RCPs.

Best fit nonstationary return level results are compared with stationary model return level values of every model and RCP scenarios. There are various increases and decreases which can be seen among the time series' results but it can be concluded that on average nonstationary models produce mostly lower return levels for mid and longer return periods for all durations however most of the nonstationary model maximum results are significantly higher than stationary model maximum return level results for all storm durations and return periods. However future projections can reveal different results for different regions. While it is found that stationary return level estimates for projections reveal higher values in this study, DeGaetano et al. (2017) computed future precipitation recurrence probabilities for NY State to consider the future flood risk. The study reveals that at the end of the century, NYS will face a median change of between 20 and 30% increase in one-hundred-year recurrence interval precipitation amounts.

Observed data driven stationary return level values are compared with projected data driven return level values for 10-15 minutes and 1-6 hours storm duration. In this comparison averages and maximum values of projected data driven return level values are used. The comparison results suggest that for 10-15 minutes and 1 hour storm duration; return level values that are derived from observed data are greater almost for all storm durations and return periods. On the other hand for six hours comparison, return level values that are derived from observed data driven models are greater than average projected data driven return level results but smaller than maximum of these projected data driven return level values. If every single projected data driven model results are compared with observed data driven models results it can be seen that observed data driven models reveal greater return level values than all projected data driven models for 10-15 minutes and 1 hour. This means a reduction in the magnitude of extreme precipitation over time. Simonovic et al. (2017) found that a reduction in extreme precipitation in central regions of Canada and increases in other regions based on CanESM2 results but also mentioned the GCM based uncertainty and the difference between ensemble and single model results. In this study also a general decrease in extreme rainfall detected for the Ankara. However for all return periods, six hours storm duration projected data driven model results do not fit the general trend. On the other hand there are uncertainty caused by different aspects of the data and lack of practice as stated in the literature which complicate the analyses especially for future conditions. For instance Fadhel et al. (2017) show that the uncertainty in the future IDF curves resulted from the use of different reference periods to bias-correct the RCM, and that the effect of the reference period on future climate projections is significant and Kara (2014), concluded that all RCMs may underestimate precipitation. Moreover Arnbjerg Nielsen et al., (2013) state the lack of understanding of how to quantify the impacts of climate change and the insufficiency of long term rainfall statistics so the understanding of consequences of climate change stays limited**.**

CHAPTER 5

OVERVIEW OF URBANIZATION: ANKARA CASE

During the last century the number of people living in urban areas has globally increased rapidly. At the beginning of the twentieth century, only 14% of the world population lived in an urban areas, today 55% of the global population reside in urban areas (United Nations, 2018). This increase in urban population is expected to continue until at least 2050 and reach 68% (United Nations, 2018). Since urbanization is one of the main consequences of urban population growth, it is expected that increase in the urban population lead to urbanization over that period.

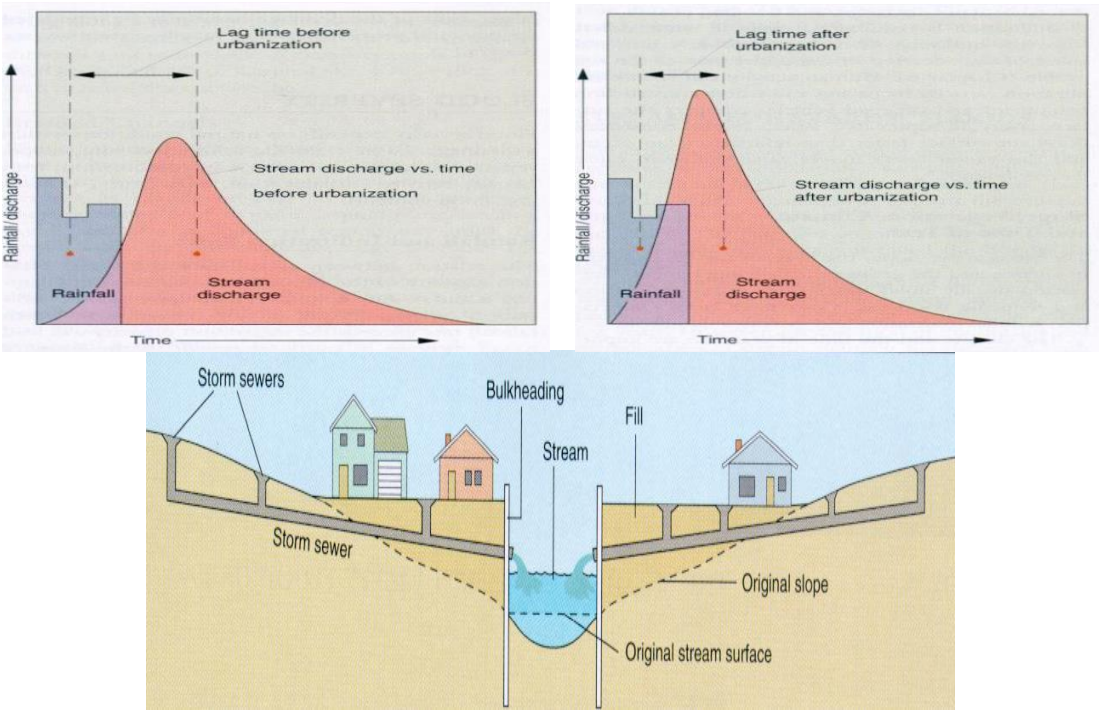

Figure 5.1. Urbanization Effect in a Basin - (surface runoff increases both in volume and in peak discharge value)

Urbanized areas become more vulnerable to flood hazard under conditions of high precipitation intensity (Sun et al., 2011). As a consequence of urbanization impervious surface area increases and that increase brings about significant effects on the hydrological cycle in the urban areas. Increased proportion of impervious surface result in shorter lag times between onset of precipitation and end up with higher runoff peaks and total volume of runoff (Figure 5.1) (Shuster, Bonta, Thurston, Warnemuende & Smith 2005). The conversion of pervious (permeable) land to impervious (non-permeable) surfaces change the hydrologic characteristics of the landscape by reducing infiltration into the soil and evapotranspiration from vegetation which results in a dramatic increase in the rate and volume of stormwater runoff (Guidelines for NYC, 2012).

This chapter presents the development of the urbanization process in Ankara based on the official maps, to investigate the rate of change and trends in urban and green areas in the Province. Late 50s, early 80s, mid 90s and early 2010s situation is briefly compared. In order to assess the effects of urbanization on the urban stormwater network of Ankara, the dynamics of the expansion of urban areas has been investigated. For the analysis of the impacts of urbanization on the stormwater network performance, an assessment of the historical development of the urban areas which leads to land use and land cover change has been carried out. The available maps of Ankara are obtained from GCom and made into processable by Özkil (2015) are used to evaluate the total urbanized and green areas together with the road network.

5.1. LAND USE CHANGE IN ANKARA AND PILOT STUDY AREA

The outputs produced from the land cover change maps showed that urban areas exhibited a very high rate of increase, especially after 1960s for Ankara. The striking expansion of the city of Ankara can be explained with improved construction and transportation technology, expansion policy, migration and rising population. For instance the change in the rural and urban population for Ankara is shown in Figure 5.2. After 80s, the rural population started to decline and for the recent years the rural population is almost became negligible for the demographic statistics. This decline in

the rural population is one of the significant reasons that cause an increase in the urban population. Previous uncontrolled urbanization rate can be explained with the above mentioned points while for the recent years the need or demand for newly built houses especially after the recent earthquakes occurred in the country is increased. Moreover the unit price of newly built residential buildings has a continuous increase due to the intention that ownership is better than tenancy that makes it an investment instrument (Coskun and Jadevicius, 2017). This investment intention may also trigger the demand for residential buildings

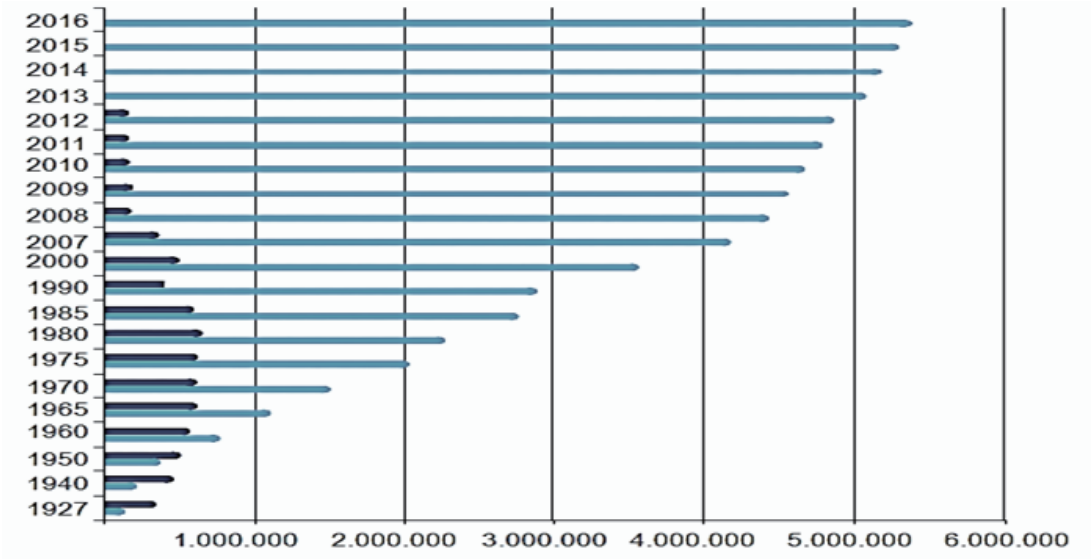

Figure 5.2. Historical Change of City and Village Population in Ankara - Year vs. Population (in Millions) (*Ankara Development Agency, 2018*) Black: Rural population, Grey: Urban population)

As the urbanized area increases in accordance with the population, this growth expands the impervious surfaces. Furthermore, if the expansion that is caused by population growth is fast enough over a region with certain spatial size, then such an expansion ends up with pressure on urban infrastructure that consequently causes illegal built up areas and other socioeconomic and environmental problems.

The change of urbanization (build-up areas), green area and road network for the three periods which derived from the land use change maps (late 1950s - Early 80s, Early 80s - Mid 90s and Mid 90s – recent (2013)) was shown in Figure 5.3. Urban

area, green area and road network are computed for all four maps and total size (area and length) is calculated for the corresponding years. Figure 5.3 compares the cumulative size of expansion of urban areas, green areas and road network for the periods (1959-2013) considered in this study. The expansion size compared with the reference period; for instance the urban area increased about 8 times in 80s compared with the late 50s and about 20 times in early 2010s when compared with the late 50s. Also road network and green area progress in time is given in Figure 5.3 which displays the general trend.

The increase in urbanization is continuous on the other hand this increase has a peak in mid 80s and starts to decrease until mid-90s; then again an intense increase can be seen. Considering the green areas; the rate of change between late 50s to early 80s and early 80s to mid-90s are not remarkable, we can see the significant increase for the green areas between mid-90s to current period which doubles the reference period green area in size. In Figure 5.4 the ratio of green area to urban area is presented. While the green area was 4 times greater than the urban area in late 50s, this situation is reversed in time. There reason for this transformation is drastic increase in the urban areas while the green areas remain almost constant until the mid-90s. Overall we can say that the urban area increased about 20 times while green area increased only 2 times with respect to late 50s.

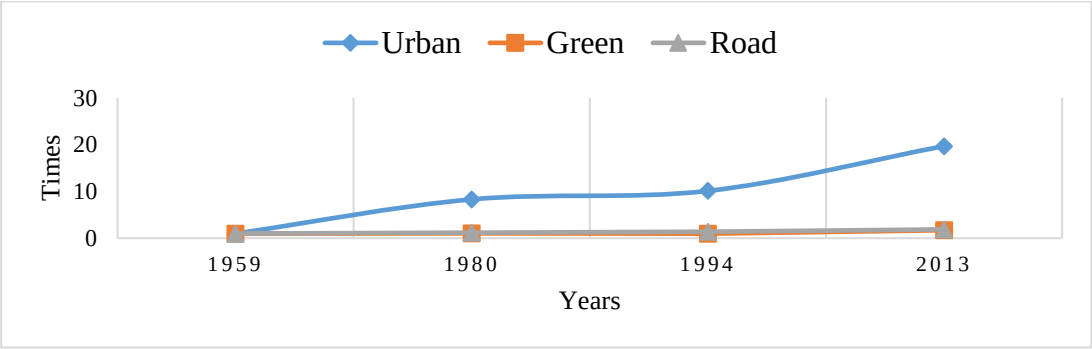

Figure 5.3. Areal Ratio with Respect to Late 50s

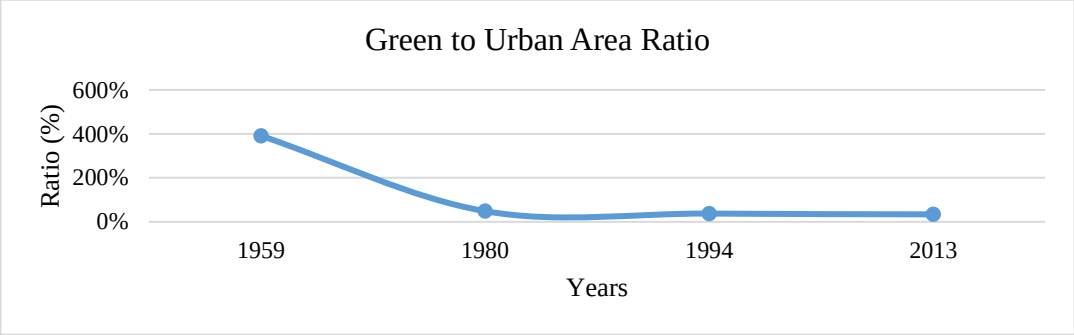

Figure 5.4. Ratio of Green to Urban Area

It is very clear that, Ankara city urbanisation has concentrated after 1960s. These change mentioned above can be seen from the Figure 5.5 which exhibits the last 60 years of urban transformation images for Ankara. The Ankara freeway (blue polyline) remained constant in the graphs to make the comparison easier. Another significant transformation has occurred in the open vast spaces of Ankara. While most of the land turned into dense urbanized areas, the properties of public institutions such as university campuses and military zones tend to remain undeveloped which is also valid for the pilot study area. Development of the urban area boundaries in Ankara City which is presented in Figure 5.5 supports the remarkable increased rates of urbanization mentioned above.

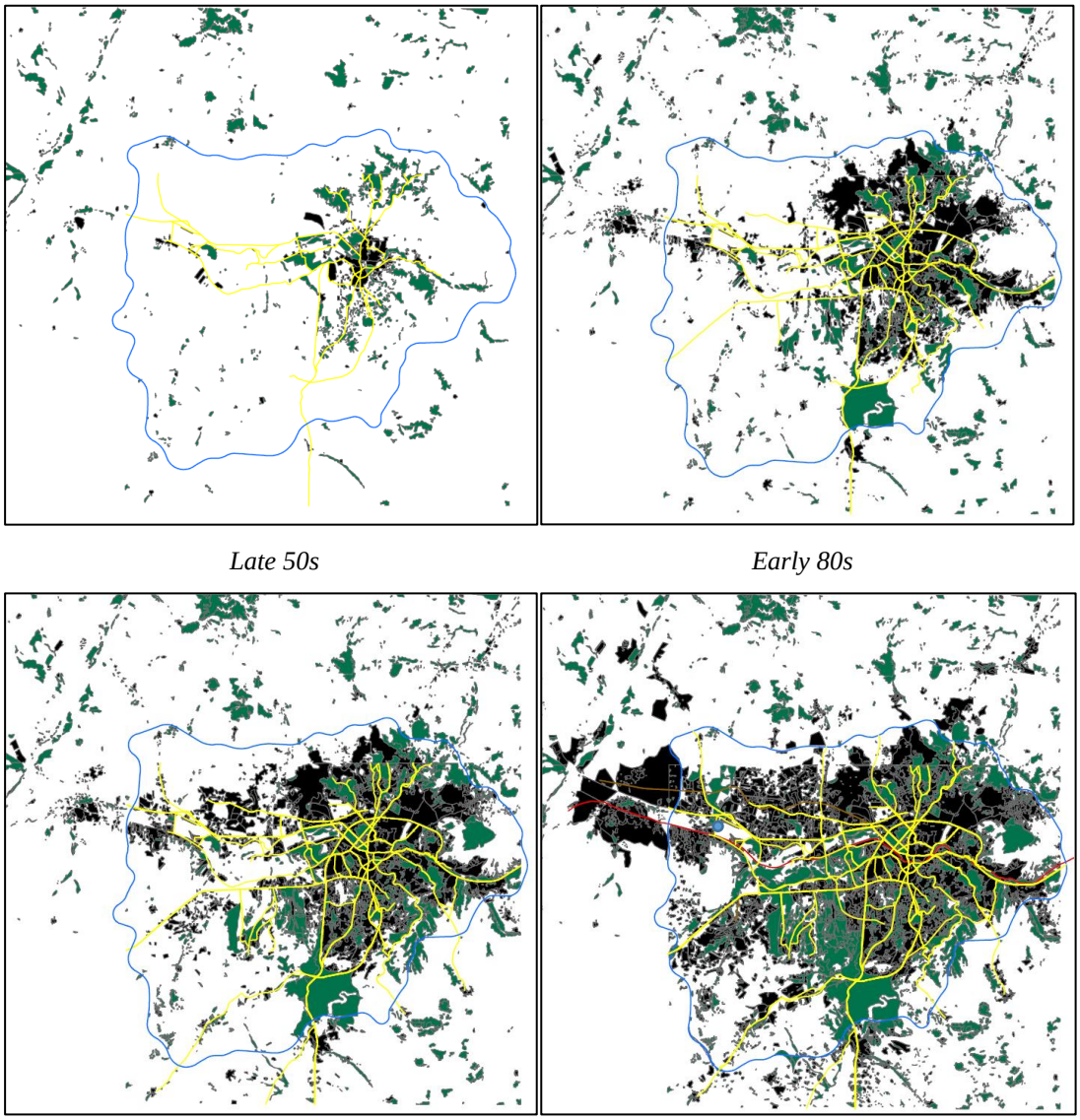

Late 50s *Early 80s*

Mid 90s *Early 2010s*

Figure 5.5. Last 60 Years Urban Transformation of Ankara (Black=Urban, Green=Green Areas)

In this circumstances it can be said that urbanization can generate a considerable increase in the proportion of impervious surfaces and, consequently, the conversion of pervious surfaces to impervious landscape results in increased rate and volume of stormwater runoff.

Figure 5.6. Urban Transformation of Pilot Study Area- Left 2003 and Right 2018

In Figure 5.6 (Google Earth Pro, 2018) the fifteen years transformation can be seen and compared from the maps of the same area for the year 2003 and 2018. For our pilot study area, the general implications for Ankara is applicable for the urban transformation; the open spaces that are stayed undeveloped are generally representing publicly owned areas such as Turkish Sugar Factories and Military.

Area of urban and green and length of road network computed for four different periods to capture the change and trend of urban and green area together with road network for Ankara. Land use/cover types of pilot study area are calculated in order to calculate composite runoff coefficient that considers the effect of different land use/cover types.

In our pilot study area (Figure 5.6), there are several type of cover such as building (roof), parking lot, asphalt, slab on grade (concrete), bituminous sub-ballast, etc. which can be seen in Table 5.1. These cover types have different range of runoff coefficients not only related with the material but also related with the slope of the cover (TDT, 2016; Burke, B. and Burke, T, 2015). There are various land use and

land cover type within the pilot study area. In order to find a better runoff coefficient for the future, both current land use type and the potential development of the undeveloped area are considered. Consequently a composite runoff coefficient is calculated by using weighted average of the land cover types. The reason to choose a single runoff coefficient rather than calculating it for every sub-basin is that the existing (baseline) network is designed considering this approach.

To find out the potential development rate of the undeveloped area for the pilot study area to use in the composite runoff calculations, the rate of increase in the developed area (pervious to impervious) is decided with the general population growth rate, urbanization rate of Ankara and the characteristics of the pilot study area. For instance the undeveloped (grass, natural land, landscaped) area cannot be transformed totally because of the construction constraints, spatial constraints, legal constraints and permits that limits the conversion of pervious surfaces for the pilot study area. The general trend in urbanization is still tend to increase but not as a boom as in previous decades. Also the regulations brings new restrictions and make effort to expand or urbanize in a sustainable way. When all of these above taken into account the maximum convertible part of the total undeveloped area is 90% (90% of undeveloped area can be transformed developed area over time) and the potential cover type is building, slab on grade or asphalt. In these circumstances the calculated runoff coefficient for the future composition of land is 0.9 which can be seen in Table 5.1.

Table 5.1. Cover Types and Runoff Coefficient – Pilot Study Area

Type	Area m²	Runoff Coefficient
Building (Roof)	51,629	0.95
Car Park	18,500	0.95
Landscaped Area	4,650	0.50
Green Area	16,500	0.30
Asphalt-Sub-Ballast	149,000	0.95
Slab on Grade	49,000	0.95
Undevelopped	5,272	0.30
Potential Development Area	47,449	0.95
Composite Runoff Coefficient		**0.90**

As well as precipitation analyses, land use/land cover change is also taken into consideration in the present study. The outputs produced from the land cover change maps which belong to different periods (starting from late 50s to present time) showed that urban areas exhibited a very high rate of increase, especially after 1960s for Ankara. As Çamur et al. (2009) indicates, increased accessibility of people and rising quality of housing construction attract population to near rural fringe settlements and these settlements experience high rate of population growth, lose their rural characteristics and transform into urban or semi-urban areas. Urbanization, green area and road network change between late 1950s to early 2010s are derived from the land use maps (late 1950s - Early 80s - Mid 90s and early 2010s). Urban area, green area and road network are computed for all four maps and total size (area and length) is calculated for the corresponding years. The expansion size compared with the reference period; for instance the urban area increased about 8 times in 80s compared with the late 50s and about 20 times in early 2010s when compared with the late 50s.

The increase in urbanization is continuous on the other hand this increase has a peak in mid 80s due to mainly migration from rural areas and also internal migration as mentioned in Köle (2012). Urbanization continues with a decreasing trend until mid-90s; then again an intense increase can be seen towards the early 2010s due to mainly urban transformation and population increase. Overall it can be concluded that the urban area increased about 20 times while green area increased only 2 times with respect to late 50s. Al-Ruzouq et al. (2018) represent that the expansion of built areas increased the fraction of impervious land and runoff coefficient and Sun et al. (2011) emphasized in their research that runoff increase was highly correlated with the increase in the percentage of urban areas, which are similar results in this study in terms of land use analyses results.

CHAPTER 6

CLIMATE CHANGE AND ALTERATIONS IN THE PRECIPITATION REGIME: STORMWATER NETWORK ANALYSIS

This chapter presents the assessment of stationary and nonstationary models results and demonstrate the behaviour of an existing stormwater network. Same as current (baseline) design, 15 minutes storm duration 2 year return period values of observed and future stationary and nonstationary models are used to re-evaluate the pilot study area stormwater network. Stationary and best fit nonstationary model results are used to figure out the effect of various climate models. Observed (1950-2015) and projected (2015-2098) annual maximum storm durations for Ankara province is used. First the existing design is checked whether or not a revision is needed for the new rainfall intensities and land use change (runoff coefficient). Then, the shifts in existing design (pipe diameter change) due to changing conditions (climatic and land use) are simulated. 15 minutes 5 year return period is also calculated due to literature, global and national standards for such an area and facility (Fortunato et al., 2014; B.Burke and T. Burke, 2015; AWSA).

For stomwater network, there are standards and criteria that must be considered and satisfied for an appropriate design. For instance minimum pipe size varies due to different standards, regulatory bodies and cities; for the so-called baseline (existing) network pipe size (diameter) between Ø300 mm- Ø1200 mm is considered. Also maximum and minimum slope is taken into account when deciding the pipe size. Velocity is another criteria, values for maximum and minimum velocity get different values 0.5 m/s<V < 5 m/s or 0.4 m/s<V < 4 m/s ranges are the commonly used values for stormwater network design. The maximum spacing of manholes, minimum depth of storm sewers are other criteria that must be satisfied during the design process. The comparison of different standards that administrations use such

as Bursa Water and Sewerage Administration (BWSA), AWSA, AWSA Masterplan, İLBANK (Turkey's Bank of Provinces) can be found in Efe (2006), and Regulations on Stormwater Collection, Storage and Discharge Systems prepared by Ministry of Environment and Urbanization can be found in Official Gazette of the Republic of Turkey on 23.07.2017. But to adhere the baseline network design assumptions only the intensity and runoff coefficient changed as design inputs. Additionally, pipe diameters are revised in order to obtain more optimal outcomes for the stormwater network under changing conditions.

6.1. STORMWATER NETWORK ANALYSIS IN ETIMESGUT PILOT STUDY AREA

Stormwater network design and management is examined considering the findings in Chapters 3, 4 and 5 for a railway critical infrastructure located in Etimesgut pilot study area.

In order to figure out the performance of current (existing) stormwater network of pilot study area rainfall return levels that are obtained from observation and projection periods with stationary and nonstationary models are used to calculate intensity input of rational formula. In addition land use/cover change effect is integrated as composite runoff coefficient. Analysis conducted for the following cases; climate change effect applied to existing network by using projection and observation rainfall return levels as intensity input to calculate the peak runoff for the first case. For this case only the intensity has changed and the behaviour of existing stormwater network is observed. For the second case only runoff coefficient has changed and the effect is observed. As the third case, both rainfall return levels and runoff coefficient have changed and the changes in pipe capacities (percent fullness) of existing network is observed. Furthermore, rainfall return level input has changed together with pipe diameter revisions as scenario four and rainfall return level input and runoff coefficient have changed as scenario five together with revision in pipe diameters for a more optimal size within the design criteria.

Existing network design considered the time of concentration 15 minutes and the return period 2 years so the same duration and return period is used for the analyses in this study. On the other hand the minimum return period that recommended is 5 - 10 years (Burke, B. and Burke, T., 2015, Efe, 2006) for urban stormwater networks for the areas with such a critical facility. If there is greater possibility of damage and loss, then also larger frequencies are recommended. So the baseline network capacity is recalculated for 15 minutes 5 years return period values additionally. These (15 minutes - 5 years) design storm depths were also obtained from the observation and projection results. But only observation period results were used for the analyses because the 15 minutes -5 years storm intensities of projections were lower than the baseline design intensity. The operational status of the stormwater network is described as unsatisfactory if the specified hydraulic criteria (e.g. excess pipe capacity, velocity is out of the range) is violated. In this study the capacity surcharge of pipes which is the excess of percent fullness ratio, is described as a failure, where a failure.

Table 6.1 shows pipe capacities for climate change and Figure 6.1 demonstrates percent fullness (maximum capacity) experienced by each pipe for case one.

Table 6.1. Percent Fullness of Models without Pipe Revision-Climate Change

	%0-%20	**%20-%40**	**%40-%60**	**%60-%80**	**%80-%100**
st mpi45	87%	12%	0%	0%	0%
st gfdl45	85%	13%	1%	0%	0%
st hg45	83%	15%	2%	0%	0%
nst mpi45	87%	12%	0%	0%	0%
nst gfdl45	86%	13%	1%	0%	0%
nst hg45	83%	15%	2%	0%	0%
st mpi85	80%	14%	6%	0%	0%
st gfdl85	98%	2%	0%	0%	0%
st hg85	97%	3%	0%	0%	0%
nst mpi85	80%	14%	6%	0%	0%
nst gfdl85	98%	2%	0%	0%	0%
nst hg85	97%	3%	0%	0%	0%
st obs 2 years	69%	18%	9%	4%	0%
nst obs 2years	69%	18%	8%	4%	0%
Baseline Design	69%	19%	8%	4%	0%

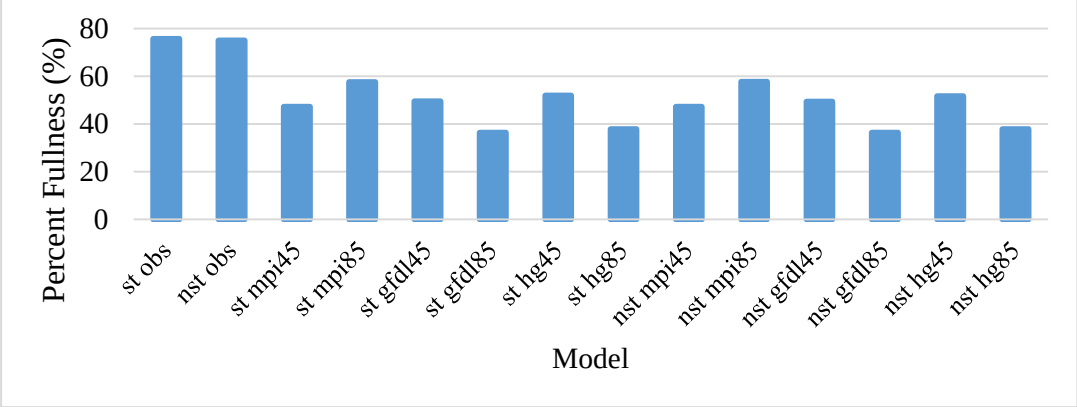

Figure 6.1. Maximum Capacity Experienced during the Projection Period by Each Pipe

As shown in Table 6.1, for the current climate conditions, 96% of the network pipe volume is under the 60% capacity for the baseline design. Only the 4% of the network pipe volume shows a maximum pipe capacity higher than 60%. The 69% of the network pipe volume is reaching a maximum capacity lower than 20%. With regard to the climate change scenario, remarkable changes in the system performance can be observed when compared with current conditions in terms of pipe capacity ranges. Specifically, the maximum pipe capacity reached about the 85% of the network pipe volume stay within the %0-%20 range, while about %15 falls in the %20-%40 range. There are no pipe flows that exceed 60% capacity for all the climate change scenarios. On the other hand observed data in stationary and nonstationary conditions exhibit a parallel capacity range with the baseline design.

Figure 6.2 demonstrates the percent fullness change for case two (for C=0.8 and C=0.9, with and without land use change scenario). Table 6.2 exhibits the pipe capacities for land use change combined with climate change scenarios without any revision for the existing network. Land use and climate change applied together as land use change scenario does not have a significant effect on the percent fullness ratio (Figure 6.2).

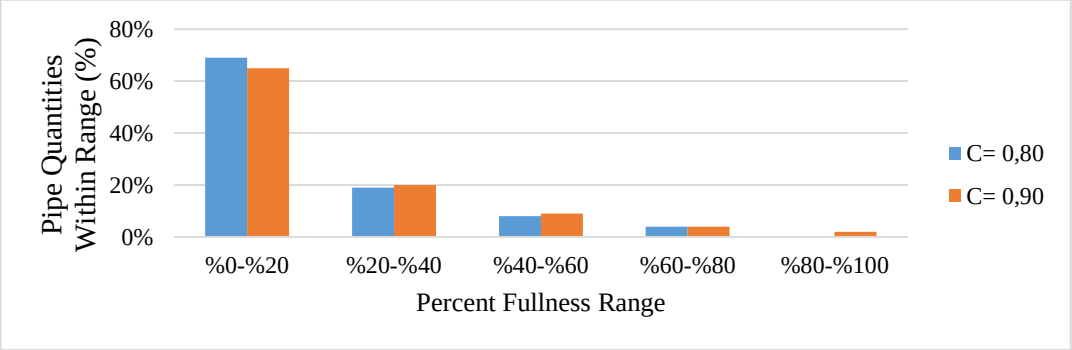

Figure 6.2. Baseline Design Percent Fullness – C=0.8 and C=0.9

Table 6.2. Percent Fullness of Models Without Pipe Revision-Climate Change and Land Use Change (C=0,90)

	%0-%20	%20-%40	%40-%60	%60-%80	%80-%100
st mpi45	85%	13%	1%	0%	0%
st gfdl45	83%	14%	3%	0%	0%
st hg45	81%	13%	6%	0%	0%
nst mpi45	85%	13%	1%	0%	0%
nst gfdl45	83%	14%	3%	0%	0%
nst hg45	81%	13%	6%	0%	0%
st mpi85	76%	16%	7%	1%	0%
st gfdl85	97%	3%	0%	0%	0%
st hg85	97%	3%	0%	0%	0%
nst mpi85	76%	16%	7%	1%	0%
nst gfdl85	97%	3%	0%	0%	0%
nst hg85	97%	3%	0%	0%	0%
st obs 2 years	66%	19%	9%	6%	1%
nst obs 2 years	66%	19%	9%	6%	1%
Baseline Design	65%	20%	9%	4%	2%

Land use change, as shown in Table 6.2, has an additional effect on the distribution of the capacity with regard to climate change scenario but nevertheless for the overall effect it can be said that baseline design can perform well under land use change revised climate change scenarios. The system operated in a satisfactory state refers the condition that the maximum volume that the network system conveys as result of climate change projections for the extreme rainfall will decline throughout the projection period. Land use change scenario (C=0.90) separately and climate change combined with land use change scenario conditions also stay satisfactory for the

baseline design. The outputs produced from the simulations show that performance of the case study stormwater network was observed to operate in a satisfactory state for the climate change scenario experiments, where an unsatisfactory state is defined as an occurrence of the conduit/pipe capacity (percent fullness) exceeding 90%. These results indicate that system performance will be satisfactory by the end of the century.

The existing stormwater network design is observed to operate in satisfactory conditions considering the projected rainfall data however a better allocation of pipe diameters can be achieved when the percent fullness data is examined. For this reason other design parameters such as velocity and minimum depth are compared. The maximum and minimum velocity and minimum water height in the channels are presented in Table 6.3 for case one. Stationary and nonstationary projection results reveal closer values and the highest velocity and depth are computed for observation period stationary and nonstationary models.

Table 6.3. Velocity-Percent Fullness-H Minimum Results for Models Obtained for Baseline Design System

	Maximum velocity (m/sn)	**Minimum velocity (m/sn)**	**Max q/Q_0 (%)**	**H minimum (cm)**
st obs 2 years	3.03	0.26	75.7	1.62
nst obs 2 years	3.02	0.25	75	1.62
st mpi45	2.44	0.2	47.3	0.54
st gfdl45	2.51	0.2	49.5	0.75
st hg45	2.59	0.21	51.9	0.75
st mpi85	2.76	0.23	57.6	1.5
st gfdl85	1.95	0.1	36.4	0.3
st hg85	2.03	0.1	37.8	0.3
nst mpi45	2.43	0.2	47.2	0.54
nst gfdl45	2.51	0.2	49.4	0.75
nst hg45	2.59	0.21	51.7	0.75
nst mpi85	2.76	0.23	57.7	1.5
nst gfdl85	1.95	0.1	36.4	0.3
nst hg85	2.03	0.1	37.8	0.3

Minimum velocity values indicate that the system is over designed and pipe diameter must be decreased or the slope must be increased in order to stay in the design ranges. RCP 8.5 based results for GFDL and HG models show lower intensities so the velocity in the pipes and the fullness decrease for these models. Also the water depth in the pipes reaches its lowest value for these models too. With regard to models results, decreasing trend of extreme precipitation, which is the outcome of projection results, can be one of the reasons that existing system stay satisfactory over time. That means stationary assumption reveals more conservative design conditions for the future.

Furthermore the existing stormwater network is redesigned in terms of pipe diameter to obtain more optimal solutions and compare them with the current quantities. Table 6.4 and Table 6.5 exhibits the pipe capacities for climate change then land use change combined with climate change scenarios respectively with revision for the existing network (case 4 and case 5).

Table 6.4. Percent Fullness of Models with Pipe Revision-Climate Change

	%0-%20	**%20-%40**	**%40-%60**	**%60-%80**	**%80-%100**	**# of >90**
st mpi45	67%	11%	10%	10%	2%	**1**
st gfdl45	67%	6%	11%	11%	5%	**1**
st hg45	67%	6%	11%	11%	6%	**1**
nst mpi45	68%	12%	10%	9%	1%	**0**
nst gfdl45	67%	6%	11%	11%	5%	**1**
nst hg45	67%	6%	12%	10%	5%	**0**
st mpi85	64%	7%	15%	11%	2%	**1**
st gfdl85	71%	7%	11%	9%	2%	**0**
st hg85	70%	6%	10%	10%	4%	**2**
nst mpi85	64%	8%	15%	11%	2%	**1**
nst gfdl85	71%	7%	11%	9%	2%	**0**
nst hg85	70%	6%	10%	10%	4%	**2**
st obs 2 years	59%	8%	15%	14%	4%	**1**
nst obs 2 years	60%	7%	16%	14%	3%	**0**
st obs 5 years	52%	10%	16%	15%	7%	**2**
nst obs 5 years	53%	11%	14%	17%	6%	**1**

In the climate change and revised system scenario, the system performance increases; about the 15% of the network pipe volume shows a maximum pipe

capacity higher than 60% and about 25% the network pipe volume shows a maximum pipe capacity higher than 40% for the projection scenarios. The surcharged range (80%-100%) network pipe volume is equal to 3% but these pipe volumes do not exceed the 90% capacity ratio significantly which can also be seen in Table 6.4. The revision of the system by pipe diameter, which is represented in Table 6.6, results in a reduction of the oversized network. In the 15 minutes 5 years scenario that is originated from observed stationary and nonstationary return levels, the system produces a better drainage system performance, if compared with the baseline scenario. The maximum pipe capacity within 0%-20% reached 52%. About 40% of the network pipe volume has a maximum pipe capacity higher than 40% capacity ratio and about the 16% of the pipes is within 60%-80% capacity range (Table 6.4).

Table 6.5. Percent Fullness of Models with Pipe Revision-Climate Change and Land Use

	%0-%20	**%20-%40**	**%40-%60**	**%60-%80**	**%80-%100**	**>%90**	**>%100**
st mpi45	67%	8%	11%	9%	5%	2%	0%
st gfdl45	66%	6%	9%	9%	10%	4%	1%
st hg45	65%	6%	9%	10%	10%	6%	1%
nst mpi45	67%	9%	11%	8%	4%	1%	0%
nst gfdl45	67%	5%	9%	10%	9%	4%	1%
nst hg45	65%	7%	10%	9%	9%	5%	0%
st mpi85	62%	7%	9%	14%	7%	2%	0%
st gfdl85	70%	6%	10%	10%	4%	1%	0%
st hg85	69%	6%	10%	7%	7%	4%	1%
nst mpi85	62%	8%	10%	14%	6%	2%	0%
nst gfdl85	71%	6%	9%	10%	5%	2%	0%
nst hg85	69%	6%	10%	7%	7%	4%	1%
st obs 2	56%	11%	9%	13%	11%	4%	0%
nst obs 2	56%	10%	10%	13%	10%	4%	0%
st obs 5	50%	11%	12%	14%	11%	7%	3%
nst obs 5	50%	11%	12%	13%	12%	6%	0%

In addition to climate change scenario, also the new composite runoff coefficient (0.9) is applied to the design. The revised system performance simulated under these new conditions and results are given in Table 6.5. The surcharged range (80%-100%)

of network pipe volume has increased and there are pipe volumes that exceed the 90% and 100% capacity ratio significantly.

The hydraulic performance of the baseline and revised system for the observed and projected rainfall data has been compared in terms of the pipe capacity ratio associated with various pipe capacity range (0-20%, 20-40%, 40-60%, 60-80% and 80-100%). It can be seen that system continuity can be satisfied with various design conditions, including climate change and land use, for all return level results. The remarkable point is that the system can perform with lower pipe diameters than it is designed. Table 6.6 shows the diameter change, quantities of small size and large size pipes in meters for every diameter (200 mm to 1600 mm) and total quantities of small (200 mm to 600 mm) and large (800 mm to 1600 mm) size pipes. Table 6.7. exhibits the % change in pipe length for every diameter after revision compared with baseline design. Figure 6.3 also shows the total small and large size pipe quantities (lengths in meters) of baseline (existing) design and revised network's small and large size pipe quantities due to climate change scenarios.

Table 6.6. Pipe Quantities for Models (in meters) Small (200-600 mm) and Large (800-1600 mm) Size-After Revision

Small Size Pipes	Ø200	Ø300	Ø400	Ø500	Ø600	Total
Baseline Design	-	2,557	618	132	330	3,638
	Ø200	**Ø300**	**Ø400**	**Ø500**	**Ø600**	**Total**
st mpi45	-	3,514	299	751	163	4,727
st gfdl45	-	3,504	605	455	153	4,717
st hg45	-	3,447	503	574	194	4,717
nst mpi45	-	3,376	437	751	163	4,727
nst gfdl45	-	3,447	662	455	153	4,717
nst hg45	-	3,447	473	603	194	4,717
	Ø200	**Ø300**	**Ø400**	**Ø500**	**Ø600**	**Total**
st mpi85	-	3,358	340	787	164	4,650
st gfdl85	-	3,966	621	434	113	5,134
st hg85	-	3,966	621	434	113	5,134
nst mpi85	-	3,301	397	787	164	4,650
nst gfdl85	-	3,966	621	434	113	5,134
nst hg85	-	3,966	621	434	113	5,134
	Ø200	**Ø300**	**Ø400**	**Ø500**	**Ø600**	**Total**
st obs 2 years	-	3,214	504	383	450	4,550
nst obs 2 years	-	3,226	492	383	450	4,550
st obs 5 years	-	3,169	234	252	790	4,444
nst obs 5 years	-	3,169	273	217	786	4,444
Large Size Pipes	**Ø800**	**Ø1000**	**Ø1200**	**Ø1400**	**Ø1600**	**Total**
Baseline Design	1,089	441	45	-	-	1,575
	Ø800	**Ø1000**	**Ø1200**	**Ø1400**	**Ø1600**	**Total**
st mpi45	462	24	-	-	-	486
st gfdl45	450	45	-	-	-	496
st hg45	395	101	-	-	-	496
nst mpi45	385	101	-	-	-	486
nst gfdl45	450	45	-	-	-	496
nst hg45	395	101	-	-	-	496
	Ø800	**Ø1000**	**Ø1200**	**Ø1400**	**Ø1600**	**Total**
st mpi85	462	101	-	-	-	563
st gfdl85	55	24	-	-	-	79
st hg85	55	24	-	-	-	79
nst mpi85	462	101	-	-	-	563
nst gfdl85	79	-	-	-	-	79
nst hg85	55	24	-	-	-	79
	Ø800	**Ø1000**	**Ø1200**	**Ø1400**	**Ø1600**	**Total**
st obs 2 years	562	101	-	-	-	663
nst obs 2 years	562	101	-	-	-	663
st obs 5 years	330	415	24	-	-	769
nst obs 5 years	330	415	24	-	-	769

For the 15 minutes 5 years return levels, increase in the rainfall intensity cause system failure; about 10% of the pipes excess capacity for the baseline (existing) network. The current system also can perform well under the 15 minutes 5 years return period loads with revisions in pipe diameter such as increase in large size and decrease in small size quantities which can be seen from Table 6.6, 6.7 and Figure 6.3. The revised network for 2 years 15 minutes rainfall intensities can also be designed with several changes in pipe diameter for 15 minutes 5 years return period loads which at the end result increase in small size pipes and decrease in large size pipes with respect to existing (baseline) design pipe quantities.

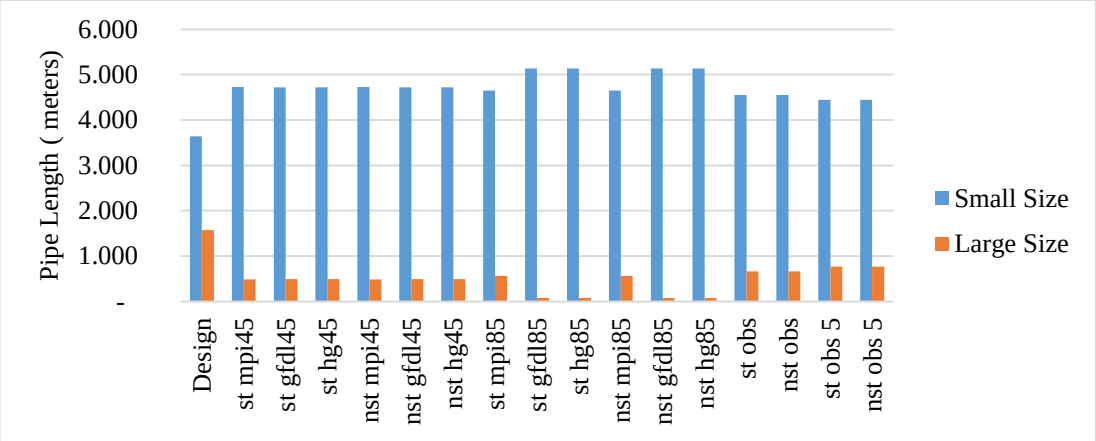

Figure 6.3. Small vs. Large Size Pipe Quantities – Baseline and Revised System Pipe Lengths in Meters

Table 6.7. Pipe Diameter Change for the Models Compared with Baseline Design

Model	Ø300	Ø400	Ø500	Ø600	Total Change (Small Size)	Ø800	Ø1000	Ø1200	Total Change (Large Size)
st mpi45	37%	-52%	469%	-51%	**30%**	-58%	-95%	-100%	**-69%**
st gfdl45	37%	-2%	245%	-54%	**30%**	-59%	-90%	-100%	**-69%**
st hg45	35%	-19%	335%	-41%	**30%**	-64%	-77%	-100%	**-69%**
nst mpi45	32%	-29%	469%	-51%	**30%**	-65%	-77%	-100%	**-69%**
nst gfdl45	35%	7%	245%	-54%	**30%**	-59%	-90%	-100%	**-69%**
nst hg45	35%	-23%	357%	-41%	**30%**	-64%	-77%	-100%	**-69%**
st mpi85	31%	-45%	496%	-50%	**28%**	-58%	-77%	-100%	**-64%**
st gfdl85	55%	0%	229%	-66%	**41%**	-95%	-95%	-100%	**-95%**
st hg85	55%	0%	229%	-66%	**41%**	-95%	-95%	-100%	**-95%**
nst mpi85	29%	-36%	496%	-50%	**28%**	-58%	-77%	-100%	**-64%**
nst gfdl85	55%	0%	229%	-66%	**41%**	-93%	-100%	-100%	**-95%**
nst hg85	55%	0%	229%	-66%	**41%**	-95%	-95%	-100%	**-95%**
st obs 2	26%	-18%	190%	36%	**25%**	-48%	-77%	-100%	**-58%**
nst obs 2	26%	-20%	190%	36%	**25%**	-48%	-77%	-100%	**-58%**
st obs 5	24%	-62%	91%	139%	**22%**	-70%	-6%	-48%	**-51%**
nst obs 5	24%	-56%	64%	138%	**22%**	-70%	-6%	-48%	**-51%**

Furthermore the effect of design revision due to changing climatic conditions is reflected in terms of cost in Table 6.8. Only the cost associated with pipe diameter is calculated by using actual project unit price. Concrete and reinforced concrete which is determined according to the pipe diameters (small size or large size group) unit prices are different that is why total cost decreases with model results.

Total cost of models that reveal lower rainfall intensity has the lowest ones such as stationary GFDL model RCP8.5 or HG model RCP8.5. In general RCP4.5 results reveal higher total cost than RCP8.5 results probably because of the increasing temperature and decreasing precipitation, besides MPI model stationary and nonstationary results. Observed data driven design alternatives have the higher cost among the all alternatives, yet they are still lower than the existing design.

Table 6.8. Cost Comparison of Models after Revision (in Euros)

	Ø300-Ø600 Cost	Ø800-Ø1200 Cost	Total-Euro
Baseline Design	260k	833k	1,093k
st mpi45	338k	257k	595k
st gfdl45	337k	262k	599k
st hg45	337k	262k	599k
nst mpi45	338k	257k	595k
nst gfdl45	337k	262k	599k
nst hg45	337k	262k	599k
st mpi85	332k	298k	630k
st gfdl85	367k	42k	409k
st hg85	367k	42k	409k
nst mpi85	332k	298k	630k
nst gfdl85	367k	42k	409k
nst hg85	367k	42k	409k
st obs 2 years	325k	351k	676k
nst obs 2 years	325k	351k	676k
st obs 5 years	318k	407k	725k
nst obs 5 years	318k	407k	725k

Overall, the total cost results of alternative design options indicate that the storm sewer system can be built at a lower total cost not only for all climate change and land use options but also for the 2 and 5 years 15 minutes observed data driven return level results. On the other hand the unit cost of pipes are unique to the project (regarding this, information that have been presented in this study cannot be used or reproduced without permission) due to tender method and cannot be generalized.

The system operated in a satisfactory state and it can be said that according to climate change projections for the extreme rainfall, the maximum volume that the system face will not exceed baseline design criteria throughout the projection period. Combination of climate change and land use change conditions also stay satisfactory for the baseline design which used 15 minutes storm duration and 2 years return period as intensity input. It can be said that the current network system can perform appropriately under the loads from 1950-2015 and 2015-2098 periods that are delivered by stationary and nonstationary assumption. On the other hand the system may fail under the loads derived separately or together by longer storm duration

(over 15 minutes and more) or higher return periods (such as 5 years and more) that is computed from stationary and nonstationary observed data analysis which is a preferred design input for such a critical facility and area.

By contrast with this study, the general outcome of the future period studies with regard to stormwater networks in literature is that current systems will probably fail and cannot withstand considering the future climate conditions. For instance Thakali et al. (2016) specify that the present capacity of most urban drainage systems is expected to be overload in the near future and the analysis of the present stormwater facilities of the Flamingo and Tropicana watershed showed that these facilities are unable to sustain their performance under the loads resulting from the projected climate scenario. Furthermore Osman (2014), also showed that in the future the urban drainage system of the area that he studied could react differently in terms of increase in number of surcharged sewers and from manholes surface flooding and Larsen et al. (2008) pointed out that a 100-year event in the control period for Sweden will be shorten due to climate change scenarios and damages caused by urban flooding will probably occur more frequently.

6.2. STORMWATER NETWORK SYSTEM IN ANKARA PROVINCE: GENERAL ASSESSMENT

With regard to stormwater network design in Ankara, there are two important aspects; one is selection of the design parameters and the other is application of these parameters in construction phase in an appropriate environment. For instance selecting an appropriate design load (e.g. storm duration and return period) is important for the network design on the other hand if the runoff cannot be routed correctly to the system then surface flooding occur. Infrastructure is relatively a long term investment and conditions may change during the proposed design life such as decrease in pervious land, population growth etc. lasting with increasing load exposure for the system, so monitoring is an essential part for a vital stormwater management process.

Selecting the optimum parameter is another issue, for the changing environmental conditions together with urbanization brings out the need for a new approach. Design parameters cannot be assumed stationary for such a long term design lives so temporal, spatial or other changes must be considered for the design process which makes involvement of multiple bodies to the design process necessary. While selecting the design approach and parameters also a risk based approach should be applied; for this not only physical damage but also environmental and social cost of the event must be considered. The cost of designing a network for 10 minutes 10 years return period rainfall will probably be higher than a 15 minutes 2 years return period rainfall based design as the design intensity increases which brings out the larger pipe diameters. Nevertheless decision making mechanism must take into account not only the extra cost derived by the design parameter but also the cost of loss of life, reputation, interruption of business etc. Because Ankara is the capital of Turkey, centre of the bureaucracy, transportation hub for high speed rail and host of many entities that are determining bodies of economic and social state of affairs design process of stormwater network must consider the above mentioned conditions.

CHAPTER 7

SUMMARY, CONCLUSIONS, AND RECOMMENDATIONS

7.1. SUMMARY

In the present study, rainfall analysis for the past, the present and the future conditions, which enables us to incorporate climate change and variability into infrastructure design and management, is performed and discussed for stationary and non-stationary conditions for the past (1950-2015 period) observed data and for the future projections (2015-2098 period) for Ankara province -Turkey. Official records of Turkish State Meteorological Services for observation period and the results of RCP4.5 and the RCP8.5 scenarios regional climate model solutions based on the HadGEM2-ES, MPI-ESM-MR and GFDL-ESM2M models for future periods have been used.

Daily future projections are disaggregated to finer scales and used for the future conditions analysis. Nonstationary GEV and stationary GEV models for observed and future data is obtained. Also partial periodic analysis besides whole period analysis is conducted to capture the difference and change within long term data for the observation period. Rainfall extreme value frequency analysis is performed for observation and future periods with model results for stationary and nonstationary conditions for Ankara province and design criteria and performance of current as well as potential infrastructure designed with current codes and standards is investigated.

Moreover land use change - urbanization and their potential effect on stormwater network is investigated to avoid present and future problems such as floods. The type and rate of change is examined, past and current land use-land cover situation is

compared and possible effects of these variations on stormwater network is investigated. Stormwater network is examined considering the nonstationarities and future conditions for the pilot study area. The pre-studies of a framework is presented which can be used to investigate spatial changes together with climatic variations that increase the hydrologic risk for the whole Ankara municipal area.

The outcomes of this study can be used as a tool to rehabilitate and future design of stormwater network of Ankara. In order to perform a novel and holistic design approach the framework given in this study can be used as a baseline; analyses which are conducted for the pilot study area can be applied to the city of Ankara through the development and adaptation of the process. Also it can be said that simple engineering design cannot be trusted solely; evolution of the parameters such as rainfall intensity or runoff coefficient brings out the requirement of periodic assessment and evaluation. The various outcomes of studied climate models and scenario results prove that parameter selection must rely on analyses and include probable changes and uncertainty.

Stormwater design variations for model and RCP combinations reveal that lower rainfall intensity has the lower costs such as stationary GFDL model RCP 8.5 or HG model RCP 8.5. In general RCP 4.5 results reveal higher total cost than RCP 8.5 results except MPI model stationary and nonstationary results. Observed data driven design alternatives have the higher cost among the all alternatives. Overall, the total cost results of alternative design options indicate that the storm sewer system can be built at a lower total cost for all options. These economic implications should be evaluated for the feasibility of future network design in order to find an optimum solution.

7.2. CONCLUSIONS

Present study showed that, the stationary GEV models were capable of fitting extreme rainfall data for all storm durations but the non-stationary GEV models showed advantage over the stationary models according to diagnostic tests and values. The differences in return level estimates between two observation periods

(1950-1975 and 1976-2015), entire period and nonstationary assumption models support the need to update the current design parameters such as return level, return period, runoff coefficient with the most recent data and approaches. The differences also reveal the need to conduct analysis using future climate data. Nonstationary model results are in general exhibited smaller return level values with respect to stationary model results of each storm duration for the observed data driven model results.

Considering the projected data driven model results; it can be concluded that on average nonstationary models produce mostly lower return levels for mid and longer return periods for all durations and similar results for short (2 and 5 years) return periods except one hour storm duration for the projected data.

Almost all the nonstationary model maximum return level results are significantly higher than stationary model maximum return level results for all storm durations and return periods for the projected data driven model results.

Observed data driven stationary return level values are compared with projected data driven return level values for 10-15 minutes and 1-6 hour storm duration. Return level values that are derived from observed data are greater almost for all storm duration and return period for 10-15 minutes and 1 hour storm duration. Return level values that are derived from observed data driven models are greater than average projected data driven return level results for six hour comparison but smaller than maximum of these projected data driven return level values.

In terms of land use change, the expansion size compared with the reference period (late 50s). The urban area increased about 8 times in 80s compared with the late 50s and about 20 times in early 2010s when compared with the late 50s while green area increased only 2 times with respect to late 50s in Ankara province. This reveals that Ankara has and will have risks of facing the urban floods which causes and will cause disasters, social life problems and economical lost.

All the analyses reveal that the current network system in Etimesgut pilot study area can sustain its performance hence stationary observation period analyses results can be used for the design values. Yet nonstationary results allow to make a risk based design, by using quantiles of nonstationary return level results. While stationary analysis produce single value, nonstationary analysis introduce a range of values changing with the corresponding covariate, a set of design values that can be evaluated according to risk perception and experience of the designer together with regulations and standards. Nonstationary return level estimates can be an essential part of engineering risk assessment purpose. Ignoring the stationary assumption may result with substantial overestimation as well as underestimation of extremes, which brings out the failure of infrastructure or waste of money.

The framework applied in this thesis can be applied anywhere (e.g. for Ankara province) since enough data is available if the extremes are the concern. The projection period return level estimates can also be applied not only the pilot study area but also the region that the projection grid cover.

Also application of observation and projection data analysis and their integration to an actual Etimesgut pilot stormwater network together with land use/land cover change analysis (considering the development) is a novel framework that can be used for Ankara.

Quantification and incorporation of climate change can be achieved by using above mentioned framework that is expressed in Chapter 2 and applied in Chapters 3, 4, 5 and 6.

7.3. RECOMMENDATIONS

To improve the results of the analyses conducted in this study and to extend the contribution for the future studies (to scientific research and application studies for society welfare), the following suggestions were presented:

- Climatic conditions effect urban hydrology so it is highly recommended that the effects of climate change be studied and incorporated into urban infrastructure design which has high investment costs and service life. Furthermore not only the land but also the climatic conditions must be evaluated within the urban catchment as the atmospheric pattern can exhibit changes even within the catchment.

- The outcome of the present study clearly shows that land use change and urbanization directly affect urban hydrology by increasing peak flows and capacity ratios of pipes. Therefore, the catchment that is subject to change should be investigated carefully and the reaction of characteristics of that catchment be considered in terms of sensitivity. Therefore land use change / urbanisation characteristics of the area should be monitored for long periods and stormwater network rehabilitation and/or network design studies should be performed accordingly.

- Rapid urbanization, with its accompanying land use changes increasing impervious areas, can cause localised in the peak discharge. While conducting a land development process land use and land cover of existing situation as well as future periods must be considered.

- Addition of various other Global Climate Models (GCMs) and working with model ensembles, improvement in the disaggregation process by using various types of Bartlett-Lewis Rectangular Pulse Model in terms of extreme production for future projections are advised.

- An urban catchment has complex and dynamic features and characteristics so it should be vital to use 1D, 2D or combination of these to get better results. Also, such models enable to work with various scenarios, enable to integrate present and future conditions and allow to use and couple data that is driven from other sources such as GIS, etc.

- Infrastructure system should be monitored as a whole, any effect which is caused by land use change, refurbishment, etc. or an instant event such as flash flood in a part of the system should be integrated in order to identify the responses of subdivisions and basins so that networks be tracked properly.

- As urban infrastructure has high rate of investment and long term projects, a cost benefit analysis is recommended nevertheless while considering the costs besides economic, social and environmental costs should be considered and rather than conventional analyses a value based analyses should be considered.

- The framework represented in this study should be applied to other urban areas in order to get an impression for the current and future conditions considering the changing climate.

- The parameters derived in this study for Ankara will be a base not only for design/redesign, rehabilitation of stormwater network but also for research studies concerned with climate change, land use change and their effect over urban flooding for Ankara.

REFERENCES

Abdellatif, M., Atherton, W., & Alkhaddar, R. (2013). Application of the stochastic model for temporal rainfall disaggregation for hydrological studies in North Western England. *Journal of Hydroinformatics*, 15(2), 555-567.

Alam, S. (2014). *Construction of the intensity-duration-frequency (idf) curves under climate change*. Master of Science, University of Saskatchewan.

Ankara Development Agency, (2018). Ankara statistics 2017. Retrieved from http://www.ankaraka.org.tr/tr/istatistiklerle-ankara-2017_4028.html.

Arnbjerg-Nielsen, K., Willems, P., Olsson, J., Beecham, S., Pathirana, A., Gregersen, I. B., & Nguyen, V-T. V. (2013). Impacts of climate change on rainfall extremes and urban drainage systems: A review. *Water Science and Technology*, 68(1), 16-28. Doi: 10.2166/wst.2013.251.

Arnold, C. L., & Gibbons, C. J. (1996). Impervious surface coverage: the emergence of a key environmental indicator. *Journal of the American Planning Association*, 62(2), 243-258.

Asikoglu, O. L., & Ciftlik, D. (2015). Recent rainfall trends in the Aegean region of Turkey. *J. Hydrometeor.*, 16, 1873–1885. doi: 10.1175/JHM-D-15-0001.1

Bahadur, A., Tanner, T., and Pichon. F. (2016). *Enhancing Urban Climate Change Resilience: Seven Entry Points for Action.* Manila. Asian Development Bank. ©ADB.

Batuman, B. (2013). City profile: Ankara. *Cities*, 31. 578–590. 10.1016/j.cities.2012.05.016

Bauer, M. E., Heinert, N. J., Doyle, J. K., & Yuan, F. (2004). Impervious surface mapping and change monitoring using landsat remote sensing. *Proceedings of American Society for Photogrammetry and Remote Sensing (ASPRS) Annual Conference*, Denver, CO, USA.

Bauer, M. E., Loffelholz, B. C., & Wilson, B. (2007*). Impervious timating and Mapping Impervious Surface Area by Regression Analysis of Landsat Imagery*. Chapter In (Eds.) Weng, Q., Remote Sensing of Impervious Surfaces. CRC Press, Boca Raton, FL, USA.

Bayazit, M. (2015). Nonstationarity of hydrological records and recent trends in trend analysis: A State-of-the-art Review. *Environmental Processes,* 2, 527-542.

Berg, N., Hall, A., Sun, F., Capps, S., Walton, D., Langenbrunner, B., & D. Neelin, (2015). Twenty-first-century precipitation changes over the los angeles region. *J. Climate*, 28, 401–421. https://doi.org/10.1175/JCLI-D-14-00316.1

Burke, C. B., & Burke, T. T. (2015). Stormwater Drainage Manual 2015. Indiana Local Technical Assistance Program (LTAP) Publications. 100.

Busuioc, A., Dobrinescu, A., Birsan, M., Dumitrescu, A., & Orzan, A. (2015). Spatial and temporal variability of climate extremes in Romania and associated large-scale mechanisms. *Int. J. Climatol.*, 35, 1278-1300. doi:10.1002/joc.4054

Buttstadt, M., & Schneider, C. (2014). Climate change signal of future climate projections for Aachen, Germany, in terms of temperature and precipitation. *Mareike*, 68(2), 71-83.

Cai, Y., & Hames, D. (2010). Minimum sample size determination for generalized extreme value distribution,communications in statistics. *Simulation and Computation,* 40(1), 87-98. doi: 10.1080/03610918.2010.530368

Çamur, C. K., & Yenigül, S. B. (2009). The Rural-Urban transformation through urban sprawl: an assessment of Ankara metropolitan area. *The 4th International Conference Of The International Forum on Urbanism (IIFoU),* Amsterdam/Delft.

Chalmers P. (2014). Climate change: implications for buildings, key findings from the intergovernmental panel on climate change fifth assessment report.

Cheng L., AghaKouchak A., & Phillips T. (2015). Non-stationary return levels of cmıp5 multi-model temperature extremes. *Climate Dynamics*, 44(11), 2947-2963. doi: 10.1007/s00382-015-2625-y.

Cheng, L. (2014). *Frameworks for univariate and multivariate non-stationary analysis of climatic extremes*, PhD. Dissertation, UC Irvine.

Cheng, L., & AghaKouchak, A. (2014). Nonstationary precipitation intensity-duration-frequency curves for infrastructure design in a changing climate. *Sci. Rep.* 4, 7093. doi:10.1038/srep07093

Coles, S. (2001). *An Introduction to Statistical Modeling of Extreme Values*, Springer, London.

Coles, S. G., & Sparks, R. S. J. (2006). Extreme *value methods for modelling historical series of large volcanic magnitudes.* Chapter 5, Statistics in Volcanology.

Collet L., Beevers, L., & Prudhomme C. (2017). Assessing the impact of climate change and extreme value uncertainty to extreme flows across Great Britain. Water, 9(2),103.

Coskun Y., & Jadevicius A. (2017). Is there a housing bubble in Turkey?. *Real Estate Management and Valuation,* 25(1), 48-73.

Crawford, M., & Seidel, S. (2013). Business Weathering (the Storm: Building Business Resilience Building Business Resilience. Washington, DC.: Center for Climate Change and Energy Solutions. Retrived from: www.c2es.org/docUploads/business-resilience-report-07-2013-final.pdf

Cukur, H. (2011). Daily precipitation variations of selected meteorological stations in Turkey. *Procedia - Social and Behavioral Sciences*, 19, 617-626.

Danandeh Mehr, A. and Kahya, E. (2016). Climate change impacts on catchment-scale extreme rainfall variability: Case Study of Rize Province, Turkey. *Journal of Hydrologic Engineering*, 10.1061/(ASCE)HE.1943-5584.0001477 , 05016037.

DeGaetano, A. T., & Castellano, C. M. (2017). Future projections of extreme precipitation intensity-duration-frequency curves for climate adaptation planning in New York State. *Climate Services*, 5, 23-35.

Eckersten, S. (2016). Updating *rainfall intensity-duration-frequency curves in sweden accounting for the observed increase in rainfall extremes*, Examensarbete 30.

EEA, (2017). *Landscapes in transition, an account of 25 years of land cover change in Europe.* EEA Report No 10/2017, European Environment Agency.

Efe, M. (2006). *Review of modelling softwares used in design and operation of sewerage and storm water collection systems*, (Master's Thesis), Graduate School of Natural and Applied Sciences, Istanbul Technical University.

Efstratiadis, A., and D. Koutsoyiannis, An evolutionary annealing-simplex algorithm for global optimisation of water resource systems, (2002). *Proceedings of the Fifth International Conference on Hydroinformatics*, Cardiff, UK, 1423-1428, International Water Association, (http: //itia.ntua.gr/el/docinfo/524/)

Ekström, M., Gutmann, E., Wilby, R. L., Tye, M. R., & Kirono, D. G. C. (2018). Robustness of hydroclimate metrics for climate change impact research. *Wiley Interdisciplinary Reviews (WIREs): Water,* 5, e1288. doi:10.1002/wat2.1288

Elshorbagy, A., Lindenas, K., & Azinfar, H. (2018). Risk-based quantification of the impact of climate change on storm water infrastructure. *Water Science*, 32(1), 102-114.

Fadhel, S., Rico-Ramirez, M. A., & Han, D. (2017). Uncertainty of intensity duration–frequency (IDF) curves due to varied climate baseline periods. *Journal of Hydrology,* 547, 600-612.

Fix, M. J., Cooley D., Sain, S. R., & Tebaldi, C. (2018). A comparison of U.S. precipitation extremes under RCP8.5 and RCP4.5 with an application of pattern scaling. *Climatic Change*, 146, 335-347. doi:10.1007/s10584-016-1656-7

Fortunato, A., Oliveri, E., & Mazzola, M. (2014). Selection of the Optimal Design Rainfall Return Period of Urban Drainage Systems. *16th Conference on Water Distribution System Analysis,* 742 – 749. doi:10.1016/j.proeng.2014.11.502.

Gavidel, S. Z., & Rickli, J. L. (2015). Triage as a core sorting strategy in extreme core arrival scenarios. *Journal of Remanufacturing*, 5(9), 1-13

Gilbert, R. O. (1987). *Statistical Methods for Environmental Pollution Monitoring*. Wiley, NY.

Gilleland, E. (2016). *Extreme Value Analysis, Package 'extRemes'*

Gilleland, E., & Katz, R. (2016). extRemes 2.0: An Extreme Value Analysis Package in R. *Journal of Statistical Software*, 72(8), 1-39. doi: 10.18637/jss.v072.i08

Gilleland, E., & Katz, R. (2011). New software to analyze how extremes change over time. *Transactions American Geophysical Union*, 92(2), 13–14. doi:10.1029/ 2011eo020001

Gilleland, E., Bukovsky, M., Williams, C. L., McGinnis, S., Ammann, C. M., Brown, B. G., & Mearns, L. O. (2016). Evaluating NARCCAP model performance for frequencies of severe-storm environments. *Advances in Statistical Climatology, Meteorology and Oceanography*, 2, 137-153.

Goldstein, J., Mirza, M., Etkin, D., & Milton, J. (2003). Hydrologic Assessment: Application of Extreme Value Theory for Climate Extreme Scenarios Construction. *14th symposium on global change and climate variations, American meteorological society 83rd annual meeting,* Long Beach.

Governorate of Ankara, (2018). Geography and demographics. [online] Available at: http://eng.ankara.gov.tr/geography-and-demographics. [Accessed 01 June 2018].

Governorship of Etimesgut, (2018). District introduction. [online] Available at: http://www.etimesgut.gov.tr/kaymakamligimizin-tanitimi. [Accessed 02 June 2018].

Gül, G., Aşıkoğlu, Ö., Gül, A., Gülçem, Y. F., & Benzeden, E. (2014). Nonstationarity in flood time series. *Journal of Hydrologic Engineering*, 19, 1349-1360

Hailegeorgis, T. T., & Alfredsen, K. T. (2017). Analyses of extreme precipitation and runoff events including uncertainties and reliability in design and management of urban water infrastructure. *Journal of Hydrology*. 544. 290-305

Haktanir, T., & Citakoglu, H. (2014). Trend, independence, stationarity, and homogeneity tests on maximum rainfall series of standard durations recorded in Turkey. *Journal of Hydrologic Engineering*, 19, 9. DOI: 10.1061/(ASCE)HE.1943-5584.0000973.

Harisaweni, Z., & Fadhilah, Y. (2016). The use of BLRP model for disaggregating daily rainfall affected by monsoon in Peninsular Malaysia. *Sains Malaysiana*, 45 (1). 87-97.

Helsel, D. R., & Hirsch, R. M. (2002). Statistical methods in water resources techniques of water resources investigations. *U.S.Geological Survey*, 522 p.

Hettiarachchi, S., Wasko, C., & Sharma, A. (2018). Increase in flood risk resulting from climate change in a developed urban watershed – the role of storm temporal patterns, *Hydrol. Earth Syst*. 22, 2041-2056.

Hirabayashi, Y., Mahendran, R., Koirala, S., Konoshima, L., Yamazaki, D., Watanabe, S., Kim, H., & Kanae, S. (2013). Global flood risk under climate change, *Nat. Clim. Change*, 3, 816–821.

Hooten, M. B., & Hobbs, N. T. (2015). A guide to Bayesian model selection for ecologists. *Ecological Monographs*, 85, 3-28. doi:10.1890/14-0661.1

Hosseinzadehtalaei, P., Tabari, H., & Willems, P. (2017). Precipitation intensity–duration–frequency curves for central Belgium with an ensemble of Eurocordex simulations, and associated uncertainties. *Atmospheric Research*, 200, 1-12. doi:10.1016/j.atmosres.2017.09.015

Huntington, T. G. (2006). Evidence for ıntensification of the global water cycle: review and synthesis. *Journal of Hydrology*, 319, 83-95. http://dx.doi.org/10.1016/j.jhydrol.2005.07.003

IPCC, (2012). Managing the risks of extreme events and disasters to advance climate change adaptation. *A Special Report of Working Groups I and II of the Intergovernmental Panel on Climate Change*.

IPCC, (2013). Climate change 2013. *The Physical Science Basis. Contribution of Working Group I to the Fifth Assessment Report of the Intergovernmental Panel on Climate Change.*

IPCC, (2014). Climate change 2014. *Impacts, Adaptation, and Vulnerability. Part A: Global and Sectoral Aspects. Contribution of Working Group II to the Fifth Assessment Report of the Intergovernmental Panel on Climate Change*.

IPCC, (2014). Climate change 2014. *Synthesis Report. Contribution of Working Groups I, II and III to the Fifth Assessment Report of the Intergovernmental Panel on Climate Change.*

January 2018 was fifth warmest January on record. (2018). Retrieved May 20, 2018, from https://climate.nasa.gov/news/2683/january-2018-was-fifth-warmest-january-on-record/

Kaczmarska, J. M., Isham, V. S., & Northrop, P. (2015). Local generalised method of moments: an application to point process-based rainfall models. *Environmetrics*, 26, 312–325. doi: 10.1002/env.2338

Kara, F. (2014). *Effects of climate change on water resources in Omerlı basin*. PhD. Dissertation. Middle East Technical University

Kara, F., Yucel, I., & Akyurek, Z. (2016). Climate change impacts on extreme precipitation of water supply area in Istanbul: use of ensemble climate modelling and geo-statistical downscaling. *Hydrological Sciences Journal*, 61(14), 2481-2495. doi: 10.1080/02626667.2015.1133911

Kendall, M. G. (1975). *Rank correlation methods*, 4th edition, Charles Griffin, London.

Kirshen, P., Caputo, L., Vogel, R., Mathisen, P., Rosner, A., & Renaud, T. (2014). Adapting urban infrastructure to climate change: A drainage case study. J. *Water Resour. Plann. Manage.*,10.1061/(ASCE)WR.1943-5452.0000443, 04014064

Köle, M. M. (2012). *Ankara örneklemi üzerinde iklim değişikliğinin su kaynakları yönetimine etkisi.* Doktora Tezi, Ankara Üniversitesi, Sosyal Bilimler Enstitüsü.

Kossieris, P., Koutsoyiannis, D., Onof, C., Tyralis, H., & Efstratiadis, A. (2012). HyetosR: *An R package for temporal stochastic simulation of rainfall at fine time scales*. European Geosciences Union General Assembly 2012, Geophysical Research Abstracts, Vol. 14, Vienna, 11718, European Geosciences Union.

Kossieris, P., Makropoulos, C., Onof, C., & Koutsoyiannis, D. (2016a). A rainfall disaggregation scheme for sub-hourly time scales: Coupling a Bartlett-Lewis based model with adjusting procedures, *Journal of Hydrology*, 556, 980-992.

Kossieris, P., Makropoulos, C., Onof, C., & Koutsoyiannis, D. (2016b). *HyetosMinute,* A package for temporal stochastic simulation of rainfall at fine time scales, Version 2.0.

Kundzewicz, Z. W. (2003). Extreme precipitation and floods in the changing world, Water Resources Systems—Hydrological Risk, Management and Development. *Proceedinss of symposium HS02b held during IUGG2003 al Sapporo*.

Kundzewicz, Z. W., & Robson, A. J. (2004). Change detection in hydrological records-a review of the methodology. *Hydrological Sciences Journal*, 49(1), 7-19. doi: 10.1623/hysj.49.1.7.53993

Kundzewicz, Z. W., Kanae, S., Seneviratne, S. I., Handmer, J., Nicholls, N., Peduzzi, P., Mechler, R., Bouwer, L. M., Arnell, N., Mach, K., Muir-Wood, R. G., Robert, B., Wolfgang, K., Gerardo, B., Yasushi, H., Kiyoshi, T., & Boris, S. (2014). Flood risk and climate change: global and regional perspectives. *Hydrological Sciences Journal*, 59(1), 1-28. doi: 10.1080/02626667.2013.857411

Kusunoki, S., (2017). Future changes in global precipitation projected by the atmospheric model MRI-AGCM3.2H with a 60-km size. *Atmosphere,* 8, 93

Larsen, A. N., Gregersen, I. B., Christensen, O. B., Linde, J. J., & Mikkelsen, P. S. (2008). Future development in extreme one-hour precipitation over Europe due to climate change. *In 11ICUD, 11the International Conference on Urban Drainage, Edinburgh, Scotland*, 31st August-5th September 2008 (Vol. CD-ROM). Sheffield, UK: University of Sheffield.

Lawrence, D. M., Hurtt, G. C., Arneth, A., Brovkin, V., Calvin, K. V., Jones, A. D., & Pitman, A. (2016). The Land use model intercomparison project (LUMIP) contribution to CMIP6: rationale and experimental design. *Geoscientific Model Development*, 9(9), 2973-2998.

Li, J., Johnson, F., Evans, J., & Sharma, A. (2017). A comparison of methods to estimate future sub-daily design rainfall. *Advances in Water Resources*, 110. 10.1016/j.advwatres.2017.10.020.

Liew, S. C., Raghavan, S. V., & Liong, S.Y. (2014). How to construct future IDF curves, under changing climate, for sites with scarce rainfall records?. *Hydrol. Process.,* 28, 3276–3287. doi:10.1002/hyp.9839

Lu, Y., & Qin, X. S. (2012). Comparison of stochastic point process models of rainfall in Singapore. *Proceedings of 2012 International Conference of World Academy on Science, Engineering and Technology (WASET),* 68, 1234-1238.

Mann, H. B. (1945). Non-parametric tests against trend, *Econometrica,* 13,163-171.

McGarigal, K. (2017). *ECO602: Analysis of Environmental Data, Week 8 Notes,* Retrieved from:
http://www.umass.edu/landeco/teaching/ecodata/schedule/likelihood.pdf

Meld, (2013). Climate change adaptation in Norway Meld. St. 33 (2012–2013) Report to the Storting (white paper) Recommendation of 7. May 2013 from the Ministry of the Environment, approved in the Council of State the same day. (White paper from the Stoltenberg II Government).

Miralles-Wilhelm, F., Clarke, L., Hejazi, M., Kim, S., Gustafson, K., Muñoz-Castillo, R., & Graham, N. (2017). *Physical impacts of climate change on water resources.* Discussion Paper. World Bank, Washington, DC.

NOAA, (2018). NOAA National Centers for Environmental information, *Climate at a Glance: Global Time Series,* published April 2018, retrieved on April 30, 2018, from http://www.ncdc.noaa.gov/cag/

Notaro, V., Liuzzo, L., Freni, G., & La Loggia, G. (2015). Uncertainty analysis in the evaluation of extreme rainfall trends and its implications on urban drainage system design. *Water,* 7(12), 6931-6945.

NYC, (2012). *Guidelines for the Design and Construction of Stormwater Management Systems.* Developed by the New York City Department of Environmental Protection in consultation with the New York City Department of Buildings.

Onyutha, C., Tabari, H., Taye, M. T., Nyandwaro, G. N., & Willems, P. (2015). Analyses of rainfall trends in the Nile River basin. *J Hydro Environ Res*, 13, 36–51.

Osborn, T. J., Gosling, S., Wallace, C., & Dorling, S. (2015). The Water Cycle in a Changing Climate. *7th World Water Forum. Faircount Media Group*, London, 14–19.

Osman, Y. (2014). Monitoring the future behaviour of urban drainage system under climate change: a case study from north-western England. *Open Engineering*, 5(1). doi:10.1515/eng-2015-0003

Özkil, A. (2015). *Searching for the Crumbles of Nature in the Metropolitan Ankara.* Unpublished manuscript. Middle East Technical University, Ankara

Ozturk, T., Turp, M. T., Türkeş, M., & Kurnaz, M. L. (2018). Future projections of temperature and precipitation climatology for CORDEX-MENA domain using RegCM4.4. *Atmospheric Research*, 206, 87-107. doi:10.1016/j.atmosres.2018.02.00

Papagiannaki, K., Lagouvardos, K., Kotroni, V., & Bezes, A. (2015). Flash flood occurrence and relation to the rainfall hazard in a highly urbanized area, *Nat. Hazards Earth Syst. Sci*., 15, 1859-1871.

Partal, T., & Kahya, E. (2006). Trend analysis in Turkish precipitation data. *Hydrol. Process.*, 20, 2011-2026. doi:10.1002/hyp.5993

Peck, A., Prodanovic, P., & Simonovic, S. P. (2012). Rainfall intensity duration frequency curves under climate change: city of London, Ontario, Canada. *Can. Water Res. J.*, 37(3), 177–189. http://dx.doi.org/10.4296/cwrj2011-935

Pinheiro, M., & Grotjahn, R. (2015). *An Introduction to Extreme Value Statistics.*

Pohl, B., Macron, C., & Monerie, P-A. (2017). Fewer rainy days and more extreme rainfall by the end of the century in Southern Africa. *Scientific Reports*, 7, 46466. doi: 10.1038/srep46466

Pohlert T. (2016). *Non-Parametric Trend Tests and Change-Point Detection.* R package Version 0.2.0.

Ritschel, C., Ulbrich, U., Névir, P., & Rust, H. W. (2017). Precipitation extremes on multiple timescales – Bartlett–Lewis rectangular pulse model and intensity–duration–frequency curves. *Hydrology and Earth System Sciences*, 21(12), 6501.

Rodriguez-Iturbe, I., Cox, D. R., & Isham, V. (1987a). Some models for rainfall based on stochastic point processes. *Proceedings of the Royal Society*, 410, 269–288.

Rodriguez-Iturbe, I., Febres de Power, B., & Valdes, J. B. (1987b). Rectangular pulses point process models for rainfall: analysis of empirical data. *Journal of Geophysical Research*, 92, 9645–9656.

Rosenberg, E. A., Keys, P. W., Booth, D. B. (2010). Precipitation extremes and the impacts of climate change on stormwater infrastructure in Washington State. *Climatic Change*. 102, 319. https://doi.org/10.1007/s10584-010-9847-0

Rozos, E., Efstratiadis, A., Nalbantis, I., & Koutsoyiannis, D. (2004).Calibration of a semi-distributed model for conjunctive simulation of surface and groundwater flows, *Hydrological Sciences Journal*, 49(5), 819-842.

Sarhadi, A., & Soulis, E. D. (2017). Time-varying extreme rainfallintensity-duration-frequency curvesin a changing climate, *Geophys. Res.Lett.*, 44. doi:10.1002/2016GL072201

Scotto, M. G., Barbosa, S. M., & Alonso, A. M. (2011). Extreme value and cluster analysis of European daily temperature series. *Journal of Applied Statistics*, 38, 2793–2804.

Seneviratne, S. I., Nicholls, N., Easterling, D., Goodess, C. M., Kanae, S., & Kossin, J. (2012). Changes in climate extremes and their impacts on the natural physical environment. Cambridge University Press, Cambridge, UK, and New York, NY.

Sensoy, S., Türkoğlu, N., Akçakaya, A., Ulupınar, Y., Ekici, M., Demircan, M., Atay, H., Tüvan, A., & Demirbaş, H. (2013). Trends in Turkey climate indices from 1960 to 2010, *6th Atmospheric Science Symposium*, 24 - 26 April 2013, ITU, Istanbul, Turkey.

Shanableh, A., Al-Ruzouq, R., Yilmaz, A., Siddique, M., Merabtene, T., & Imteaz, M. (2018). Effects of land cover change on urban floods and rainwater harvesting: a case study in Sharjah, UAE. *Water,* 10(5), 631. doi:10.3390/w10050631

Shuster, W. D., Bonta, J., Thurston, H., Warnemuende, E., &. Smith, D. R. (2005). Impacts of impervious surfaces on watershed hydrology: A review, *Urban Water J.*, 2(4), 263–275.

Sienz, F., Schneidereit, A., Blender, R., Fraedrich, K., & Lunkeit, F. (2010). Extreme value statistics for North Atlantic cyclones. *Tellus A,* 62(4), 347–360.

Simonovic, S. P. (2012). *Floods in a changing climate: Risk management*, 194. Cambridge: Cambridge University Pres

Simonovic, S. P., Schardong, A. Sandink, D., & Srivastav, R. (2016). A Web-based tool for the development of intensity duration frequency curves under changing climate. *Environmental Modelling & Software Journal*, 81:136-153.

Simonovic, S. P., Schardong, A., & Sandink, D. (2017). Mapping extreme rainfall statistics for canada under climate change using updated intensity-duration-frequency curves. *ASCE Journal of Water Resources Planning and Management,* 143(3), 04016078-1 -04016078-12.

SMS, (2018*). Republic of Turkey, the ministry of forestry and water affairs, state meteorological service*, 2017 Annual Climate Assessment Report, February 2018

Šraj, M., Viglione, A., Parajka, J., & Blöschl, G. (2016). The influence of non-stationarity in extreme hydrological events on flood frequency estimation. *Journal of Hydrology and Hydromechanics,* 64, 426-437

StormWater Forestry, (2018). Green infrastructure. [online] Available at: http://www.stormwaterforestry.ca/green-infrastructure.html [Accessed 12 May 2018].

Sun, Z., Guo, H., Li, X., Huang, Q., & Zhang, D. (2011). Effect of LULC change on surface runoff in urbanization area. *Proceedings of the ASPRS 2011 Annual Conference,* Milwaukee, Wisconsin, May 1–5.

Tayanç, M., İm, U., Doğruel, M., & Karaca, M. (2009). Climate change in Turkey for the last half century. *Climatic Change,* 94, 483-502.

TDT, (2016). *Hydraulic Design Manual*. Texas Department of Transportation.

Thakali, R., Kalra, A., & Ahmad, S. (2016). Understanding the effects of climate change on urban stormwater infrastructures in the las vegas valley. *Hydrology,* 3, 34.

Trenberth, K. E. (1998). Atmospheric moisture residence times and cycling: Implications for rainfall rates with climate change. *Climatic Change,* 39, 667-694.

Turunçoğlu, U. U., Türkeş, M., Bozkurt, D., Önol, B., Şen, Ö. L., & Dalfes, H. N. (2018). *The Soils of Turkey*. World Soils Book Series. Springer, Cham.

Umbricht, A., Fukutome, S., Liniger, M. A., Frei, C., & Appenzeller, C. (2013). *Seasonal variation of daily extreme precipitation in Switzerland.* Scientific Report. MeteoSwiss, 97, 122.

United Nations, (2018). *World urbanization prospects: The 2018 revision*. New York.

Vahedifard, F., Tehrani, F. S., Galavi, V., Ragno, E., & AghaKouchak, A. (2017). Resilience of MSE walls with marginal backfill under a changing climate: quantitative assessment for extreme precipitation events. *Journal of Geotechnical and Geoenvironmental Engineering,* 143(9). doi:10.1061/(ASCE)GT.1943-5606.0001743

Van Der Linden, P., & Mitchell, F. J. (2009). *Ensembles: Climate change and ıts ımpacts: summary of research and results from the ensembles project*. Met Office Hadley Centre, FitzRoy Road, Exeter EX1 3PB, UK.

Villani, V., Di Serafino, D., Guido, R., & Mercogliano, P. (2016). Stochastic models for the disaggregation of precipitation time series on sub-daily scale: identification of parameters by global optimization. *CMCC Research Paper* No. RP0256. http://dx.doi.org/10.2139/ssrn.2602889

Wang, J., You, S., Wu, Y., Zhang, Y., & Bin, S. (2016). A method of selecting the block size of bmm for estimating extreme loads in engineering vehicles. *Mathematical Problems in Engineering*. 1-9. 10.1155/2016/6372197.

Wang, X., Huang, G., Liu, J., Li, Z., & Zhao, S. (2015). Ensemble projections of regional climate changes over Ontario, Canada. *J. Clim.*, 28(18), 7327–7346.

Wang, Y., & Liu, Q. (2006). Comparison of Akaike information criterion (AIC) and Bayesian information criterion (BIC) in selection of stock–recruitment relationships. *Fish. Res*. 77, 220-225.

Wehner, M., Stone, D., Mitchell, D., Shiogama, H., Fischer, E., Graff, L. S., & Krishnan, H. (2018). Changes in extremely hot days under stabilized 1.5 and 2.0 °C global warming scenarios as simulated by the HAPPI multi-model ensemble. *Earth System Dynamics*, 9(1), 299–311.

Willems, P., & Lloyd-Hughes, B. (2016). *Projected change-river flow and urban drainage.* Book Chapter; North Sea Region Climate Change Assessment, 219-237.

Willems, P., Olsson, J., Arnbjerg-Nielsen, K., Beecham, S., Pathirana, A., Gregersen, I. B., & Nguyen, V. T. V. (2013). Climate change impacts on rainfall extremes and urban drainage: a state-of-the-art review. *Geophysical Research Abstracts*, 15, EGU2013-14093-1.

Willems, P., Olsson, J., Arnbjerg-Nielsen, K., Beecham, S., Pathirana, A., Gregersen, I.B., Madsen, H., Nguyen, V.T.V. (2012). *Impacts of climate change on rainfall extremes and urban drainage.* IWA Publishing, London, UK.

WMO, (2018). *Statement on the state of the global climate in 2017*. World Meteorological Organization.

WRP, (2016). *Republic of Turkey, the ministry of forestry and water affairs, general directorate of water management.* Climate Change Impacts On Water Resources Project.

Yal, G. P., & Akgün, H. (2013). Landfill site selection and landfill liner design for Ankara, Turkey. *Environ. Earth Sci* 70, 2729-2752. doi: 10.1007/s12665-013-2334-y

Yilmaz, A. G. (2015). The effects of climate change on historical and future extreme rainfall in Antalya, Turkey. *Hydrological Sciences Journal*, 60(12), 2148-2162. doi: 10.1080/02626667.2014.945455

Yilmaz, A. G., & Perera, B. J. C. (2014). Extreme rainfall non-stationarity investigation and intensity-frequency-duration relationship. *J. Hydrol. Eng.* 19, 1160-1172. doi: 10.1061/(ASCE)HE.1943-5584.0000878

Yoon, J. H., Wang, S. Y., Gillies, R. R., Kravitz, B., Hipps, L., & Rasch, P. J. (2015). Increasing water cycle extremes in California and relation to ENSO cycle under global warming. *Nat. Commun,* 6, 8657 doi: 10.1038/ncomms9657

Yuan, X.-C., Wei, Y.-M., Wang, B., and Mi, Z. (2017). Risk management of extreme events under climate change, *J. Clean. Prod.*, 166,1169–1174, https://doi.org/10.1016/j.jclepro.2017.07.209, 2017

Zhang, X., Zwiers, F., Hegerl, G., Lambert, F., Gillett, N., Solomon, S., Stott, P., & Nozawa, T. (2007). Detection of human influence on twentieth-century precipitation trends, Nature, 448(7152), 461-465.

Zhou, Q. (2014). A review of sustainable urban drainage systems considering the climate change and urbanization impacts. *Water,* 6(4), 976-992

Zhou, Q., Arnbjerg-Nielsen, K., Mikkelsen, P. S., Nielsen, S. B., & Halsnæs, K. (2012). Urban drainage design and climate change adaptation decision making. *Kgs. Lyngby: DTU Environment,*

Zscheischler J., Westra S., Van Den Hurk, B. J. J. M. , Seneviratne, S. I., Ward, P. J., Pitman, A., AghaKouchak A., Bresch D.N., Leonard M., Wahl T., & Zhang X. (2018). Future climate risk from compound events. *Nature Climate Change,* doi: 10.1038/s41558-018-0156-3.

CURRICULUM VITAE

PERSONAL INFORMATION

Surname, Name: Oruç, Sertaç

Nationality: Turkish (TC)

Date and Place of Birth: 24 April 1982, Bursa

Marital Status: Married

Email: sertac.oruc@metu.edu.tr

EDUCATION

Degree	Institution	Year of Graduation
Executive MBA	Boğaziçi Unv.	2011
BS	ITU Civil Engineering Dept.	2005
High School	Karacabey Anadolu Lisesi	2000

WORK EXPERIENCE

Year	Place	Enrollment
2014-present	State Railways	Civil Engineer